Mathematical Model to Predict the Behavior of Deep-Draft Vessels in Restricted Waterways

EDWARD T. GATES and JOHN B. HERBICH
Ocean Engineering Program

TAMU-SG-77-206
June 1977

TEXAS A&M UNIVERSITY SEA GRANT COLLEGE

MATHEMATICAL MODEL TO PREDICT THE BEHAVIOR OF DEEP-DRAFT VESSELS IN RESTRICTED WATERWAYS

by

Edward T. Gates and John B. Herbich

Ocean Engineering Program

June 1977

TAMU-SG-77-206

COE Report No. 200

Partially supported through Institutional Grant 04-6-158-44012
to Texas A&M University
by the National Oceanic and Atmospheric
Administration's Office of Sea Grants
Department of Commerce

$5.00

Order from:

Department of Marine Resources Information
Center for Marine Resources
Texas A&M University
College Station, Texas 77843

ABSTRACT

Presently deep-draft navigation channel analysis, design and review is based on empirically derived ratios of the design vessel's dimensions. Because of radical changes in vessel operation purposes and characteristics, these ratios can no longer be safely or economically applied.

The mathematical model and related theory described in this document provide the engineer with a comprehensive tool in the design and review of deep-draft navigation channels. Through its use he will be able to predict values of squat, bank suction forces and moments, equilibrium drift and rudder angles, and heights of ship-generated waves for varied channel configurations, ship positions and ship velocities. Through the determination of channel section configuration sensitivity, an optimal design both operationally and economically can be achieved.

PREFACE

Research described in this report was conducted as part of the research program in the Coastal, Hydraulic and Ocean Engineering Group at Texas A&M University. The study was partially supported by the U. S. Army Engineer Galveston District, the NOAA Sea Grant Program, and the Center for Dredging Studies at Texas A&M University.

The manuscript was edited by Dr. Gisela Mahoney and typed for publication by Miss Jeanine M. Larpenteur.

TABLE OF CONTENTS

TABLE OF CONTENTS (contd.)

LIST OF FIGURES

LIST OF FIGURES (contd.)

LIST OF FIGURES (contd.)

LIST OF FIGURES (contd.)

LIST OF FIGURES (contd)

LIST OF TABLES

CHAPTER I

INTRODUCTION

The design and efficient operation of ports and navigation channels is an important factor in the economic stability of the United States. Recent plans to expand our country's maritime facilities through the building of offshore terminals and mono-buoys will be of great help to the petrochemical industry but will aid little in other maritime shipment problem areas. Agricultural products, dry bulk cargos, manufactured goods, etc. must still be shipped through a port facility system.

The dredged channels leading to United States port facilities are at present largely inadequate to meet the nation's maritime requirements. Quite often vessels must be lightered before entering a port. Even more often vessels will delay entering or leaving a port area until the tide and wind conditions are sufficient to provide the required depth. This leads to unnecessary cost in terms of dockage fees, vessel operating costs and lightering expense to owners and others operating under charter parties. There are very few ports in the United States that can accommodate the so-called superships and none

at all on the Gulf Coast. This denies the shipper the freight economy of this class of vessel.

Navigation channel maintenance and improvement is an extremely costly investment and competition for public tax dollars has intensified. Local, state, and federal agencies are finding it ever more difficult to get project approval and funding. Dredged material disposal sites are becoming scarce and related ecological problems are more difficult to solve. For all of these reasons it is important at this time to develop more effective and efficient navigation channel design procedures.

Present Situation and Design Procedure

Navigation channel design engineers should have an in-depth knowledge of both naval architecture and coastal engineering. This is an in-between area that neither profession has devoted much effort in developing. The naval architect's main interest is the design of the vessel. The critical design conditions are not based on ship behavior in restricted channels, but on stability and behavior in the open sea. In the past, naval architects have not shown great interest in in-channel operation. Although coastal engineers are interested in these areas, their knowledge of vessel behavior is generally lacking. University courses in navigation channel design which could supply this knowledge are not offered. Even text and reference material is not normally available.

Presently, to overcome the lack of knowledge in ship behavior, engineers are determining navigation channel dimensions by U. S. Army Engineer (USAE) design policy and by use of standard ratios of proportions of the selected design vessel. For example, there is design criterion to maintain two feet depth under the keel of the vessel. Also, a maneuvering lane is 1.8B and bank clearance is 1.5B, where B is the beam of the design vessel (51). These empirically determined relationships may have been valid in the past, but because of the great changes that have occurred in relative dimensions and operational purposes of the world's marine fleets, these policies and ratios should no longer be universally applied. It should also be noted that this criteria-ratio approach to design does not take into consideration the individual characteristics of each separate channel location such as prevailing winds and currents. Neither will it assist in the selection of the best among a number of alternate designs.

It is the author's opinion that the present relatively low level of marine accidents in navigation channels is due more to the professional capability of the channel pilots than to the adequacy of the channel designs.

Model Objectives

The theory, procedures and mathematical model described herein are presented to help fill the gap that

currently exists in related behavior of parallel mid-body commercial vessels and navigation channel design information. All of the pertinent information, theory and proposed design and review procedures and their limitations have been incorporated into the model in such a way as to provide a comprehensive analysis of the selected channel section and design vessel.

When a vessel enters a restricted waterway it is acted upon and reacts to a number of physical phenomena. Many of these can be ignored in the open sea but they become very important design considerations in this type of waterway. These phenomena cause the ship to settle, to be pulled to the near bank and to react to many forces tending to skew the ship in the channel. Also the waves and surges generated by the ship can be very dangerous to other craft, shore structures and channel banks. Certainly, consideration of the effects of these phenomena must be included in navigation channel design and review procedures.

The proposed channel design model is modular in nature, each module determining the effects of a different physical phenomenon on the ship under control of given parameters (see Fig. 1). The output will contain the individual and combined effects on the design vessel in tabulated form. Each module and its related phenomenon is discussed in detail in separate chapters of this document.

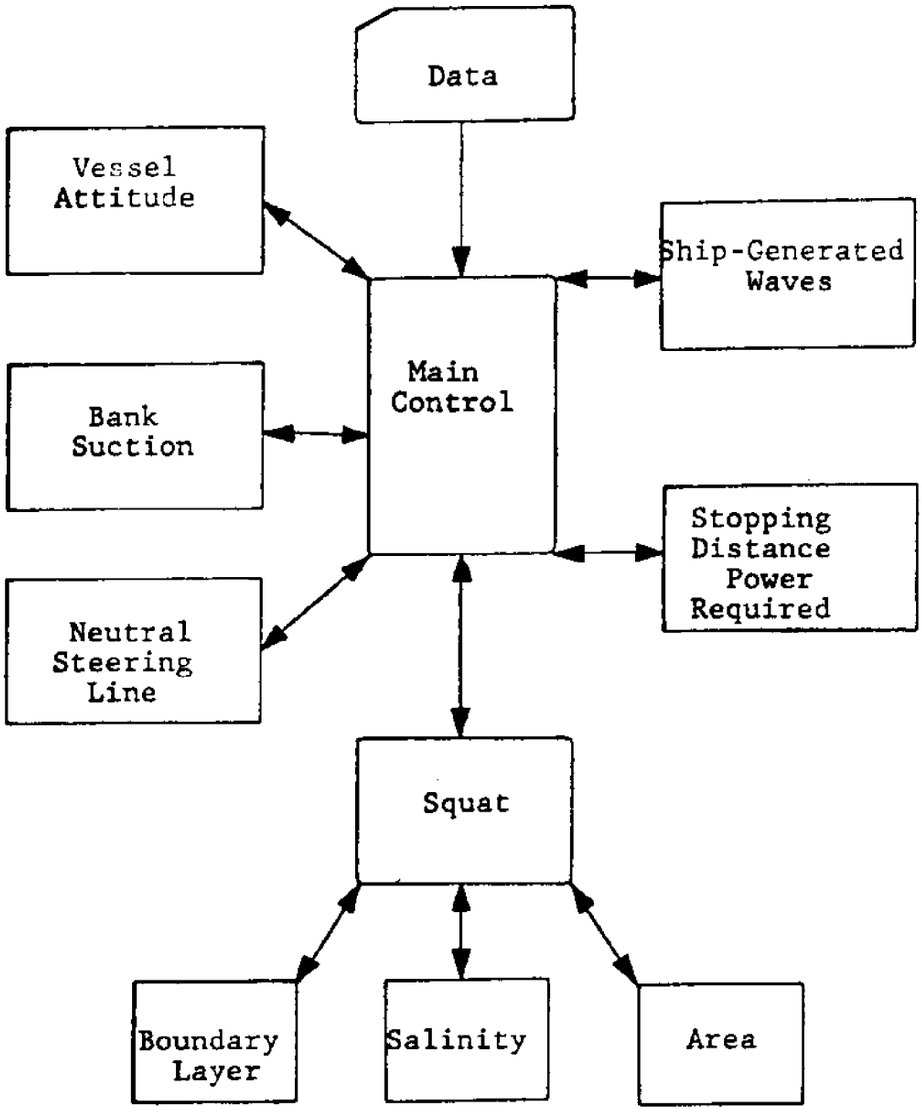

FIG. 1-CHANNEL DESIGN MODEL

The engineer can use the model as a design tool to determine the operational adequacy of the selected trial channel section. Through the variation of input data within a run or in successive runs, he can determine the operational and economic sensitivity of the changed parameters. This will produce a more nearly optimal final section. Using the model as a review tool, the engineer can determine the operational adequacy of existing navigation channels under changed conditions. When used in this manner, the model may indicate a requirement to limit certain vessel operations within the section; i.e., one-way traffic, maximum speed limitations, etc.

Present Limitations and Future Developments

Theory limitation indicators have been programmed into the model to prevent the navigation channel design engineer from exceeding the bounds of the theory where it is no longer valid or where results could be doubtful for whatever reason. These limitations are discussed in the individual chapters.

The present model is complete and accurate by today's standards and current state of the art. The accuracy of the model is more than adequate when one considers the type of input data and the requirements of the end product. It has been designed as a dynamic tool in that new modules may be added as required and existing modules

may be updated as present theory is expanded and refined. The linkage has been built in to perform these changes at relative ease to maintenance personnel.

CHAPTER II

SQUAT

Description of Problem

The movement of a vessel hull through the water results in the displacement or pushing aside of an equal volume of water lying directly in its path and the filling of a void of equal volume at the vessel's stern (20). In more detail, the water at the bow moves forward, out and down. Just aft of the bow, the forward motion of the water stops but is still out and down to make way for the vessel. Slightly back from this point the water starts to flow aft. This reverse flow continues to a point somewhat aft of the stern of the vessel, where the water closing in and upward again has a forward motion. Wherever this reverse flow occurs, the water surface is lowered. This lowering or sinking of the water surface is known as squat (22). Although this phenomenon occurs in the open sea, it is much more pronounced in restricted or shallow waterways. In restricted waters, bottom and side restrictions reduce the magnitude of the radial flow and increase the longitudinal flow, forcing a greater volume of fluid displaced by the vessel's motion to be translated under and around the hull to fill the void. Fig. 2 shows a typical differential pressure field around a moving ship. Units are in inches of water (20). This is indicative of the water surface as well.

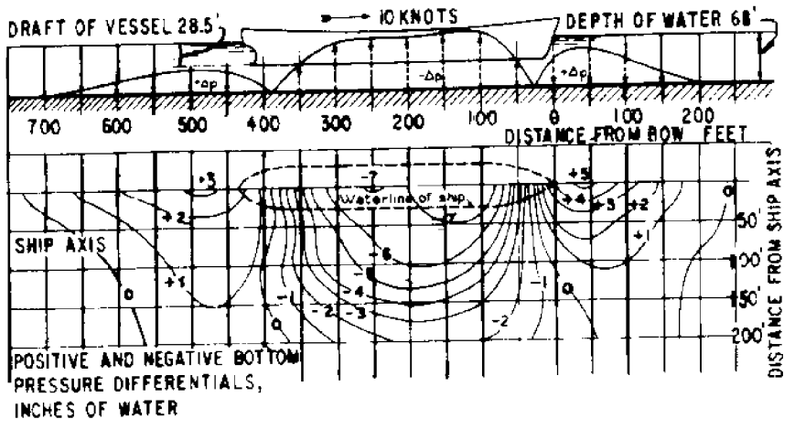

FIG. 2-TYPICAL DIFFERENTIAL PRESSURE FIELD AROUND MOVING SHIP (20)

It is interesting to note that this field at normal speeds will extend forward, aft, and to each side at least one ship length.

The squat phenomenon is a function of the speed of the vessel, the cross-sectional area of the vessel, the cross-sectional area of the channel, and the location of the vessel's sailing line with respect to the centerline of the channel, which will all be discussed in detail later. The squat will increase with speed until, under certain conditions, the vessel can actually strike the bottom of the channel.

The squat of a vessel will normally be slightly different at the bow and at the stern. This sinkage will continue with increasing speed until the speed-length ratio, $\frac{V}{\sqrt{L}}$, reaches 1.0 to 1.2, when the stern will continue to sink but the bow will begin to rise (32). This is illustrated quite well in Fig. 3 (12).

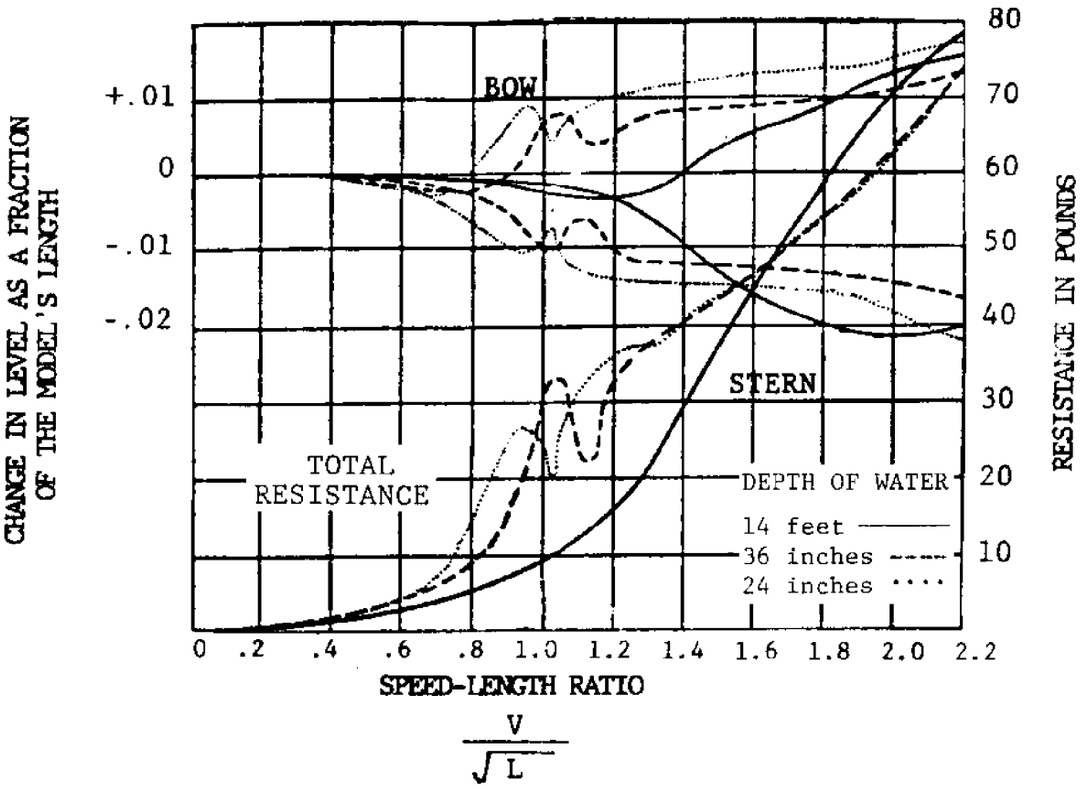

FIG. 3-RESISTANCE AND CHANGES IN LEVEL OF A 20-FOOT MODEL OF A HIGH-SPEED WARSHIP (12)

This phenomenon, squat, has been studied for many years. In 1904 Henry N. Babcock made a series of full-scale measurements of squat in the Ambrose Channel for U. S. Army Corps of Engineers (9,22). Since that time many model tests have been run at the David Taylor Model Basin (DTMB)(22,37), and the Davidson Laboratory at Stevens Institute of Technology (17,18,19). The SOGREAH Laboratory at Grenoble, France, ran a series of model tests for the Royal Dutch Shell Group producing a set of empirical curves used to predict the squat of vessels under various conditions (15).

Other tests were made in Sweden (9) and at the Institute of Marine Engineering of Odessa, U.S.S.R. (23). A series of tests run by the National Research Council of Canada in the mid 60s included not only model tests but actual observations on 190 ships in the St. Lawrence Seaway (50).

Tests made at DTMB show that a 45,000 DWT tanker with 102 ft. beam and draft of 37 ft. moving over the centerline of a restricted channel 300 ft. wide and 42 ft. deep with vertical side slopes would touch bottom at approximately 8 knots. With everything remaining the same except the widening of the channel to 500 ft., the same vessel exceeded 11 knots before a critical velocity was reached. In other test setups, supertankers of the 250,000 DWT class could attain squats of 16 ft. under certain conditions (36, 37). One can readily see that the ability to predict values of squat is of critical importance in the design of restricted waterways.

Basic Theory

The definition of squat and its basic effects are as described above. By virtue of the Bernoulli Theorem and the concepts of continuity, there must be, as described, a backflow with a resultant drop of water level adjacent to a vessel moving through the channel. The vessel, floating on the water surface, will also settle (50). Measurements taken at DTMB of the lowering of the water surface and

vessel squat indicate that the squat of the vessel is almost entirely due to the lowering of the water surface. This indicates that at normal operating speeds hydrodynamic forces have little effect on the vessel (22). This also means that if one could determine the settling of the water surface, one would also determine the squat of the vessel.

The drop in the water surface level is a function of the cross-sectional area of the channel. In a restricted-type channel this area is rather clear. However, in the open-type channel theories range from as little as a projection of the side slopes to meet the water surface to as much as ten times the beam of the vessel (32, 50). Fig. 4 shows the two types of channels considered (32).

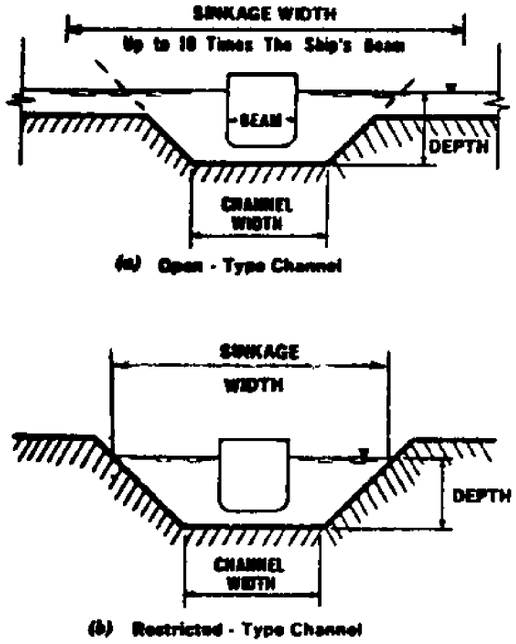

FIG. 4-TWO KINDS OF CHANNELS (32)

Squat is also a function of the velocity of the vessel and the wetted cross-sectional area of the vessel at the ship station where the amount of squat is to be determined (22,50).

A detailed derivation of the basic equation for squat is presented in Appendix III. The most useful form of the basic squat equation is:

$$\Delta d = \frac{V^2}{22.6}\left[\left(\frac{A}{A^1}\right)^2 - 1\right] \quad \ldots\ldots (1)$$

In certain cases it is necessary to know the vessel velocity which will produce a given value of squat. The equation for determining this velocity is:

$$V = \left[\frac{22.6\Delta d}{\left(\frac{A}{A^1}\right)^2 - 1}\right]^{1/2} \quad \ldots\ldots (2)$$

These equations were derived also at both the National Research Council of Canada (50) and the David Taylor Model Basin (22).

Model tests were made at the David Taylor Model Basin and squat values recorded. These values were then compared with values calculated from Eq. 1. The results of this comparison are shown in Fig. 5 (22).

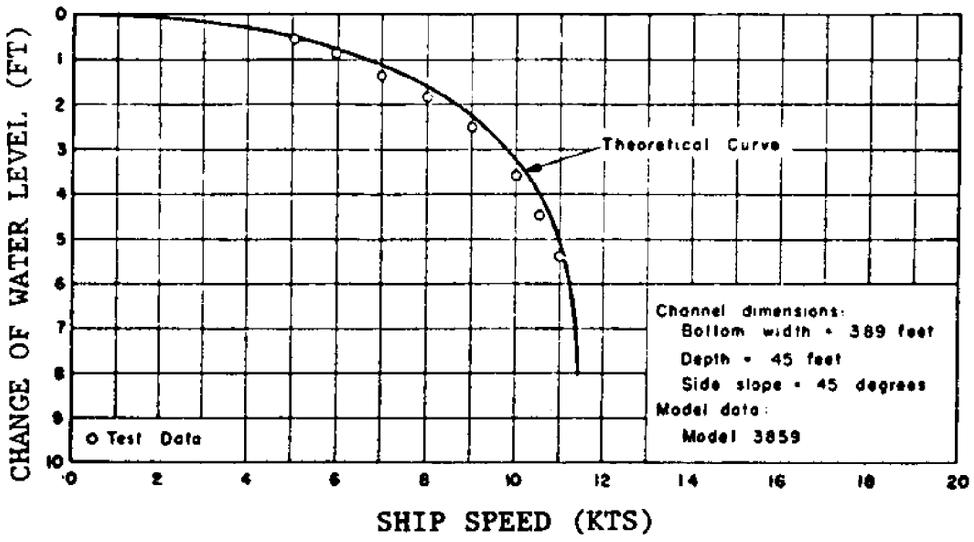

FIG. 5-COMPARISON OF THEORETICAL SQUAT CURVE WITH MODEL TEST RESULTS (22)

The fact that test values of squat are consistently greater than computed values should be noted. This consistent error will be discussed in more detail below.

The test runs at the SOGREAH Laboratory at Grenoble produced a series of curves which might be used in the determination of squat values (15, 51). Fig. 6 shows a comparison of squat values computed using the SOGREAH method versus observed model and prototype values (51).

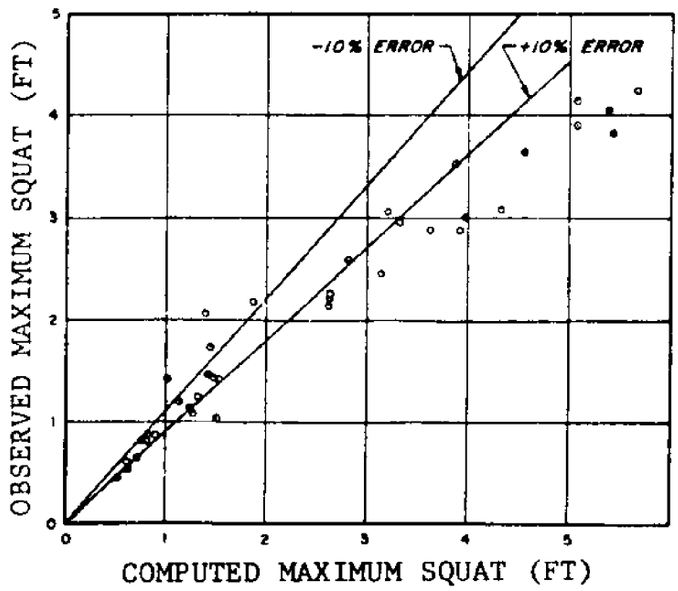

FIG. 6-OBSERVED VERSUS COMPUTED SQUAT-SOGREAH METHOD (51)

One can see that for higher values of squat the SOGREAH method (Fig. 6) computes values much greater than those actually observed. This same point was demonstrated in the Swedish test (9). Guliev (23) believes that this inaccuracy is due to the fact that the curves used in the SOGREAH method were empirically derived from model tests in fully-banked shallow water channels only. Wicker recommends that the SOGREAH method be used when the computed squat is less than 2 ft. and the theoretical equation when the squat is greater than 2 ft. (51).

The author believed that if boundary layer conditions were considered that Eq. 1 could be used satisfactorily over the entire range of squat values.

Dickson (15) has suggested approaches using the SOGREAH method of determining more accurately the values of squat for channels with unsymmetrical side slopes and for open channels. A test at DTMB clearly indicated that the channel side slopes per se, either in the restricted channel or the open-type channel, had little effect on the value of squat computed until the vessel sailing line approached the prism line of the channel (22). Because of this the author believes that satisfactory results will be obtained by using Eq. 1 with the selected channel cross-section as is.

Model tests at the Institute of Marine Engineering of Odessa, U.S.S.R.,in still water and in regular waves (head and following) in both shallow and deep water showed that the models in waves oscillated about the depressed water surface generated by squat in still water (23). This again seems to verify the validity of the theoretical solution.

Boundary Layer Considerations

Tothill used constant boundary layer thicknesses in his studies (50). He felt that a thickness of 0.5 feet on the vessel and 1.0 feet on channel would be satisfac-

tory. Field measurements were made on over one hundred deep-draft, seagoing vessels of various types. Squat readings were taken while the ships were making way in a measured section of the St. Lawrence Seaway. Static draft was measured while the ships were at rest in a navigation lock nearby. Figs. 7, 8, and 9 show comparisons of these full-size vessel squat measurements and mathematically determined squats (i.e., Eq. 1 with constant boundary layer thicknesses) for that same vessel for the bow, midships, and stern sections respectively (50).

For a vessel cross-sectional area selected near the bow, Fig. 7 shows that 56% of the squat values lay in the band $\pm$.2 ft. wide. 92.3% of the values lay in a band $\pm$.5 ft. wide.

Fig. 8 shows this comparison for a vessel cross-section taken amidships. Here 54.3% of the values lay in a band $\pm$.2 ft. wide and 87.9% of the values lay in a band $\pm$.5 ft. wide.

As shown in Fig. 9 it was found that 52.1% of the values lay in a band $\pm$.3 ft. and 70.4% of the values were found in a band $\pm$.5 ft.

These results are very good; however, it should be noted that the inclusion of constant boundary layers tends to produce greater calculated squats than those measured

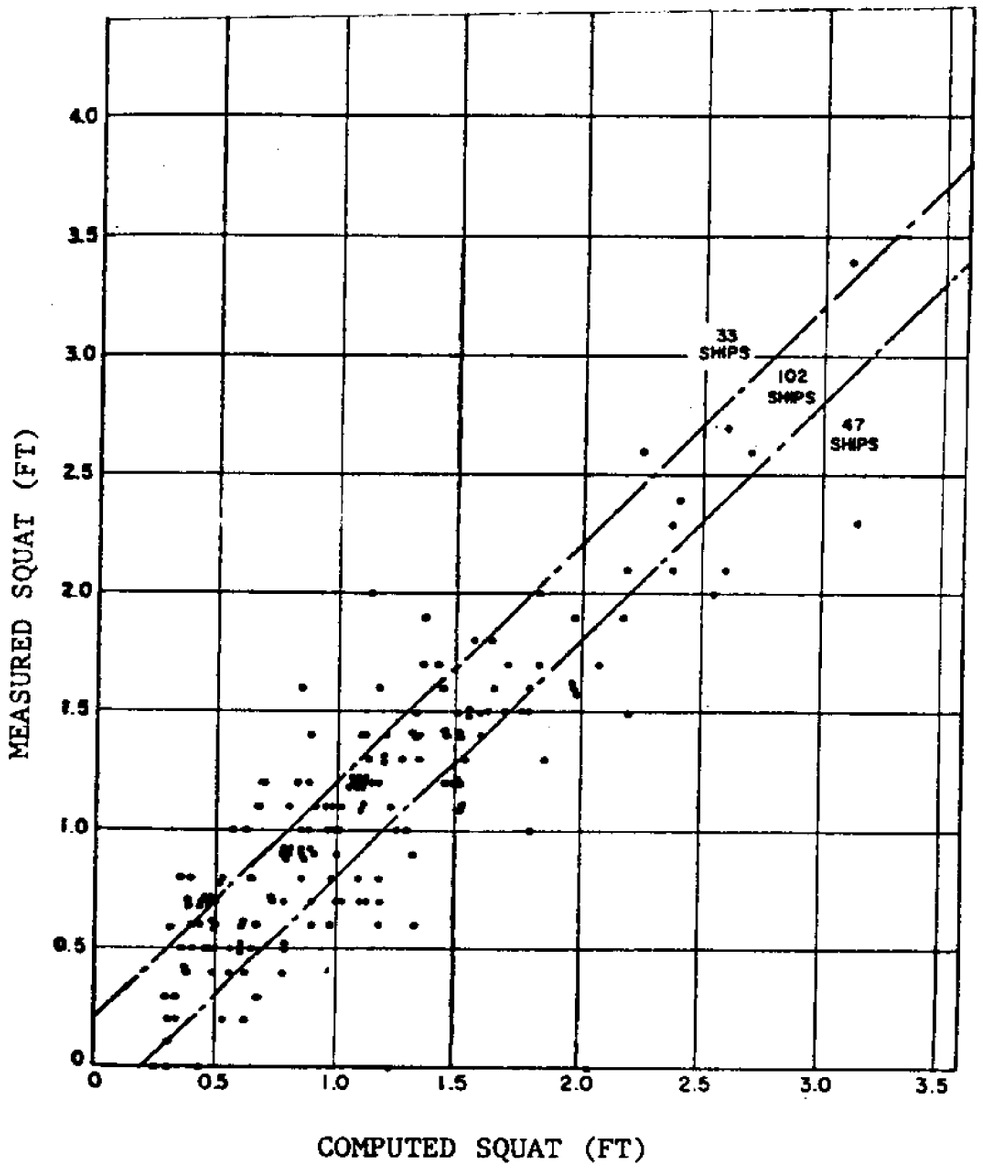

FIG. 7-COMPARISON OF FULL-SIZE SQUAT TESTS WITH THEORY-BOW (50)

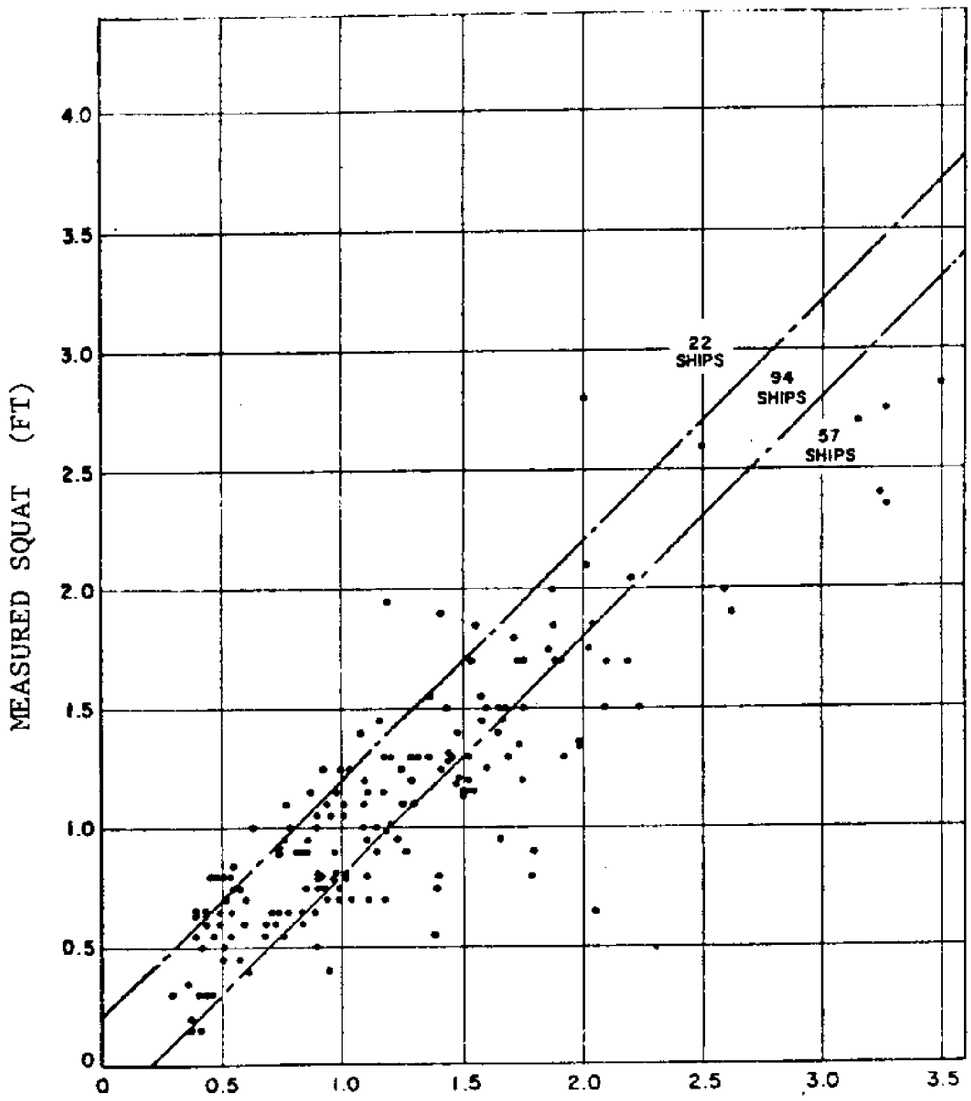

FIG. 8-COMPARISON OF FULL-SIZE SQUAT TESTS WITH THEORY-MIDSHIPS (50)

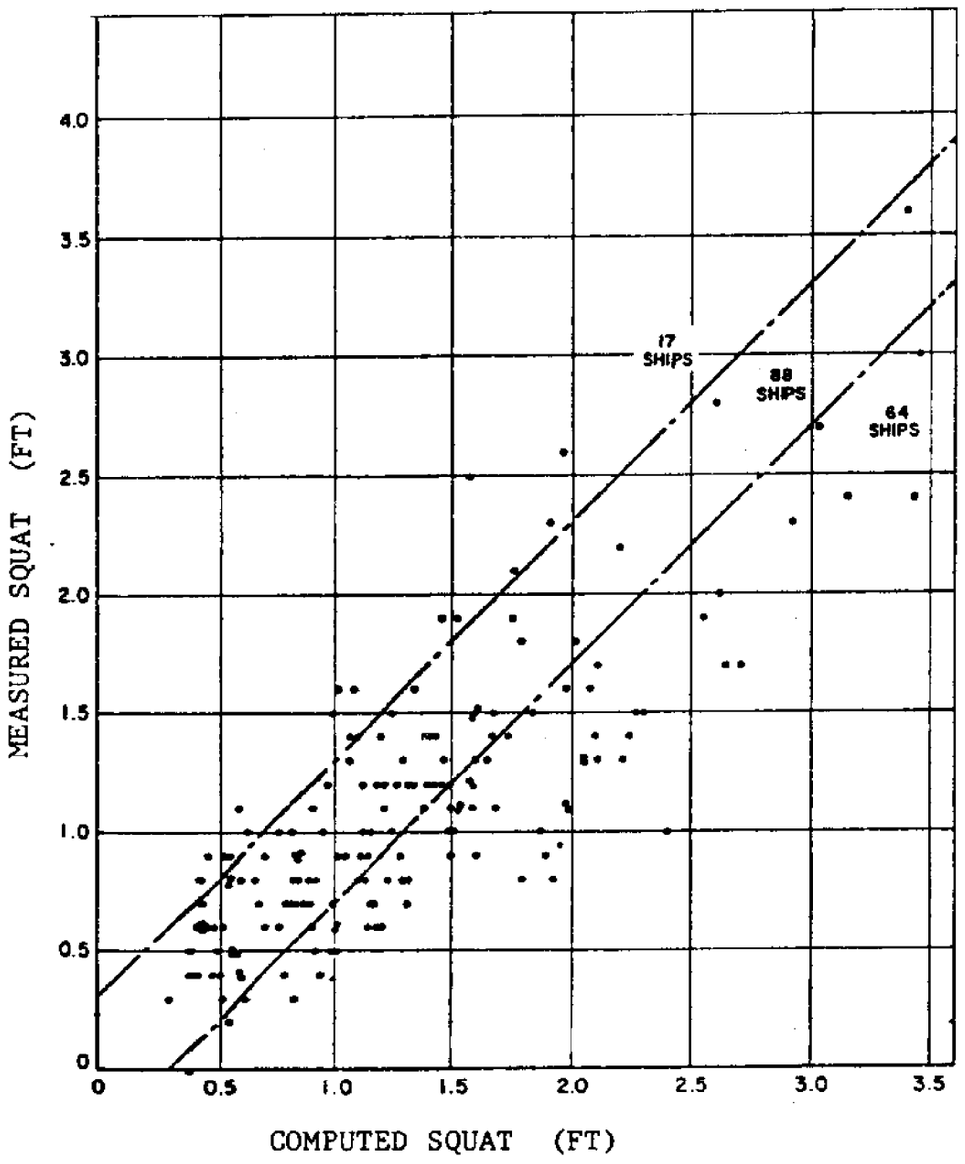

FIG. 9-COMPARISON OF FULL-SIZE SQUAT TESTS WITH THEORY-STERN (50)

in the field. Although this is good from a conservative standpoint, the author believed that more accurate squat values could be computed using Eq. 1 if more rigorously determined boundary layer values were used in the channel and vessel area calculations.

To determine the validity of this belief, displacement thicknesses were computed for both the channel and the vessel using methods detailed in Chapter III. The results of using constants and computed displacement thicknesses are compared with field data in Table 1. These measurements were part of the data taken in the above-mentioned Canadian study (50) where sufficient details of the vessels were known to allow boundary layer computations. Ship data were obtained from Lloyd's Register and are shown in Table 2 (35).

Fig. 10 shows a plot of these computed and measured values of squat. Error zones were determined by the least-squares method. The fitted curves were not forced to pass through the origin. The slope of the fitted curve for the constant boundary layer is 1.53 while the slope of the curve for the computed boundary layer is 1.02. One can see that by using computed displacement thicknesses, average errors in squat values were reduced substantially from those produced from constant thicknesses. It should be noted from both

TABLE 1. -FIELD MEASURED AND COMPUTED VALUES OF SQUAT

	SHIP DATA		MEASURED MEAN VALUES			COMPUTED BOUNDARY LAYER		CONSTANT BOUNDARY LAYER	
	LENGTH(BP) (FT)	BEAM (FT)	STATIC DRAFT (FT)	SPEED (KT)	SQUAT (FT)	SQUAT (FT)	ERROR (FT)	SQUAT (FT)	ERROR (FT)
1.	707.5	75.0	25.2	4.8	0.95	0.90	0.05-	1.10	0.15+
2.	707.5	75.0	25.3	5.0	0.70	1.00	0.30+	1.30	0.60+
3.	707.5	75.0	25.2	5.3	1.10	1.10	0.00	1.50	0.40+
4.	707.5	75.0	16.7	5.8	0.65	0.80	0.15+	1.00	0.35+
5.	707.5	75.0	25.1	3.8	0.60	0.50	0.10-	0.60	0.00
6.	707.5	75.5	18.8	4.7	0.45	0.50	0.05+	0.70	0.25+
7.	707.5	75.0	25.4	5.3	1.00	1.00	0.00	1.40	0.40+
8.	707.5	75.0	15.3	8.5	2.30	2.30	0.00	3.30	1.00+
9.	707.5	75.5	24.9	4.1	0.65	0.60	0.05-	0.70	0.05+
10.	707.5	75.5	25.2	6.2	1.50	1.80	0.30+	2.30	0.80+
11.	707.5	75.5	24.7	4.9	0.90	0.90	0.00	1.10	0.20+
12.	707.5	75.5	24.9	4.9	0.65	0.80	0.15+	1.00	0.35+
13.	565.1	75.0	25.3	6.3	1.70	1.70	0.00	2.20	0.50+
14.	476.5	69.6	25.2	6.9	1.50	2.10	0.60+	2.90	1.40+
15.	470.0	62.0	20.4	7.7	1.35	1.80	0.45+	2.60	1.25+
16.	468.0	65.0	17.9	8.3	1.75	2.10	0.35+	3.50	1.75+
17.	465.9	63.0	15.5	8.3	1.40	1.60	0.20+	2.50	1.10+
18.	353.6	48.0	15.3	8.2	0.80	0.90	0.10+	1.50	0.70+
19.	310.9	50.0	21.0	6.9	1.15	0.90	0.25-	1.30	0.15+
20.	295.9	42.0	12.5	8.3	0.60	0.70	0.10+	1.10	0.50+
21.	271.0	45.0	18.6	8.7	0.55	1.30	0.75+	2.20	1.65+
22.	236.3	36.3	10.9	10.6	1.25	1.00	0.25-	2.30	1.05+

TABLE 2. -SHIP DATA

Line No.		Length (FT)	Beam (FT)	Draft (FT)
1	Lake Winnipeg	707.5	75.0	42.5
2	Lawrencecliffe Hall	707.5	75.0	40.0
3	Saguenay	707.5	75.0	40.0
4	New Brunswicker	707.5	75.0	40.0
5	Quebecois	707.5	75.5	39.1
6	Quebecois	707.5	75.5	39.1
7	Lawrencecliffe Hall	707.5	75.0	40.0
8	Silver Isle	707.5	75.0	39.0
9	Quebecois	707.5	75.5	39.1
10	Montrealais	707.5	75.5	39.2
11	Quebecois	707.5	75.5	39.1
12	Quebecois	707.5	75.5	39.1
13	Patignies	565.1	75.0	44.1
14	Carl Trautwein	476.5	69.6	42.0
15	Manchester Commerce	470.0	62.0	37.0
16	Beltana	468.0	65.0	40.0
17	La Marea	465.9	63.0	41.5
18	Martian	353.6	48.0	18.1
19	Constance Bowater	310.9	50.0	30.0
20	Prins Willem II	295.9	42.0	18.3
21	Lawrendoc	271.0	45.0	24.0
22	Frigion	236.3	36.3	12.4

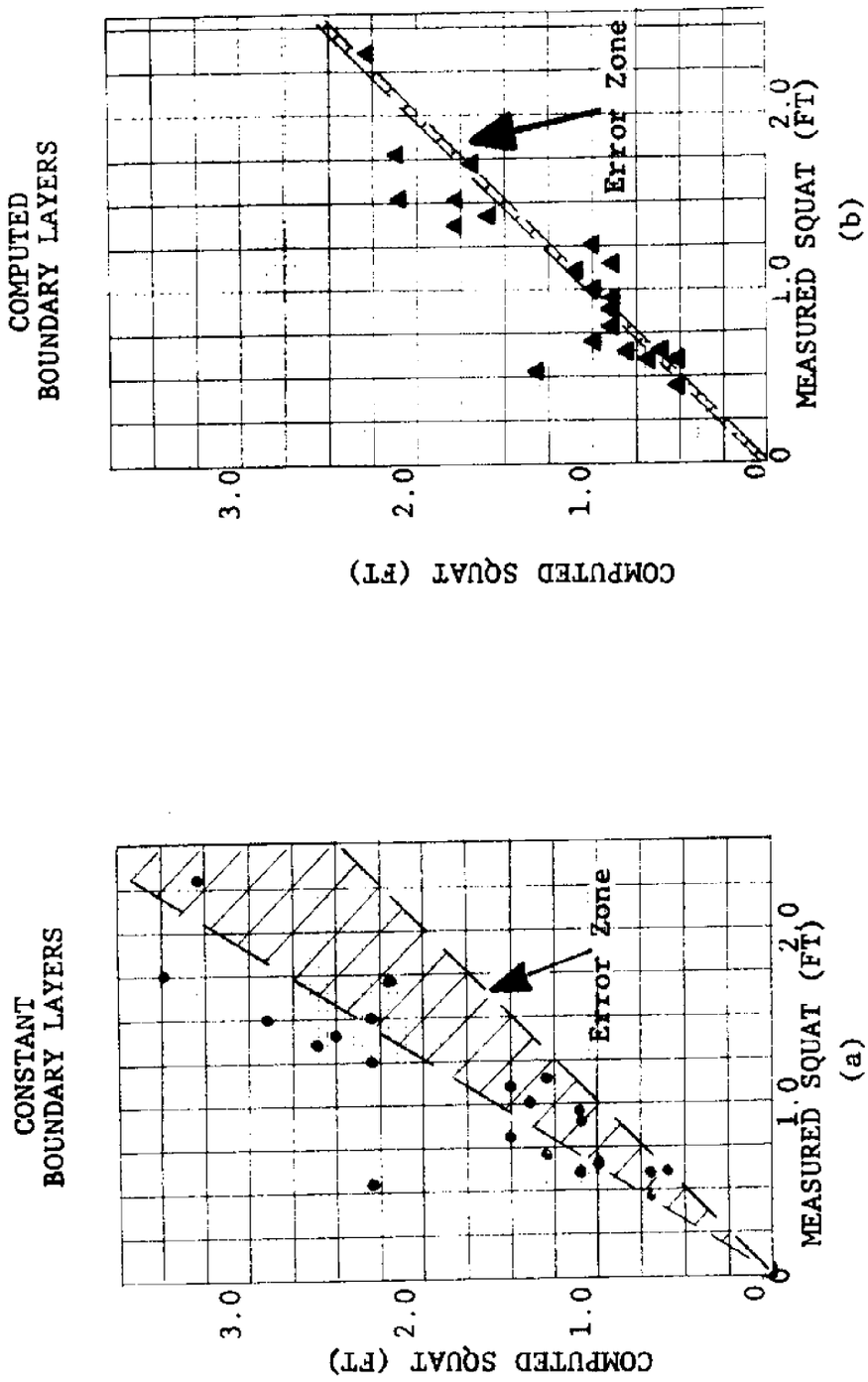

FIG. 10-EXPECTED ERROR OF SQUAT COMPUTATIONS

Table 1 and Fig. 11 that computed values of squat are normally exact or slightly greater than measured values. This is understandable since vessels underway prefer to be level or in trim slightly by the stern. The movement through the water of a vessel in trim by the stern would produce a small hydrodynamic force component in the upward direction tending to decrease the ship's draft and so the indicated squat value.

Critical Velocity

As a vessel's speed increases above a normal velocity, the stern will continue to settle while the bow will begin to rise and appear to ride on the back of its own bow wave As velocity continued to increase, a hydraulic jump is formed just aft of the mid-section of the vessel (Fig. 3). This point is known as the critical velocity. As this critical velocity is approached, there is a very rapid increase in squat for a slight increase in speed. Fig. 11 shows a family of squat versus velocity curves, clearly indicating the critical velocity as a dashed line. Note that the critical velocity corresponds to a point on the squat-velocity curve where the curve makes a tangent with the vertical (12,51). In Fig. 11, $\diamond$ equals midship section area in square feet.

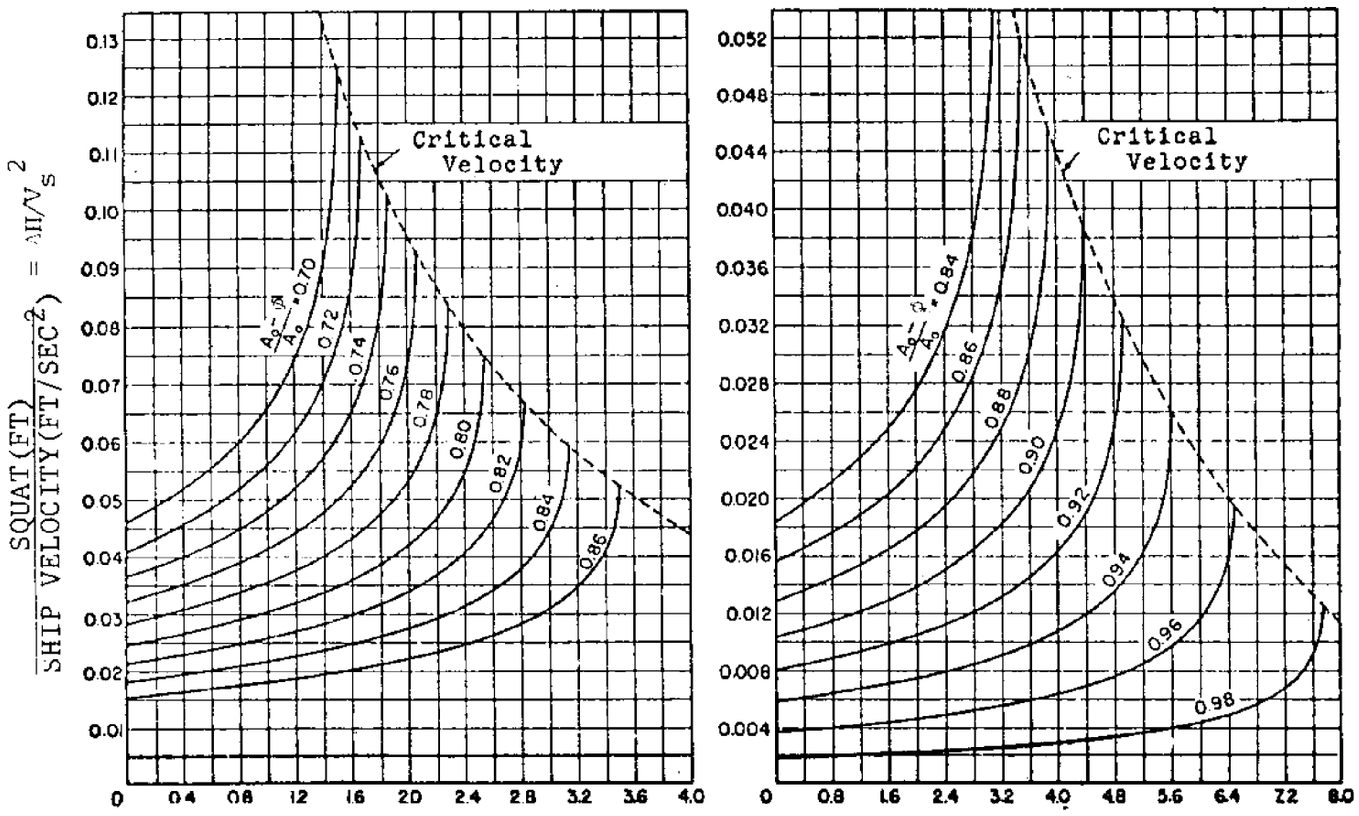

$$\frac{\text{SQUAT (FT)}}{\text{SHIP VELOCITY (FT/SEC}^2\text{)}} = \Delta H/V_s^2$$

$$\frac{\text{CHANNEL WIDTH BEFORE SQUAT (FT)} \times \text{SHIP VELOCITY (FT/SEC}^2\text{)}}{\text{CHANNEL CROSS-SECTIONAL AREA BEFORE SQUAT (FT}^2\text{)}} = W_0 V_s^2 / A_0$$

FIG. 11-CRITICAL VELOCITY (22)

Certain military vessels, both Navy and Coast Guard, may continue to increase velocity until the entire vessel is riding on the bow wave. This never occurs with commercial vessels. However, since the critical velocity like squat is a function of the cross-sectional area of the channel, and the velocity of the vessel, it is an additional aspect that must be taken into consideration in the design of a restricted waterway.

Ships in Passing and Off-Centerline Operation

When one vessel is overtaking another, or when a vessel is passing another from the opposite direction, larger amounts of squat are experienced due to the decrease in flow area caused by both vessel cross-sectional areas being at the same channel section at the same time. Since this occurrence is quite common, it must be accounted for in the design of a restricted waterway and has been included in the model.

When vessels are passing under normal conditions, they will each move off the centerline. As a vessel approaches the prism line of the channel, an additional sinking of the water surface occurs between the vessel and the near side of the channel. An attempt was made at DTMB (22) to determine the validity of using an approach similar to the one described above (utilizing the Bernoulli and continuity equations) to determine this additional squat. Additional

assumptions made were:

1. Flow divides proportionately; i.e.,

$$\frac{Q_1}{Q_2} = \frac{A_1}{A_2} \quad \ldots\ldots\ldots\ldots\ldots\ldots\ldots\ldots \quad (3)$$

where Q_1 and Q_2 are the rates of flow in Sections A_1 and A_2, the sections on each side of the centerline of the vessel.

2. Bernoulli's equation applies to both sections. This necessitates no cross-flow under the hull.

3. The change in level of the ship is the average of the change in the level of the two water surfaces on each side of the ship.

When computed values were compared with model tests, DTMB found that the calculated values were much greater than those actually observed. This seems to indicate a rather large lateral flow under the hull of the vessel. This, of course, violates Assumption 2 above. Figure 12 shows various water profiles of a ship operating off of the centerline. By comparing Section G=G and H-H, one can clearly see the difference in water surface elevation (22).

The computer model calculates the larger squat values due to the primary and secondary vessels being in a passing

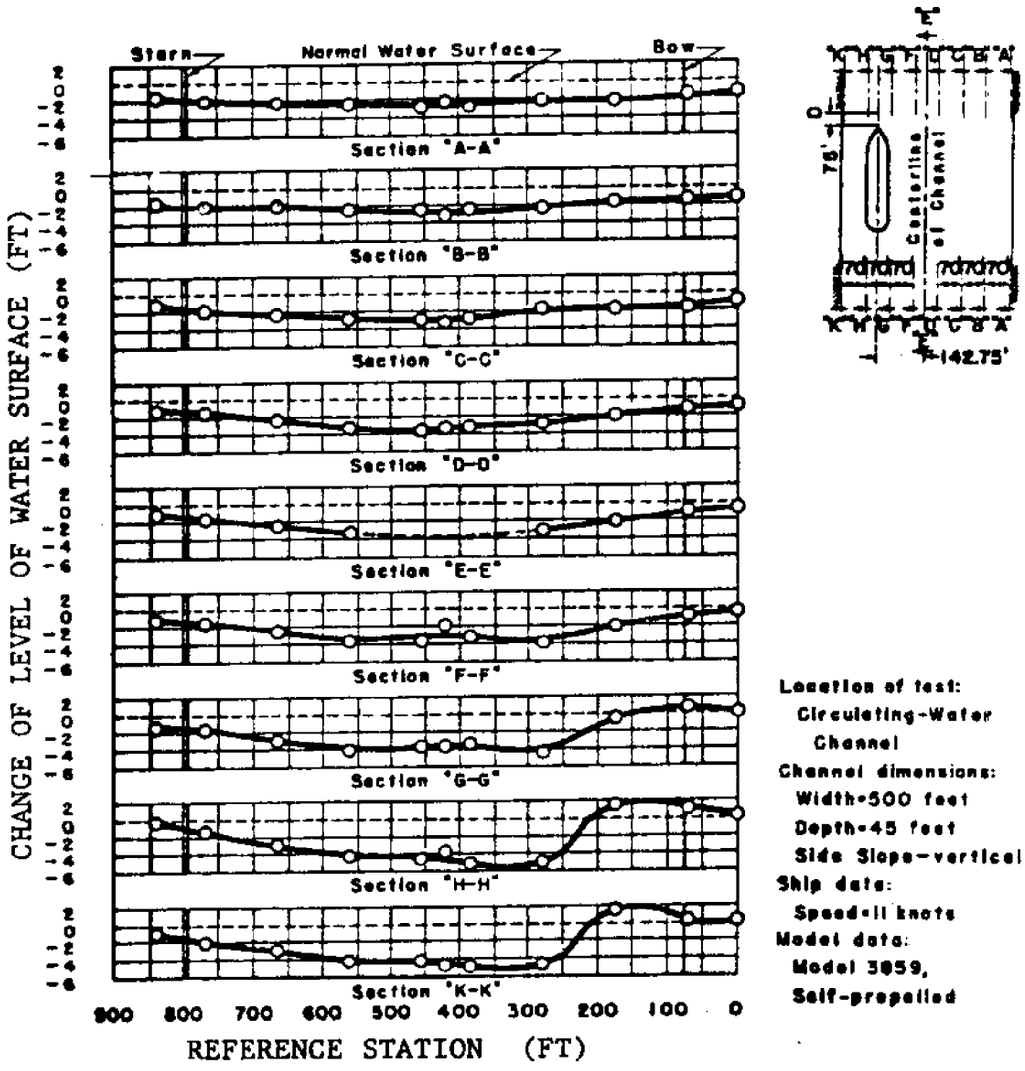

FIG. 12-WATER SURFACE PROFILE FOR A SHIP LOCATED OFF THE CENTERLINE OF A RESTRICTED CHANNEL (22)

or overtaking condition. However, it does not provide for the additional squat as the ships approach the channel prism line.

CHAPTER III

BOUNDARY LAYER CONDITIONS

The influence of viscosity is mainly confined to a thin layer close to an object moving through the fluid media. In this thin layer, the velocity goes from zero (no slip) at the object to its full value which corresponds to 99 percent of the external frictionless flow. This area of boundary shear influence is called the boundary layer. Fig. 13 shows a boundary layer for a flat plate in laminar flow without boundary separation (43).

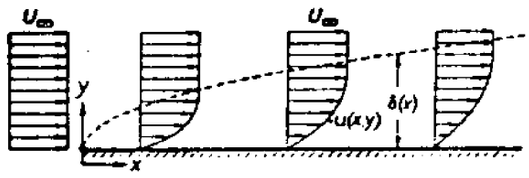

FIG. 13-SKETCH OF BOUNDARY LAYER ON A FLAT PLATE IN PARALLEL FLOW AT ZERO INCIDENCE (43)

A boundary layer is formed on the hull of a ship due to its velocity through the fluid media. A boundary layer is also formed on the channel due to the reverse flow at the midships as the vessel proceeds through a restricted waterway. Since these boundary layers tend to increase the effective cross-sectional area of the vessel and decrease the effective cross-sectional flow area of the channel, they should be taken into consideration in determining the squat of the vessel.

Although a vessel is not a flat plate, flat plate theory will be used to determine boundary layer values. The validity of this procedure will be shown later in this chapter.

Basic Theory

When a vessel moves through a real fluid, the fluid adheres to the ship. Frictional forces retard the motion of the fluid in a thin layer close to the ship called the boundary layer. Velocity of the fluid is zero at the ship and approaches the velocity of the external frictionless flow asymptotically (49). In the boundary layer the velocity gradient, $\frac{du}{dy}$, is very large. Also a small viscosity, μ, exerts an essential influence in so far as the shearing stress, $\tau=\mu \frac{\delta u}{\delta y}$, is concerned and τ may assume large values. Outside the boundary layer the viscosity is unimportant and the flow is essentially frictionless (43). This is an important concern in navigation channel design because it alters the virtual shape of the vessel (10).

A basic definition of the boundary layer, δ, is (see Figs. 13 and 14a):

$$\delta=y \text{ where } \frac{u}{U}=0.99 \quad . \quad . \quad . \quad . \quad . \quad . \quad . \quad . \quad . \quad . \quad (4)$$

A more important distance relative to the concern of this paper is the displacement thickness, δ_1. The displacement thickness indicates the distance by which the external streamlines are shifted outward due to the for-

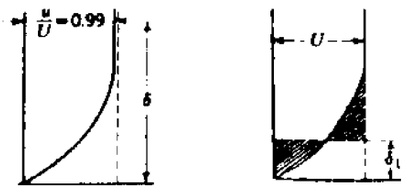

(a) (b)

FIG. 14-DEFINITIONS OF BOUNDARY LAYER THICKNESS (49)

mation of the boundary layer. It is defined by (see Fig. 14b):

$$U\delta_1 = \int_0^{\delta} (U-u)dy \quad \ldots\ldots\ldots\ldots\ldots\ldots\ldots (5)$$

where δ is the value of y where U=u. (U-u) is known as the velocity defect. δ_1 is the distance from the ship where the shaded areas in Fig. 14b are equal.

For laminar boundary layers the displacement thickness on a flat plate has been found to be (43, 49):

$$\delta_1 = \frac{1.7208X}{R_x^{1/2}} \quad \ldots\ldots\ldots\ldots\ldots (6)$$

where R_x is the local Reynolds number which depends on the distance, x, from the leading edge of the ship (plate) and the local free stream velocity, U_∞ (43, 49). The likelihood that a vessel boundary layer will be laminar is small (4), however, it has been included in the model along with appropriate switching based on Reynolds number. So far no vessel has been computed by the model to have a laminar

boundary layer. This is true because the speeds required for ship steerage are too high to allow this condition to occur for any significant distance. In fact, when making certain calculations to determine the usefulness of more complex methods of computing δ_1, the author found that the boundary layer became turbulent within inches of the bow.

As stated above, a vessel normally will have a turbulent boundary layer. The displacement thickness for this condition for a flat plate has been found to be (43, 49):

$$\delta_1 = \frac{.04625X}{R_x^{1/5}} \quad \ldots\ldots\ldots (7)$$

where the variables are as described above.

Flat plate theory used to derive Eqs. 6 and 7 above assumes a zero pressure gradient along the entire length of the plate. Although this is essentially true for the long parallel middle-body of a commercial vessel it is not true for the tapered portion of the fore-body due to entrance effects. In order to determine the magnitude of these entrance effects on δ_1 a typical computation using one of the more complex methods was performed.

Most of the methods used to calculate two-dimensional turbulent boundary layers are similar, using either momentum-

integral or energy-integral equations. Since, however, no general expressions for shear and dissipation in turbulent flow can be found by purely theoretical means, additional assumptions based on test measurements are needed. Consequently, the calculation of turbulent boundary layers is semi-empirical (43).

The method due to E. Truckenbrodt (43) was selected for use in determining the magnitude of the entrance effects. Appendix IV contains a detailed description of the method and the calculations. A channel 500 ft. wide and 45 ft. deep was used. The vessel selected had a length of 707.5 ft., a beam of 75 ft. and a draft of 40 ft. The fluid velocity was also corrected for channel restriction effects. All values such as bow shape, water temperature, salinity, etc. were selected as typical or average. Since most of the data were found or created in tabular form, a method of quadratures was used in the various integrations.

Some very interesting things surfaced during these calculations. It was found that at 10 knots the point of transition from laminar to turbulent flow occurs only about 3 inches from the stem (bow) of the vessel as shown below.

$$x = \frac{R\gamma}{U} = \frac{400{,}000(1.1342\times10^{-5})12}{10(1.68889)} = 3.2 \text{ in.} \quad \ldots\ldots\ldots \quad (8)$$

where: X = distance
R = Reynolds number at transition
γ = kinematic viscosity
U = velocity

Even when the velocity was decreased to steerage speed (5 knots), the transition point was only about 6 inches back from the stem.

Information concerning typical or specific pressure gradients or velocity profiles at the bow of a ship are not readily available. However, some data were found in Saunders (42).

The most significant outcome of the comparison of the complex method (Truckenbrodt) and the simple flat plate method (Eq. 7) was that the entrance effects at the bow on displacement thickness amounted to only 45/1000 of a foot. This is in agreement with Phillips' statement that the entrance effects were known to be negligible and were not considered in certain ship design computations; i.e., the placement of pitot tube type velocity meters, etc. (41). This is also in agreement with Kline (29) where it is stated that, "because of the necessarily approximate turbulent shear stress, only marginal gains result from the more complex integration methods of computation. Also, the mixed length

hypothesis which has been used with the fixed values of the relevant constants, gives predictions of the hydrodynamic properties of a specified boundary layer which are as reliable as experimental data. It is therefore not worth trying to improve the choice of constants." When one considers the outcome of the method comparison, the findings of others, the lack of detailed information concerning the design vessel and the good results obtained from flat plate theory as shown in Fig. 10(b) one must conclude that Eq. 7 is adequate to compute the displacement thickness used in determining squat values.

The same method is used for computing the displacement thickness on the channel. Since the local velocity is caused mainly by the back flow due to the squat phenomenon, x-distances are measured from the stem of the vessel.

In determining values of R_x in Eq. 7, an accurate method of selecting values of kinematic viscosity, γ, was required. These values of γ had to be correct for varying water density and temperature. Through a method of table look-up and interpolation the model will determine the kinematic viscosity to five-place accuracy when given the water temperature and density (see Fig. 15).

The local velocity used in determining R_x includes the

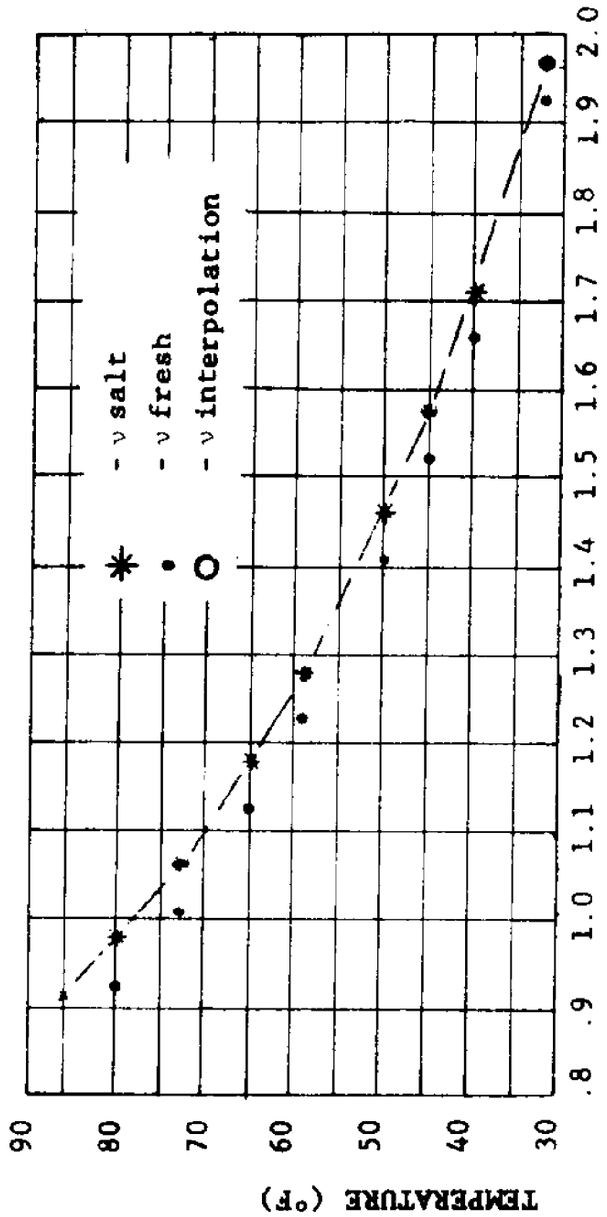

FIG. 15-INTERPOLATED KINEMATIC VISCOSITY

backflow velocity due to the squat phenomenon described in Chapter II and the correct component of water current when computing the channel displacement thickness and the ship velocity and the current component when computing the displacement thickness of the vessel.

CHAPTER IV

BANK SUCTION

Description of Problem

When a ship moves through the water, fluid is displaced at the bow and transported back around the hull to fill the void behind the stern. Flow-produced lateral pressures are balanced when the ship is proceeding in open water or on the centerline of a symmetrical channel. However, when the ship is moving parallel to, but off of, the channel centerline the forces produced are asymmetrical, resulting in a yawing moment. This yawing moment is produced by the building of a wave system between the bow of the ship and the near channel bank. Behind this bow wave, the elevation of the water between the vessel and the near bank is less than between the vessel and the centerline of the channel with a force being produced tending to move the stern toward the near bank (Fig. 16). The resulting force of the system is behind the center of gravity (CG) of the vessel (Fig. 17). These same phenomena occur when a vessel moves off of the neutral steering line (NSL) of an asymmetrical channel which will be described in detail below. This effect is called bank suction and increases directly with the distance that the vessel sailing line is from the centerline (or NSL) of the channel. A similar effect is noted between ships in either passing or overtaking maneuvers. Bank suction can be rather

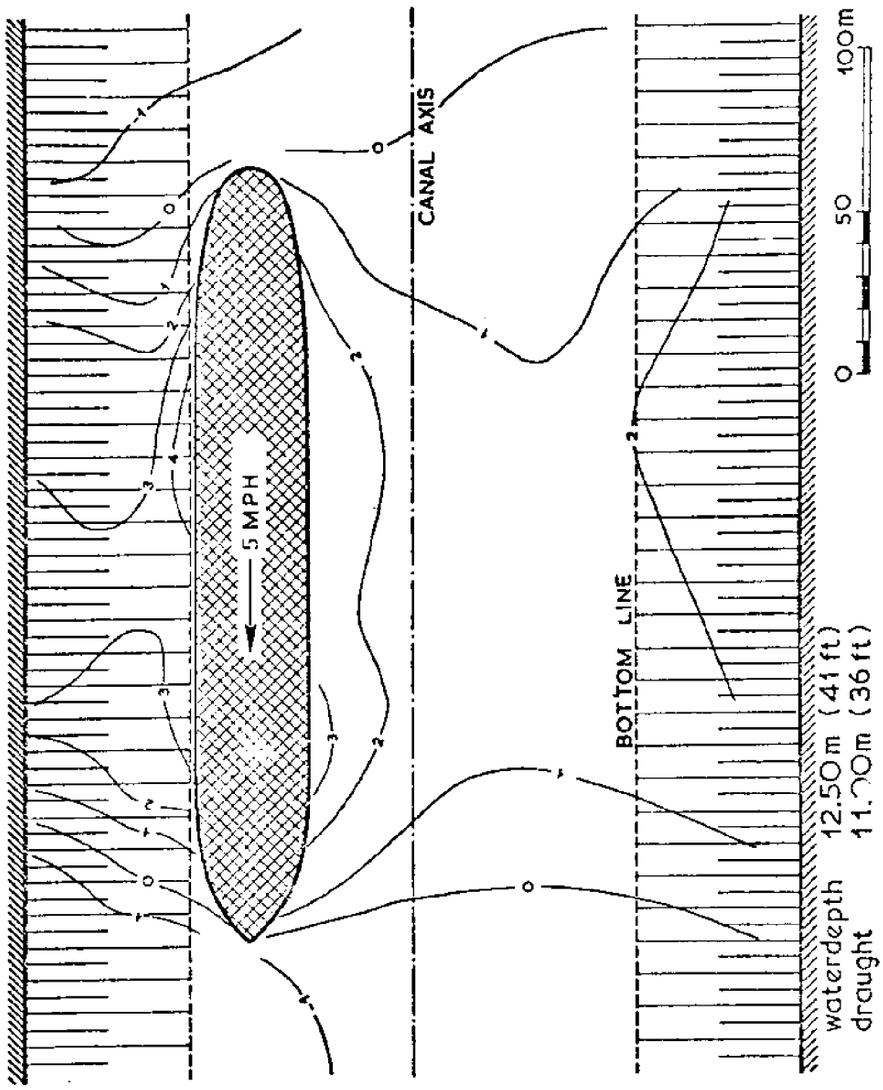

FIG. 16 LINES OF EQUAL WATER LEVEL DROP (10^{-1}m) (30)

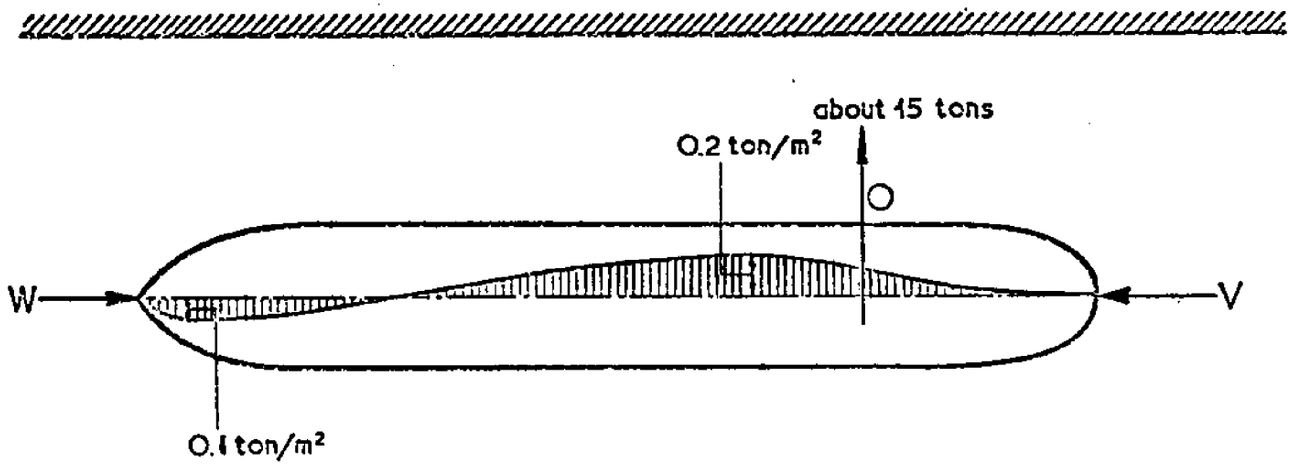

Hydrostatic pressure differences derived from Fig. 16

O=resulting suction force W=resistance V=propulsion force

FIG. 17-DIAGRAM OF TYPICAL BANK SUCTION FORCES (30)

sudden and quite severe and has been the cause of many groundings and other accidents (16, 22, 30, 44, 51).

Operational Procedures

The yawing moment caused by bank suction can be overcome by use of right rudder. This alone, however, will not prevent the gradual translation of the vessel toward the near bank. A drift angle in the direction of the centerline (or NSL) of the channel will have to be applied to overcome the lateral force and achieve an equilibrium condition. The vessel may then proceed on a sailing line off of, but parallel to, the centerline (or NSL) of the channel in a canted position. In model tests, rudder angles in excess of thirty degrees with drift angles in excess of seven degrees have been recorded (22). These maximum model test rudder angles agree with those reported by channel pilots. However, the pilots stated that drift angles in excess of twelve degrees have been experienced (11, 40).

Additional rudder control can be achieved by temporarily increasing the speed of the ship's propeller so that water velocity in the vicinity of the rudder is increased while the speed of the vessel is not changed materially (22, 30). It appears from model and prototype tests that smaller draft vessels require smaller rudder angles to obtain equilibrium. This reinforces the theory that a lateral flow under the keel of the vessel tends to aid in the filling of the de-

pression in the water surface between the vessel and the near bank (22, 30).

Determination of Forces and Moments

Schoenherr (DTMB) derived several dimensionless coefficients and force and moment determination curves (44) from model test data (22). These tests were made on full-line merchant ship hulls in symmetrical channels. The measurements were taken when the model ships were positioned parallel to the channel centerline; i.e., not in an equilibrium position. Both vessel drift angle and rudder angle were zero. These tests also indicated that bank suction effects were not greatly affected by propeller action. The procedures presented could be used to predict bank suction effects for both single and multi-screw merchant ships of relatively full form (44).

The three dimensionless coefficients derived were (44):

$$C_F = \frac{F}{\rho/2(Ld)V^2} \quad \ldots\ldots\ldots\ldots\ldots\ldots (9)$$

Where:
- C_F = dimensionless coefficient
- F = lateral bank suction force in pounds
- ρ = fluid density in slugs per cubic foot
- L = ship length in feet
- d = ship draft in feet
- V = ship velocity relative to undisturbed water in feet per second

$$\bar{X} = \frac{M}{FL} \quad \ldots\ldots\ldots\ldots\ldots\ldots\ldots\ldots\ldots\ldots (10)$$

Where: $\bar{X}$ = dimensionless coefficient
M = yawing moment in pound-feet

$$\alpha = \frac{C_F \text{ for given } H/d}{C_F \text{ for } H/d=1.40} \quad \ldots\ldots\ldots\ldots\ldots\ldots (11)$$

Where: H = channel depth in feet

The distance from the centerline, y, was expressed as a fraction of the vessel beam, B, and plotted against the dimensionless coefficient C_F for various values of W/B where W is the channel width in feet (Fig. 18).

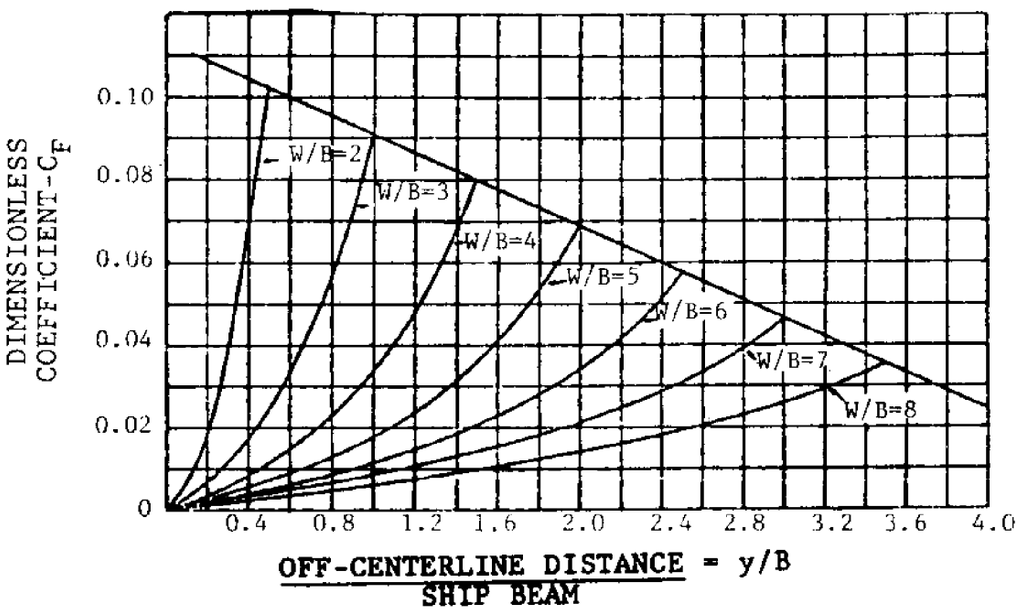

FIG. 18-CROSS-FAIRED VALUES OF C_F FOR H/d =1.40 AND VARYING W/B (44)

Values of $\bar{X}$ and α were plotted against values of H/d (Fig. 19).

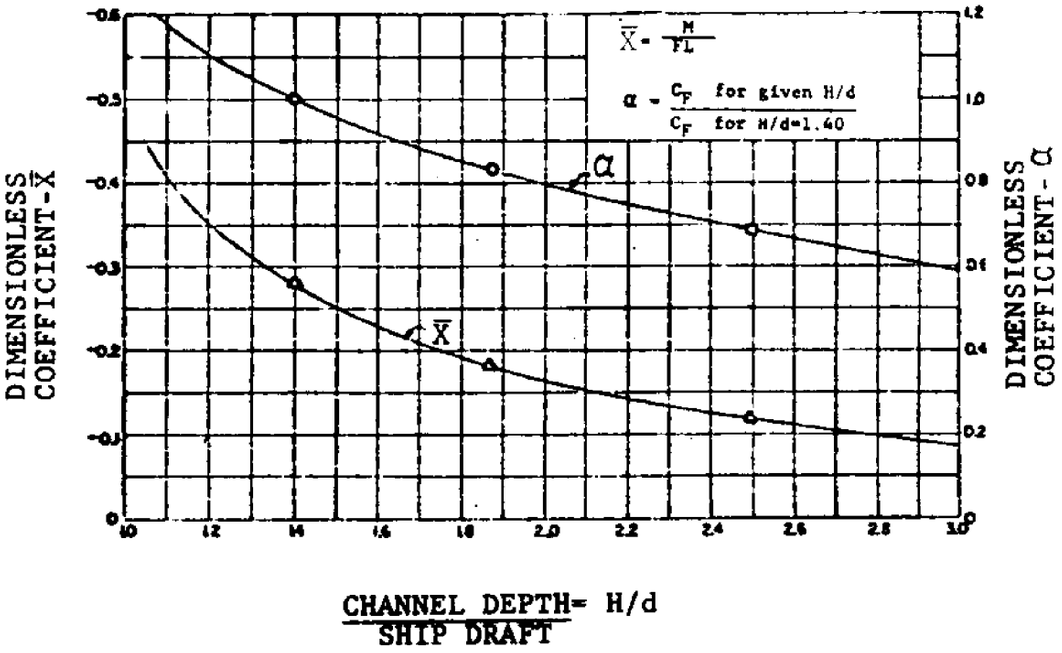

FIG. 19-VARIATION OF $\bar{X}$ AND α WITH H/d (44)

The general procedure for determining the values of the lateral force and turning moment due to bank suction is to calculate y/B, W/B and H/d for the problem to be solved. One would then enter Fig. 18 with W/B and y/B to find C_F. Then enter Fig. 19 with H/d to find $\bar{X}$ and α. The dimensionless coefficient α is to adjust for H/d values other than 1.40. One could then detemine the desired values from the following:

$$F = \frac{\rho}{2} C_F LdV^2 \alpha \quad \ldots\ldots\ldots\ldots\ldots\ldots\ldots\ldots (12)$$

$$M = \bar{X}LF \quad \ldots\ldots\ldots\ldots\ldots\ldots\ldots\ldots\ldots\ldots (13)$$

The channel design model uses the same basic procedure. Using a multiple linear regression method, 3rd-degree polynomial expressions were derived for each curve in Figs. 18 and 19 from the basic physical model test data. This provides values of the lateral force and turning moment for a symmetric channel. Figs. 20 and 21 show a comparison between measured and computed values of lateral force and turning moment respectively (see Table 3 for dimensions of Model 3859).

Asymmetric Channels

The ability to determine bank suction effects for symmetrical channels is very useful in basic navigation channel design, however, it does not reflect real world conditions very well. Because of methods of channel construction and contract payment, advanced maintenance dredging, and shoaling due to littoral drift and vessel operation, navigation channels are never completely symmetrical.

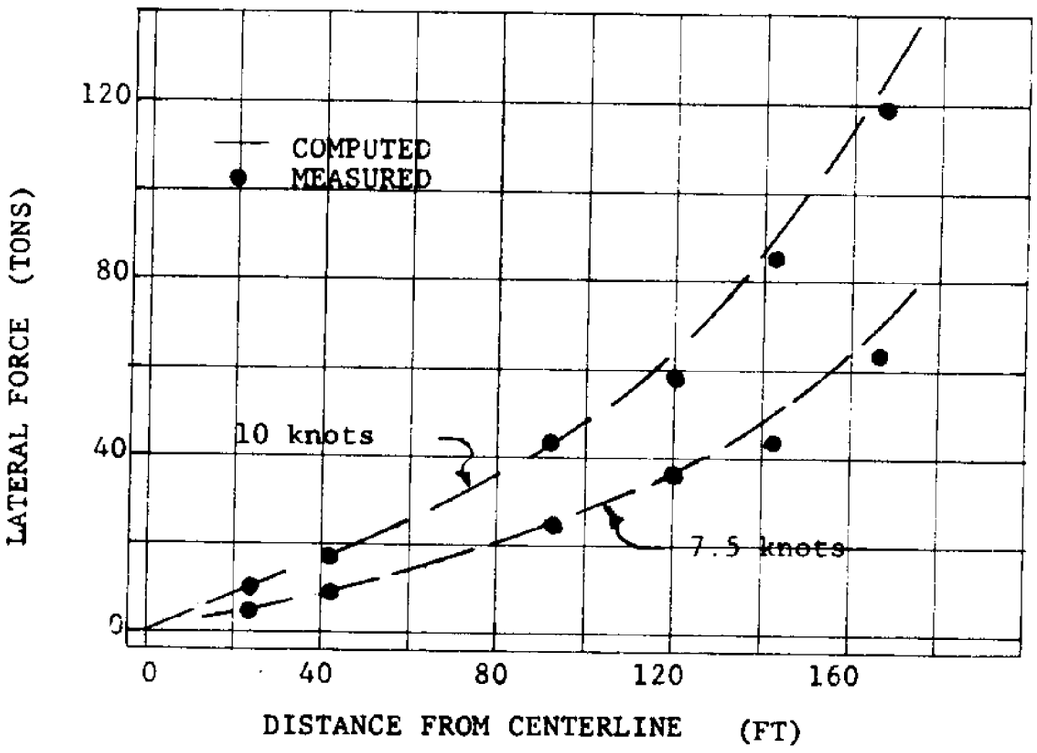

The data are for zero drift angle and zero rudder angle. Channel width 500 ft. depth 60 ft.

FIG. 20 -COMPARISON OF MEASURED AND COMPUTED LATERAL FORCES IN A SYMMETRICAL CHANNEL-MODEL 3859 (22)

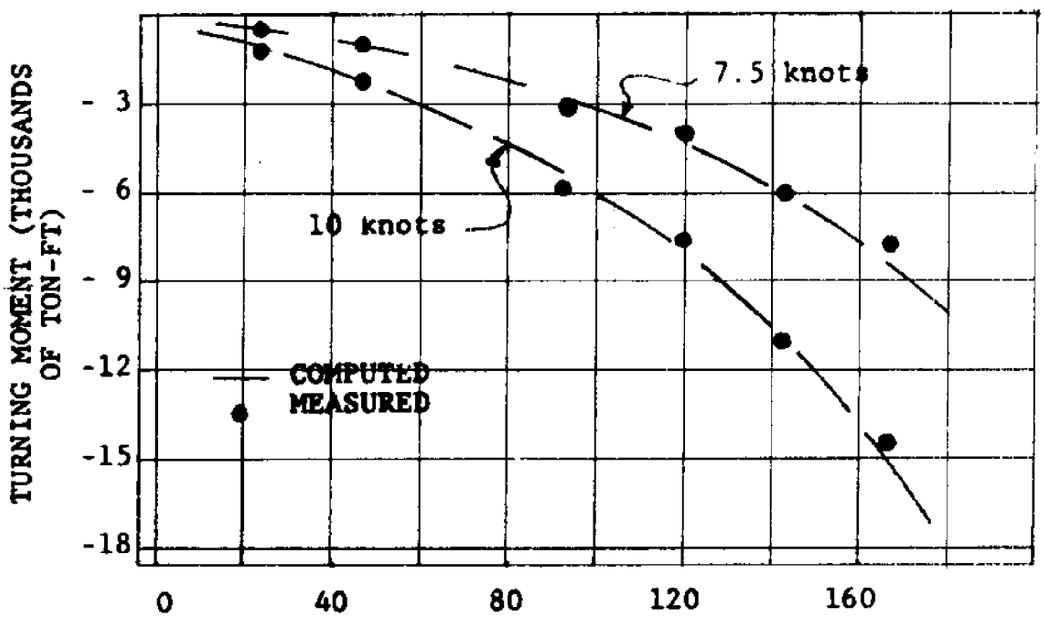

The data are for zero drift angle and zero rudder angle. Channel width 500 ft. depth 60 ft.

FIG. 21-COMPARISON OF MEASURED AND COMPUTED TURNING MOMENTS IN A SYMMETRICAL CHANNEL-MODEL 3859 (22)

When a channel is asymmetric, several important changes occur. First, the neutral steering line (NSL); i.e., the position where all lateral forces due to bank suction are counterbalanced and the yawing moment is zero, is no longer along the centerline of the channel. It will be shifted in the direction of the deeper or larger portion of the channel. Moody (37) in his tests discovered that the neutral steering line would be established along a line where the hydraulic radii on both sides of the line are equal. It can also be shown that the hydraulic radii will equal the hydraulic radius of the entire section. In asymmetrical channels, the y distance used in determining bank suction effects must be measured from this NSL and not the section centerline.

The channel design model determines if the channel is asymmetric from computed values of the hydraulic radii for the right side, left side and total channel. If the channel is asymmetric, the model will increment from the centerline in the direction of the greater hydraulic radius until a balance has been achieved. The NSL is located to an accuracy of 0.1 foot. The model also computes an effective W for the smaller side of the asymmetric channel in order to obtain good agreement with test data. This adjustment was not required for the larger side of the channel.

Due to irregularities in the bottom of most channels,

there is generally no one physical depth which can be used in the H/d ratio. For this reason the hydraulic depth, D, is computed and used.

$$D = A/W \quad \ldots\ldots\ldots\ldots\ldots\ldots\ldots\ldots\ldots\ldots (14)$$

Where: A = Area of channel in square feet

Figs. 22 through 31 show that the adjustments made for asymmetrical channels give results that agree very well with test data. It is believed that the original curve representing the test data in Fig. 31 (page 61) has been drawn incorrectly as the point of zero turning moment should be at the neutral steering line and not at the channel centerline.

A description of the model ships used in the testing (22, 37) is shown in terms of full size dimensions in Table 3.

TABLE 3. -TEST MODEL SHIP DIMENSIONS

SHIP	DRAFT (FT)	BEAM (FT)	LENGTH (FT)
3859	32.1	100.0	720.6
A	37.0	102.0	705.0
B	31.7	89.2	624.1
C	34.2	87.1	602.5
D	29.4	79.9	539.3

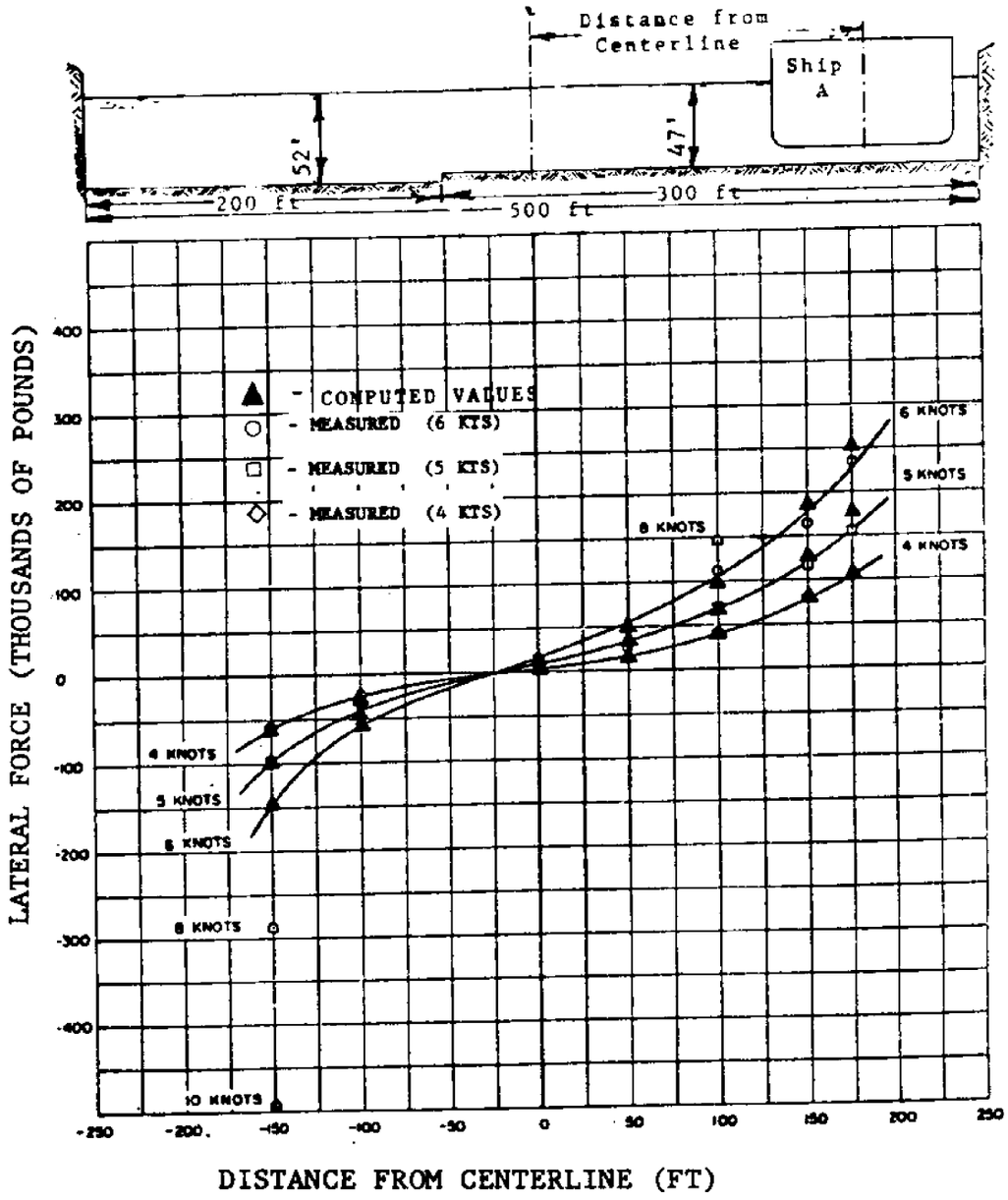

The data are for zero drift angle and zero rudder angle.

FIG. 22-LATERAL FORCES IN ASYMMETRICAL CHANNEL FOR SHIP A-(WATER SURFACE REFERENCE ELEV. 0.0 FT) (37)

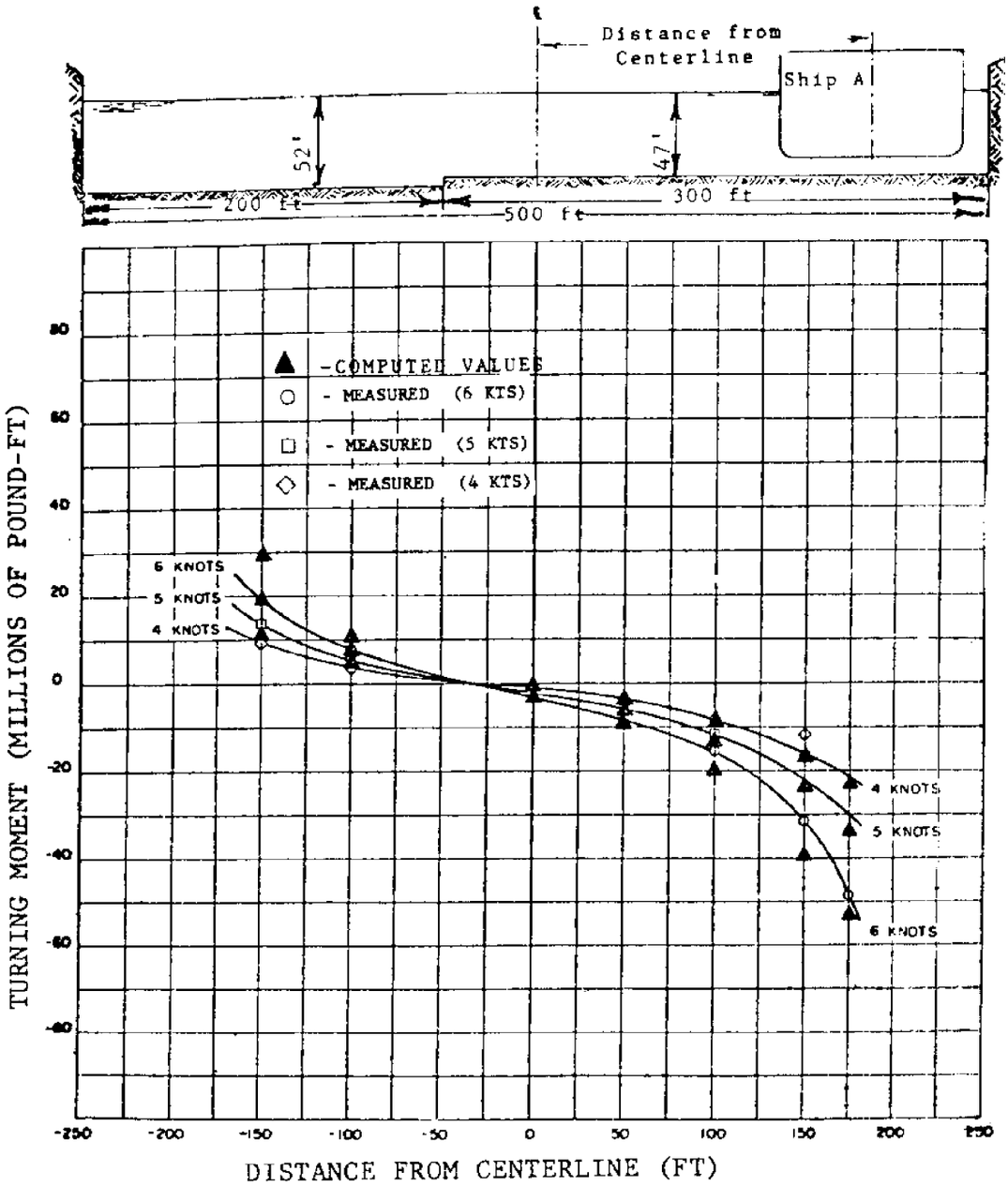

The data are for zero drift angle and zero rudder angle.

FIG. 23-TURNING MOMENTS IN ASYMMETRICAL CHANNEL FOR SHIP A-(WATER SURFACE REFERENCE ELEV. 0.0 FT.) (37)

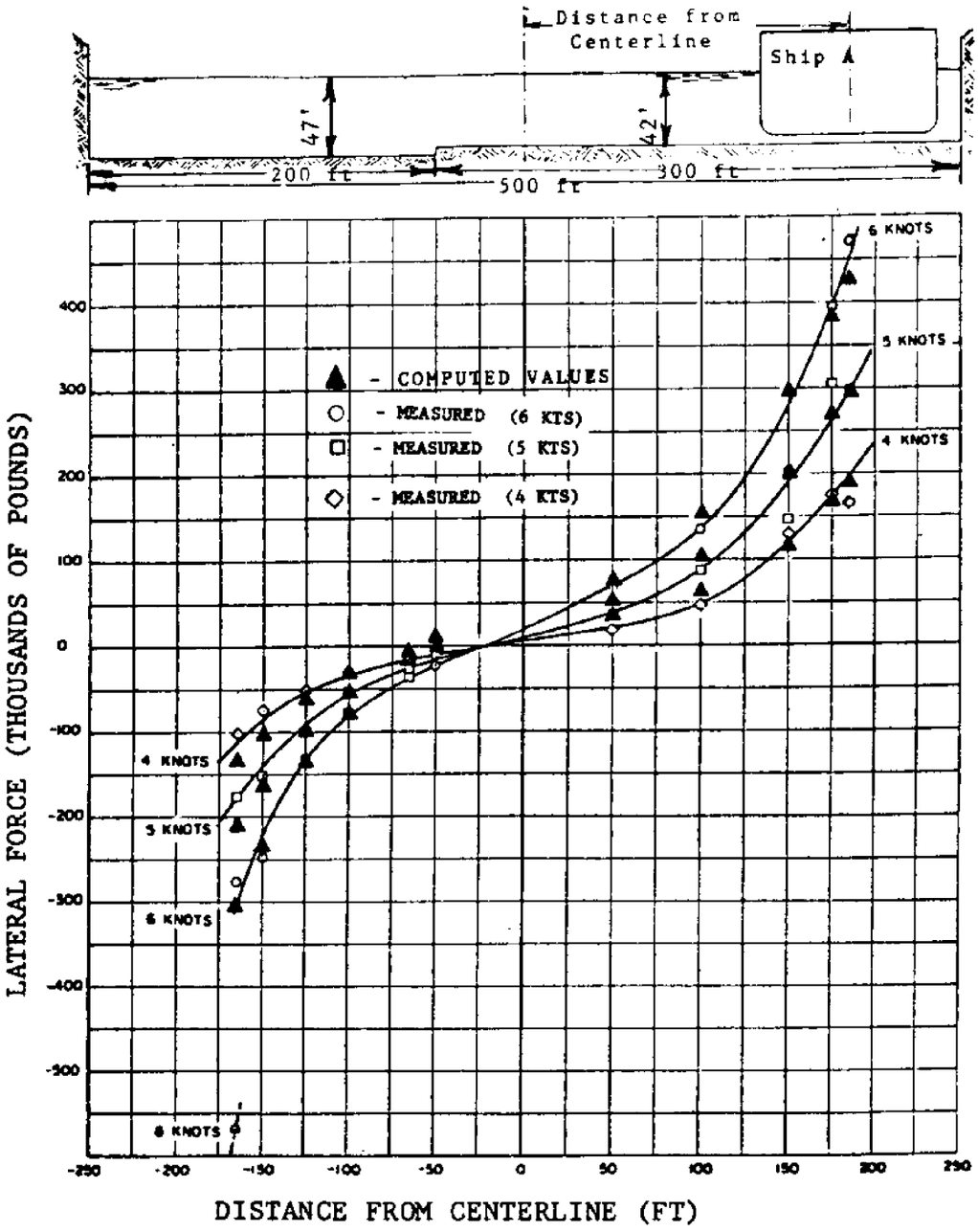

The data are for zero drift angle and zero rudder angle.

FIG. 24-LATERAL FORCE IN ASYMMETRICAL CHANNEL FOR SHIP A-(WATER SURFACE REFERENCE ELEV. -5.0 FT)(37)

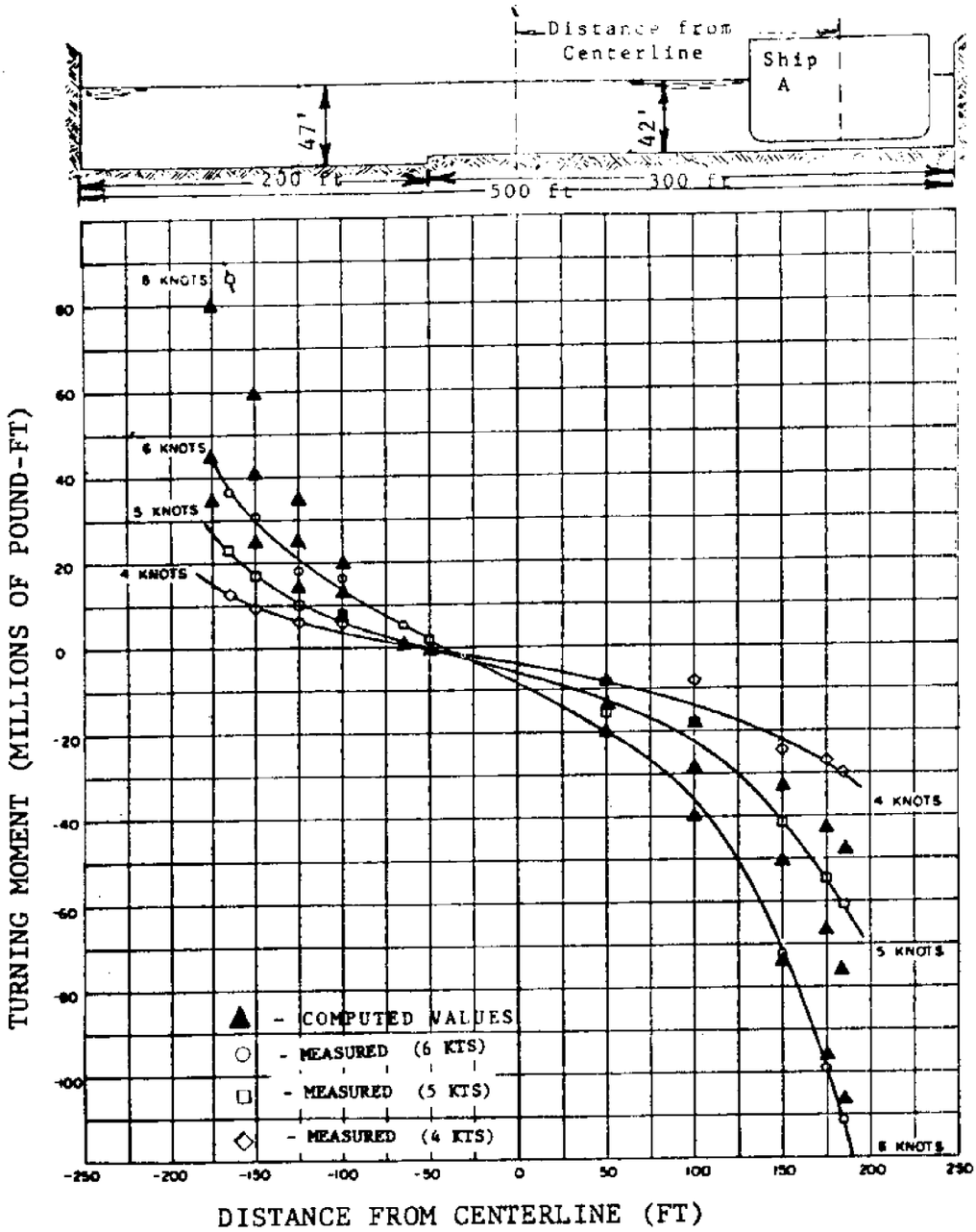

The data are for zero drift angle and zero rudder angle.

FIG. 25-TURNING MOMENTS IN ASYMMETRICAL CHANNEL FOR SHIP A-(WATER SURFACE REFERENCE ELEV. -5.0 FT.)(37)

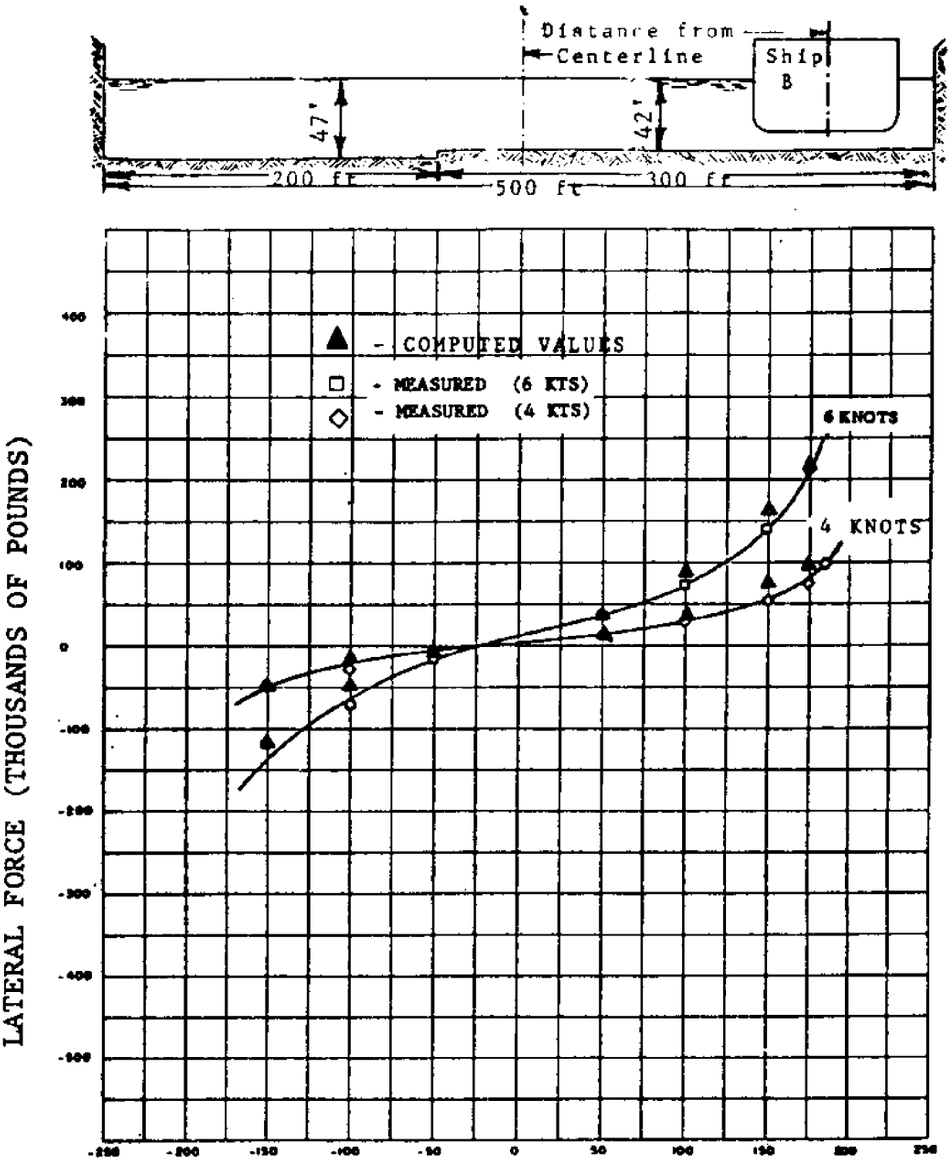

The data are for zero drift angle and zero rudder angle.

FIG. 26-LATERAL FORCES IN ASYMMETRICAL CHANNEL FOR SHIP B-(WATER SURFACE REFERENCE ELEV.-5.0 FT)(37)

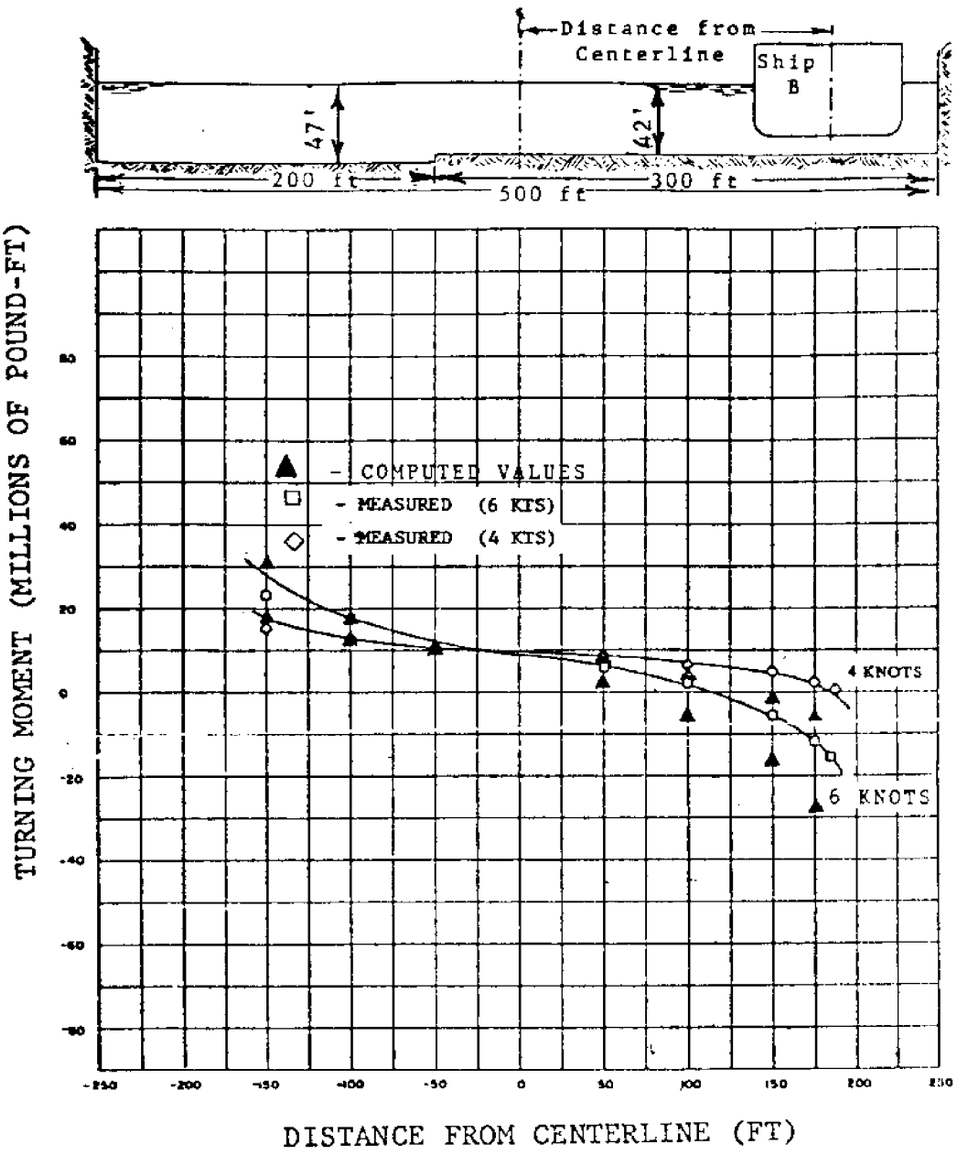

The data are for zero drift angle and zero rudder angle.

FIG. 27-TURNING MOMENTS IN ASYMMETRICAL CHANNEL FOR SHIP B-(WATER SURFACE REFERENCE ELEV. -5.0 FT) (37)

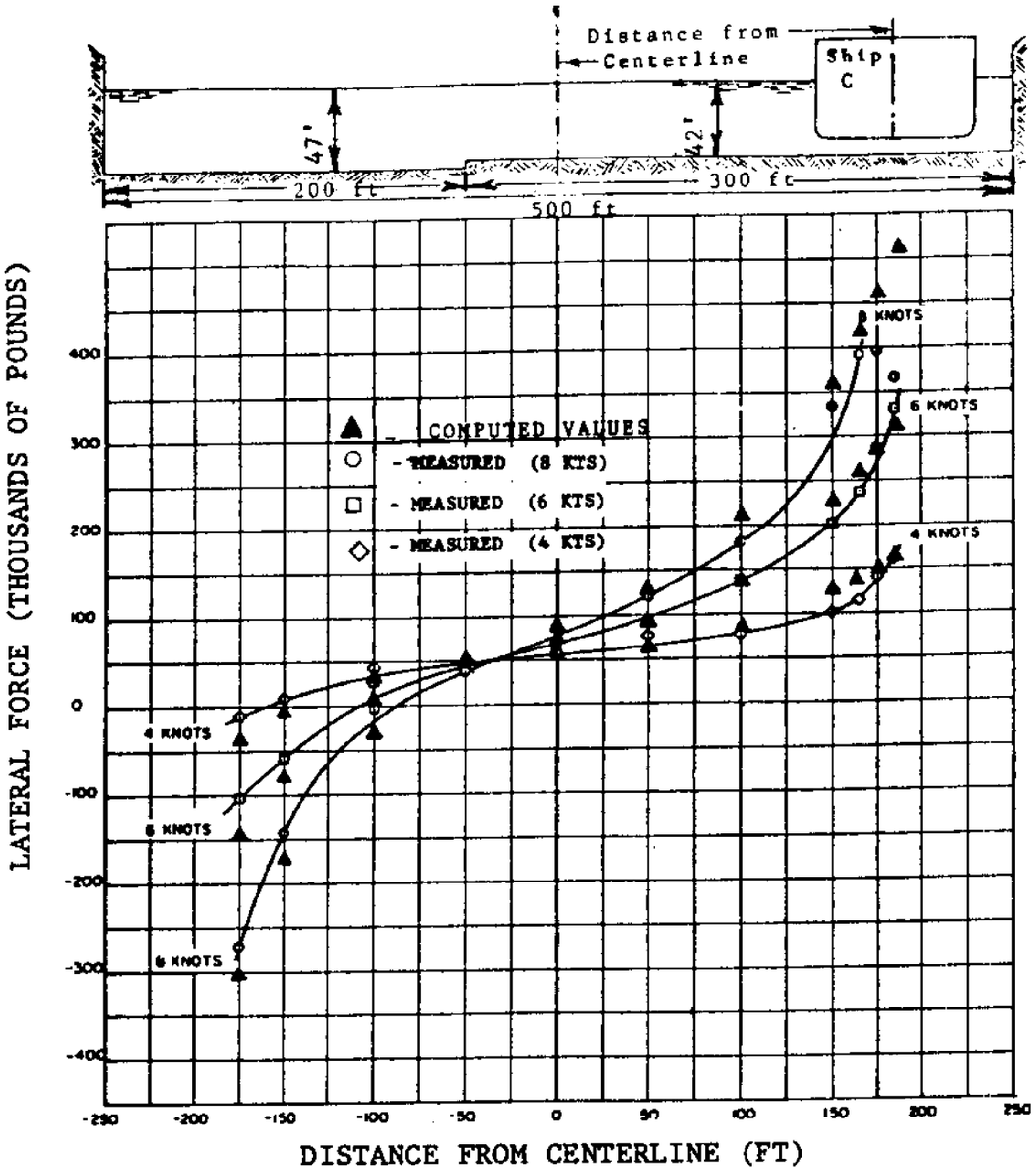

The data are for zero drift angle and zero rudder angle.

FIG. 28-LATERAL FORCES IN ASYMMETRICAL CHANNEL FOR SHIP C-(WATER SURFACE REFERENCE ELEV. -5.0 FT)(37)

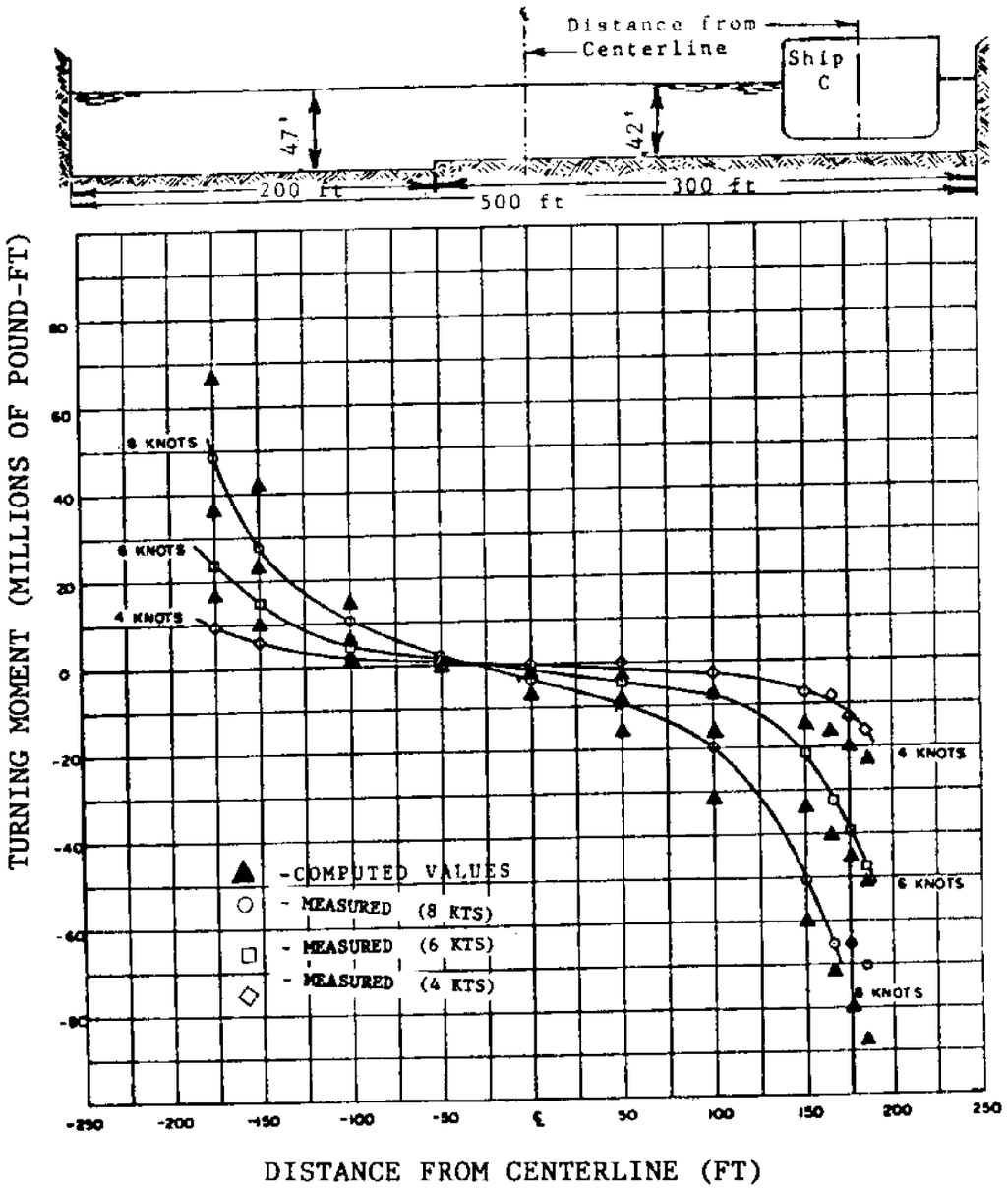

The data are for zero drift angle and zero rudder angle.

FIG. 29-TURNING MOMENTS IN ASYMMETRICAL CHANNEL FOR SHIP C-(WATER SURFACE REFERENCE ELEV.-5.0 FT)(37)

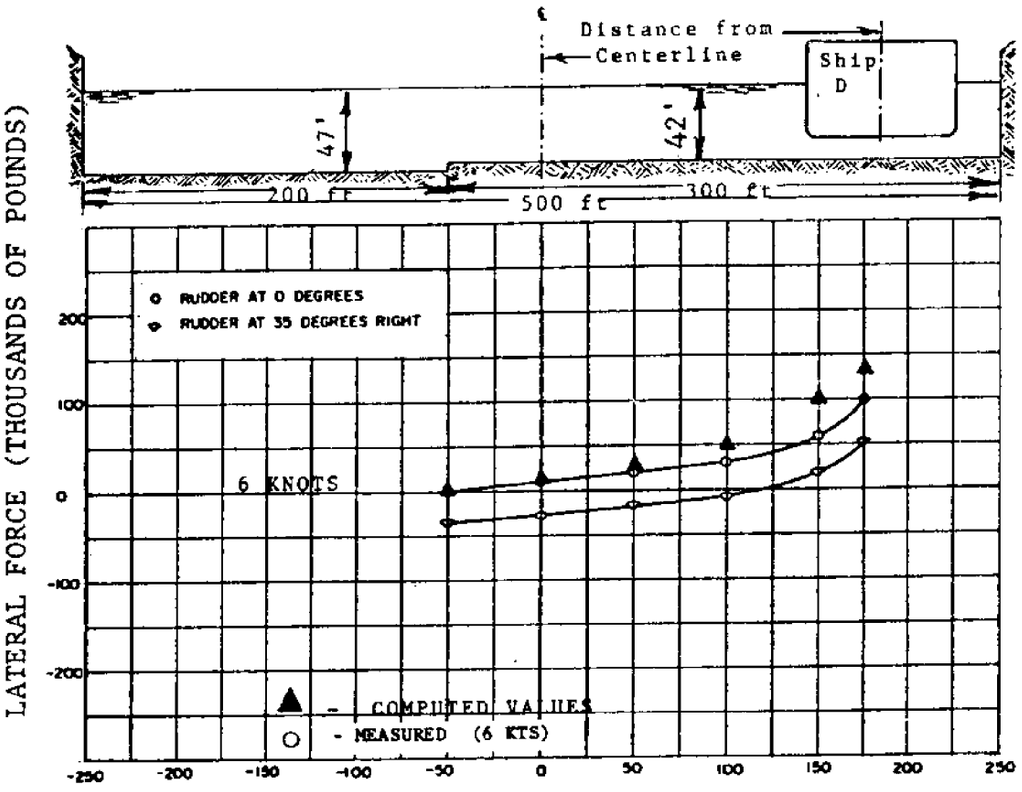

The data are for zero drift angle and zero rudder angle.

FIG. 30-LATERAL FORCES IN ASYMMETRICAL CHANNEL FOR SHIP D-(WATER SURFACE REFERENCE ELEV.-5.0 FT)(37)

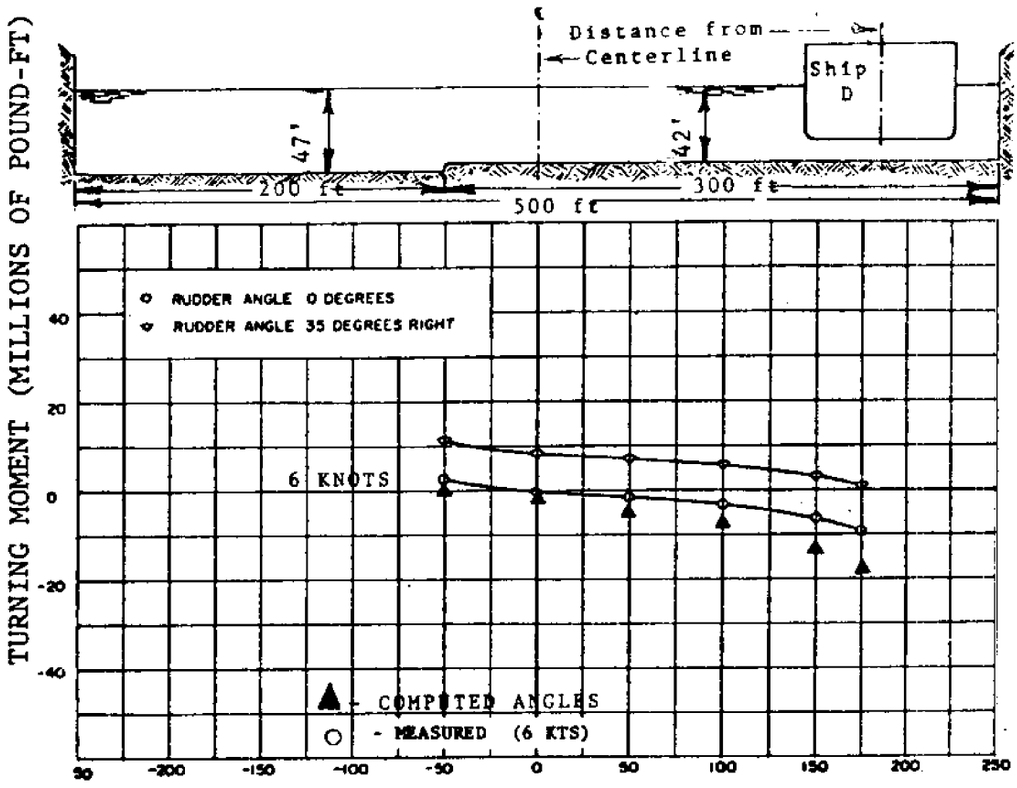

The data are for zero drift angle and zero rudder angle.

FIG. 31-TURNING MOMENTS IN ASYMMETRICAL CHANNEL FOR SHIP D-(WATER SURFACE REFERENCE ELEV.-5 FT)(37)

As stated above, asymmetric channels are most common when dealing with real ground lines as opposed to design templates. When actual field data was used, the design model found that the NSL shift from as little as a few feet to over one hundred feet from the channel centerline. Pilot reports of ship behavior in the vicinity of these channel sections is in agreement with computed model results (11).

There is a possibility, where the section is unusual; i.e., at channel entrances where section is asymmetric but almost all open water, that no NSL will be found within the channel limits. The model will print a warning message should this occur.

Open Channels

In open channels the water flowing from the over-bank areas tends to fill the void or low water surface area between the vessel and the near bank. Any computed values of lateral force and turning moment for this type channel must be reduced for this reason. Norrbin (39) found this reduction factor to be:

$$RF = e^{-2\frac{H_1}{H-H_1}} \quad \ldots\ldots\ldots\ldots\ldots\ldots \quad (15)$$

Where:
- RF = reduction factor
- H_1 = depth of water over the near bank in feet
- H = depth of water in channel in feet

He also found that when the bank height divided by the water depth (H_1/H) is less than 0.4 that the effects of bank suction are negligible. These factors have also been included in the channel design model.

CHAPTER V

VESSEL ATTITUDE

Description of Problem

The forces and moments due to bank suction discussed in Chapter IV must be neutralized by correct application of vessel drift and rudder angle to establish and maintain an equilibrium position to one side of the channel centerline or neutral steering line (NSL). The same type of attitude control is required when the vessel is encountering beam winds and/or currents.

The natural response of a vessel to bank suction forces and moments is to decrease their effects. The vessel with zero rudder angle will turn toward the centerline (or NSL) of the channel. The pilot, however, must not be too eager to take advantage of this reaction. In fact, the ship tends to assume an angular velocity which the rudder might be unable to neutralize (7).

Cargo vessels generally have a more awkward shape which adversely influences their steering. Tankers, which can be classified as big cargo ships, are noted for their bad steerability, especially in shallow water (16). One reason for this is that the bulky hull tends to mask the rudder (6).

Cargo vessel response to rudder control is very sluggish. To help overcome this, exaggerated rudder swing is given causing a larger than required rudder moment. Once the vessel begins to respond, counter rudder, also exaggerated, is applied. This technique is called "strutting" by North Sea channel pilots (16).

Basic Theory

Both Brard (7) and Bindel (6) describe the work done at the Paris Model Basin in the control of vessel attitude. However, Bindel's paper being later (1960) gives more test results and is therefore of greater interest.

A ship hull behaves like a vertical airplane wing, but the span of this wing (ship draft) is very small and the approximations of classical aerodynamics such as coefficients of lift, etc., are no longer valid (6, 7). In order to determine the effects of drift and rudder angle in producing turning moments and lateral forces, two dimensionless coefficients were formulated (6).

$$C_Y = \frac{Y}{\pi \rho S V^2 T/L} \qquad (16)$$

Where: C_Y=Lateral force coefficient
Y=Lateral force
ρ=Water density
S=Total longitudinal area (including rudder area)
V=Speed of center of gravity (G)
T=Ship draft
L=Ship length

$$C_N = \frac{N}{\frac{1}{2}\pi\rho STV^2} \quad \ldots\ldots\ldots\ldots\ldots\ldots\ldots\ldots \quad (17)$$

Where: C_N = Yawing moment coefficient

N = Yawing moment

Through model tests of cargo vessels the following expressions were formulated for the determination of C_Y and C_N along a straight course (6).

$$C_Y = .71\delta + 10.0\delta^3 - .06a - 4.0a\delta^2 + a^2\delta \quad \ldots\ldots \quad (18)$$

Where: δ = Vessel drift angle in radians

a = Rudder angle in radians

$$C_N = .83\delta - 1.95\delta^3 + .053a + 2.5a\delta^2 - .5a^2\delta \quad \ldots\ldots \quad (19)$$

Sign conventions are as shown in Fig. 32.

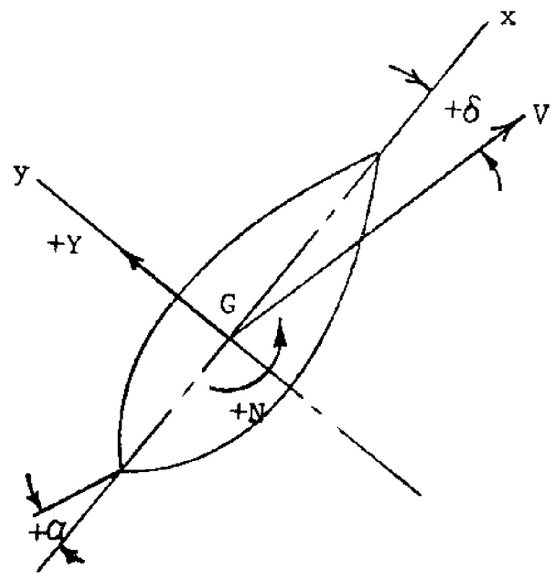

FIG. 32-SIGN CONVENTIONS FOR VESSEL ATTITUDE COMPUTATIONS (6)

In order to determine the magnitude of the lateral force and yawing moment produced by a given drift angle and rudder angle one would determine values of C_Y and C_N from Eqs. 18 and 19. Then by solving Eq. 16 for Y:

$$Y = C_Y \pi \rho \, SV^2 \, T/L \quad \ldots\ldots\ldots\ldots\ldots\ldots\ldots\ldots\ldots (20)$$

and solving Eq. 17 for N:

$$N = C_N \frac{\pi}{2} \rho \, STV^2 \quad \ldots\ldots\ldots\ldots\ldots\ldots\ldots\ldots\ldots\ldots (21)$$

and substituting the correct values in Eqs. 20 and 21, the magnitude and direction of the required force and moment can be found.

The Paris Model Basin, in determining the coefficients in Eqs. 18 and 19, ran tests with the drift angle varied from -10 degrees to +10 degrees and rudder angle from -5 degrees to +25 degrees using models 2.5 meters in length, scale 1/66. Other scales used ranged up to 1/20. It was Bindel's opinion that the scale effects for transverse forces and moments were small and that the model results were applicable to full-size ships (6).

Determination of Equilibrium Attitude

When a vessel is under the influence of bank suction effects or forces due to cross-winds or currents, the normal procedure is to neutralize the yawing moments with rudder control and the lateral forces with drift angle.

The Paris Model Basin studies were made on the centerline of the channel and some adjustment must be made for off-centerline operation. When a vessel moves off the centerline of a channel toward a bank there is a marked increase in fluid velocity between the vessel and the near bank that can be partially explained by Bernoulli effects and continuity. The exact change in velocity cannot be defined because the suspected tranverse flow under the keel of the vessel is unknown. It is this velocity increase

that must be adjusted.

A plot of dimensionless values was made to determine this adjusting coefficient (Fig. 33). One can see from Fig. 33 that the plotted points of both force and moment increase from a value of 1.0 at the centerline (NSL) of the channel in a linear form as the ratio of the off-centerline distance (y) to the half channel width (.5W) increases. This is what one would intuitively suspect. When the equation of the line was determined using a regression-type analysis, the linear fit was by far the most significant, having both "t" and "F" statistics above the 99 percent confidence level. This coefficient, C_V, is applied to attitude control produced forces and moments determined by Eqs. 20 and 21. C_V is computed by:

$$C_V = 1.0 + 2.3974101y/.5W. \quad \ldots \quad (22)$$

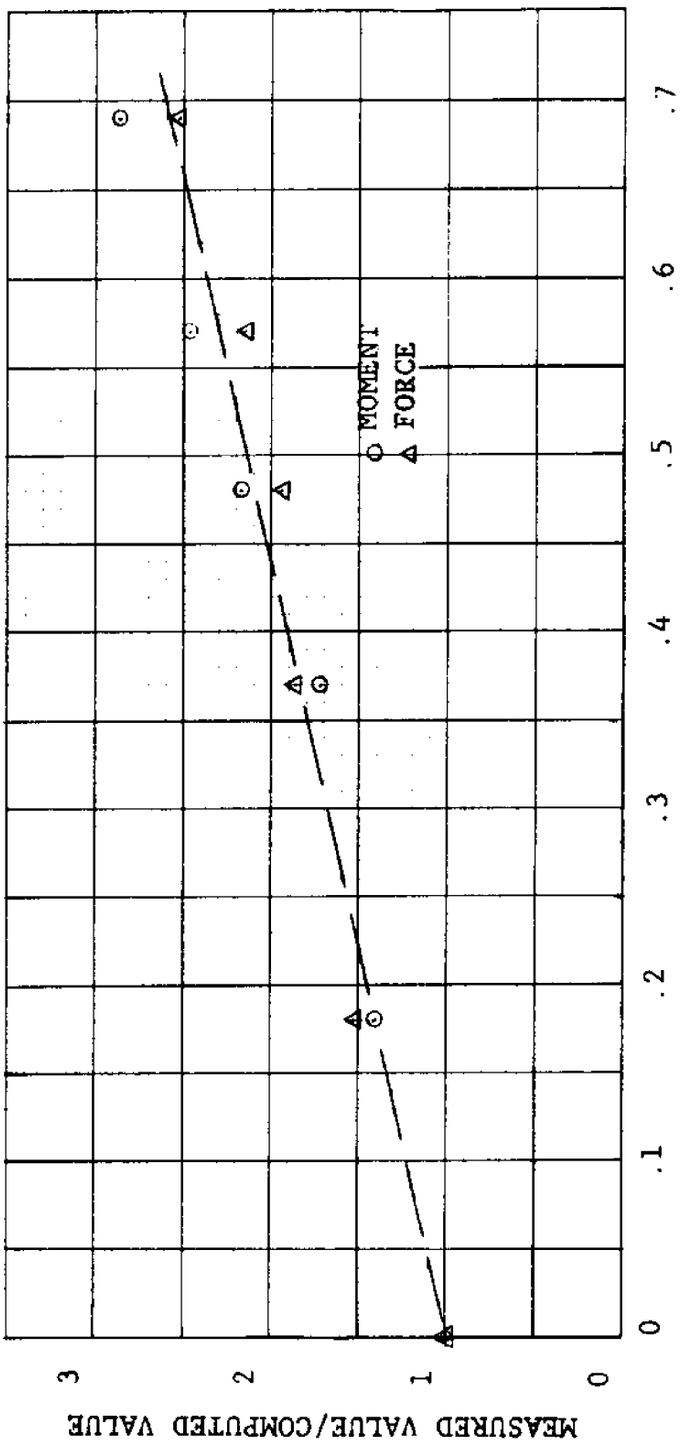

FIG. 33-INCREASE IN MOMENT AND LATERAL FORCE DUE TO FLUID VELOCITY INCREASE-SHIP VELOCITY CONSTANT

The mathematical model simulates the actions normally taken by a pilot; i.e., once the forces and moment due to bank suction, wind and currents have been computed, rudder angle in the correct direction is increased until the applied moment has been neutralized. Drift angle in the correct direction is applied until the force has been neutralized. Since the application of drift angle tends to add additional moment, the rudder angle is rechecked as each increment of drift angle is added.

The results of the computer runs are shown in Fig. 34 through Fig. 39. Curves of computed data were determined by the least-squares method. Runs were made for six different off-centerline positions, three speeds 5, 7.5 and 10 knots; and three different channel depths 45, 60 and 80 feet (22). The average difference between measured and calculated values (Tables 4 and 5) was 1.9 degrees for rudder angle and 0.15 degrees for drift angle. Differences of this magnitude are considered insignificant by ship masters (34) and channel pilots (11, 40) in that rudder commands are never given in increments of less than 5 degrees. Rudder angles may vary by $\pm$ 3 degrees while trying to maintain a straight course (11). With regard to drift angle, the ship's compass card is graduated in only 1 degree increments. Compass readings are rounded to the nearest degree for all normal operations (11, 34).

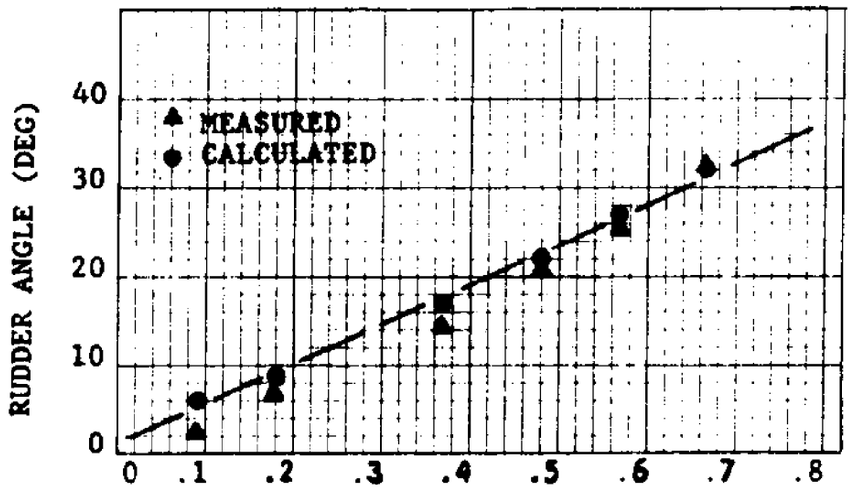

FIG. 34-RUDDER ANGLE REQUIRED FOR EQUILIBRIUM-45 FT DEPTH (22)

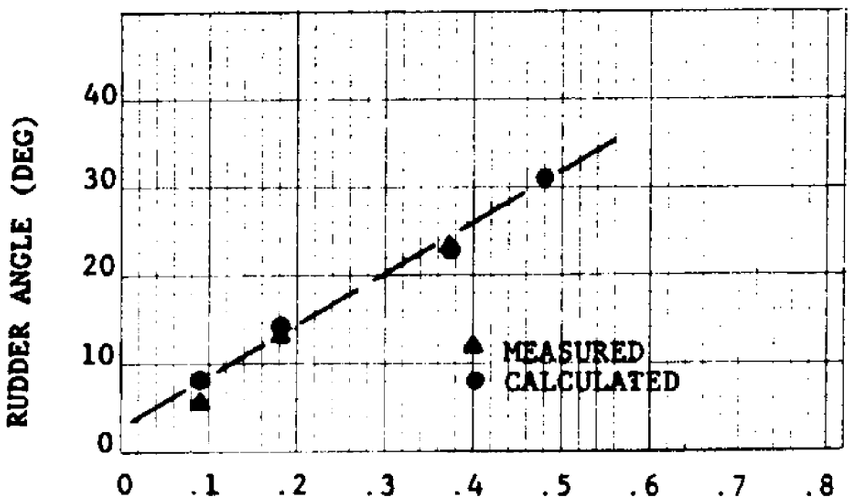

FIG. 35-RUDDER ANGLE REQUIRED FOR EQUILIBRIUM-60 FT DEPTH (22)

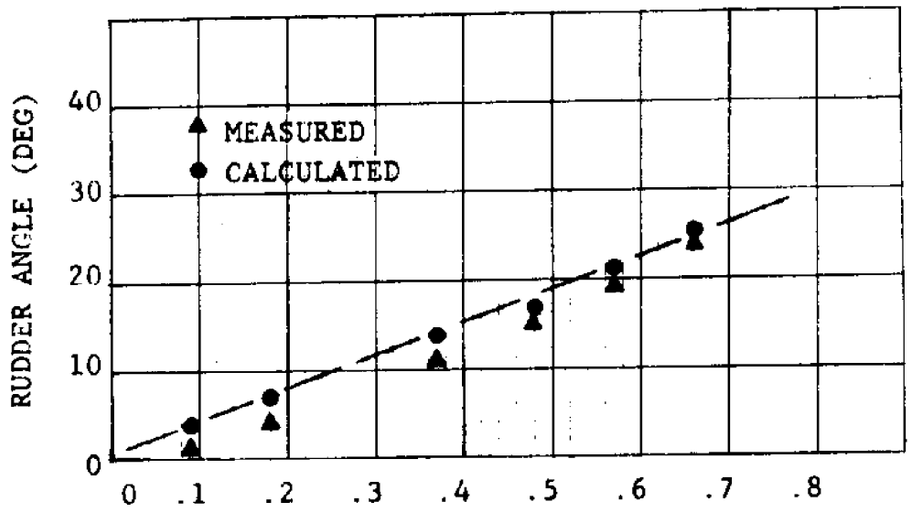

OFF-CENTERLINE DISTANCE / HALF CHANNEL WIDTH = y/.5W

FIG. 36-RUDDER ANGLE REQUIRED
FOR EQUILIBRIUM-80 FT DEPTH (22)

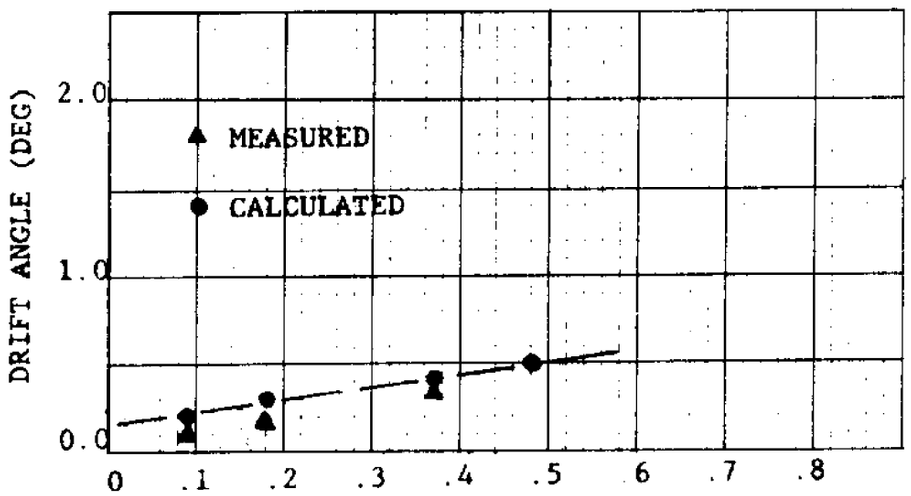

OFF-CENTERLINE DISTANCE / HALF CHANNEL WIDTH = y/.5W

FIG. 37- DRIFT ANGLE REQUIRED
FOR EQUILIBRIUM-45 FT DEPTH (22)

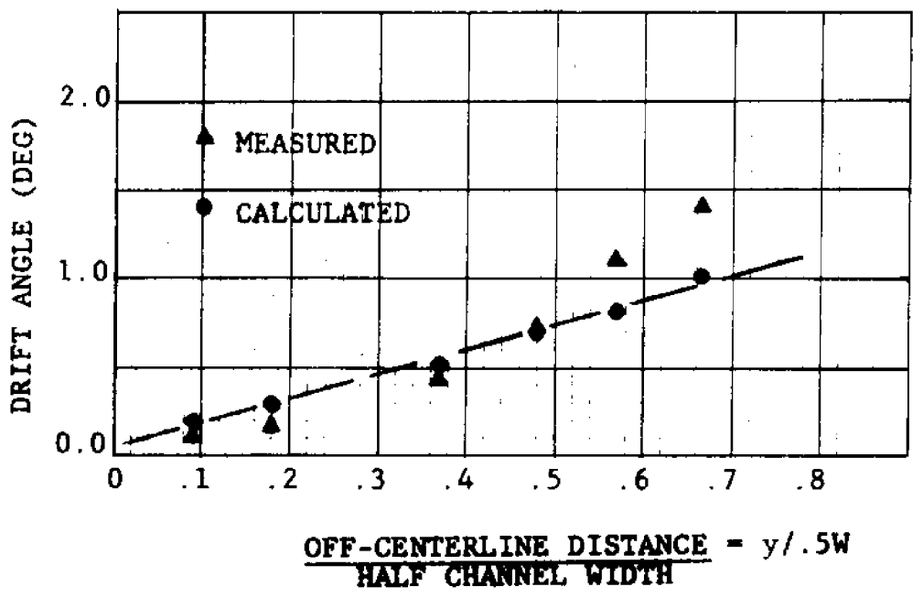

FIG. 38-DRIFT ANGLE REQUIRED FOR EQUILIBRIUM-60 FT DEPTH (22)

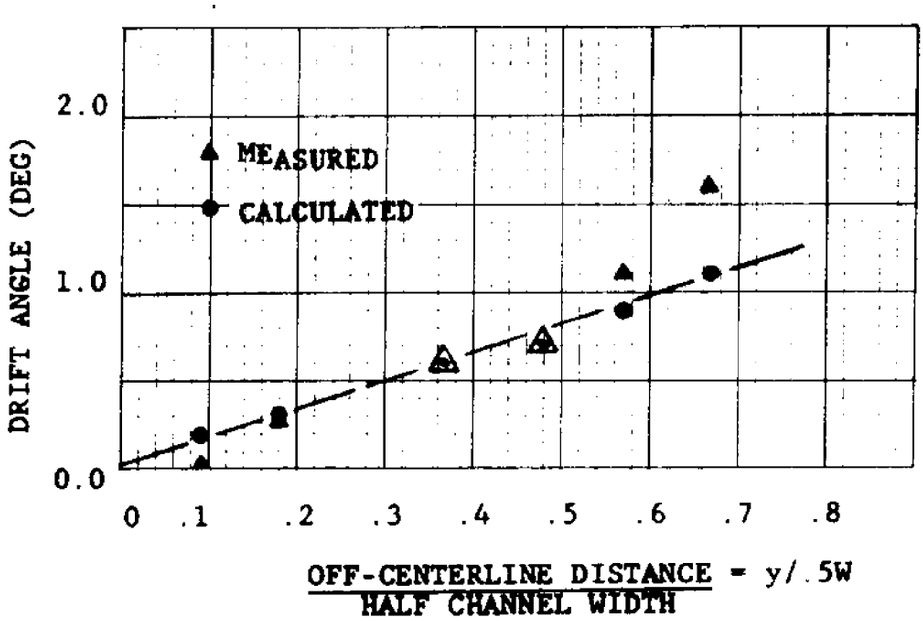

FIG. 39-DRIFT ANGLE REQUIRED FOR EQUILIBRIUM-80 FT DEPTH (22)

The same data are presented in tabular form in Tables 4 and 5. The observation has been made that the equilibrium position, once established, is relatively independent of velocity (30). This is the case when the vessel is being acted on by bank suction effects only because velocity is one of the dominant factors in both bank suction and attitude control. Bank suction effects change at the same rate as attitude control measure (drift angle and rudder movement) effectiveness with changes in velocity. This is clearly shown in Tables 4 and 5. The computed values of rudder and drift angles over the entire range of velocities for each ship position came out exactly the same in all cases even though each calculation from bank suction effect through attitude control was completely independent. It is felt that the scatter of the measured values is generally due to the many uncertainties of research measurement procedures

The above reasoning does not apply to equilibrium attitude control measures used to neutralize beam wind and current effects. Here the effects of the lateral winds and currents will remain constant while the effectiveness of the attitude control measures will vary with velocity.

TABLE 4.-RUDDER ANGLE COMPARISON-500 FT WIDE CHANNEL

DIST FROM CENTERLINE (FT)	SPEED (KTS)	45 FT. DEPTH MEASURED RUDDER ANGLE (DEG)	45 FT. DEPTH COMPUTED RUDDER ANGLE (DEG)	60 FT. DEPTH MEASURED RUDDER ANGLE (DEG)	60 FT. DEPTH COMPUTED RUDDER ANGLE (DEG)	80 FT. DEPTH MEASURED RUDDER ANGLE (DEG)	80 FT. DEPTH COMPUTED RUDDER ANGLE (DEG)
23.3	5	6.0	8.0	---	6.0	---	4.0
	7.5	7.0	8.0	2.7	6.0	1.2	4.0
	10	4.4	8.0	2.2	6.0	---	4.0
	(AVG.)	(5.8)	(8.0)	(2.5)	(6.0)	(1.2)	(4.0)
45.8	5	12.0	14.0	8.0	9.0	2.5	7.0
	7.5	14.8	14.0	6.7	9.0	3.4	7.0
	10	12.2	14.0	6.1	9.0	6.0	7.0
	(AVG.)	(13.0)	(14.0)	(6.9)	(9.0)	(4.0)	(7.0)
92.4	5	22.0	23.0	15.2	17.0	11.5	14.0
	7.5	22.6	23.0	16.6	17.0	10.0	14.0
	10	26.0	23.0	11.5	17.0	11.6	14.0
	(AVG.)	(23.5)	(23.0)	(14.4)	(17.0)	(11.0)	(14.0)
119.4	5	----	31.0	20.5	22.0	15.0	17.0
	7.5	----	31.0	22.5	22.0	----	17.0
	10	----	31.0	19.0	22.0	15.2	17.0
	(AVG.)	----	(31.0)	(20.7)	(22.0)	(15.1)	(17.0)
142.8	5	----	----	24.0	27.0	19.8	21.0
	7.5	----	----	26.2	27.0	18.8	21.0
	10	----	----	25.3	27.0	19.0	21.0
	(AVG.)	----	----	(25.2)	(27.0)	(19.2)	(21.0)
166.3	5	----	----	31.1	32.0	25.0	25.0
	7.5	----	----	----	32.0	23.1	25.0
	10	----	----	33.9	32.0	24.0	25.0
	(AVG.)	----	----	(32.5)	(32.0)	(24.0)	(25.0)

TABLE 5.-DRIFT ANGLE COMPARISON-500 FT WIDE CHANNEL

DIST FROM CENTERLINE (FT)	SPEED (KTS)	45 FT. DEPTH MEASURED DRIFT ANGLE (DEG)	45 FT. DEPTH COMPUTED DRIFT ANGLE (DEG)	60 FT. DEPTH MEASURED DRIFT ANGLE (DEG)	60 FT. DEPTH COMPUTED DRIFT ANGLE (DEG)	80 FT. DEPTH MEASURED DRIFT ANGLE (DEG)	80 FT. DEPTH COMPUTED DRIFT ANGLE (DEG)
23.3	5	.1	.2	---	.2	---	.2
	7.5	.2	.2	.2	.2	.0	.2
	10	.0	.2	.0	.2	---	.2
	(AVG.)	(.1)	(.2)	(.1)	(.2)	(.0)	(.2)
45.8	5	.2	.3	.2	.3	.2	.3
	7.5	.2	.3	.2	.3	.2	.3
	10	.1	.3	.1	.3	.4	.3
	(AVG.)	(.17)	(.3)	(.17)	(.3)	(.27)	(.3)
92.4	5	.4	.4	.3	.5	.5	.6
	7.5	.35	.4	.5	.5	.5	.6
	10	.2	.4	.5	.5	.8	.6
	(AVG.)	(.32)	(.4)	(.43)	(.5)	(.6)	(.6)
119.4	5	---	.5	.7	.7	.5	.7
	7.5	---	.5	.9	.7	---	.7
	10	---	.5	.6	.7	.9	.7
	(AVG.)	---	(.5)	(.73)	(.7)	(.7)	(.7)
142.6	5	---	---	1.0	.8	1.1	.9
	7.5	---	---	1.2	.8	1.1	.9
	10	---	---	1.1	.8	1.1	.9
	(AVG.)	---	---	(1.1)	(.8)	(1.1)	(.9)
166.3	5	---	---	1.4	1.0	1.8	1.1
	7.5	---	---	---	1.0	1.4	1.1
	10	---	---	1.4	1.0	1.6	1.1
	(AVG.)	---	---	(1.4)	(1.0)	(1.6)	(1.1)

Cross-winds and Currents

The effects of beam current components and winds have been included in the mathematical model. Components of quartering winds have also been included. The effects of these forces have been reported by many pilots as being hazardous to channel navigation, especially when maneuvering empty ships (7).

The forces are computed by the simple relation (4):

$$F = CA\left(1/2\rho V^2\right) \quad \ldots\ldots\ldots\ldots\ldots\ldots \quad (23)$$

where: A = total area affected; i.e., sail area
C = coefficient

and added to any other forces. When only force and not moment is acting on the vessel, the previously described procedure is reversed. The ship is given a drift angle to overcome the force which in turn induces a moment. Rudder control is then added to neutralize this moment.

CHAPTER VI

SHIP-GENERATED WAVES

Introduction

A ship moving through the water will create a pressure disturbance due to energy transfer. This pressure disturbance in turn will create a system of diverging and transverse waves. These ship-generated waves have been studied over a period of many years by Froude (52), Lord Kelvin (33), Lamb (33), Havelock (52), Kostyukov (31), Johnson (27) Sorensen (45), Das (14), and many others (Figs. 40 and 41). Most of these studies of ship-generated waves were conducted to determine the effects of these waves on the vessel itself, mainly resistance to vessel movement. Very little was done until quite recently to determine the effects of these waves on other vessels, marine structures, and bank erosion.

The effects of these ship-generated waves on other bodies are of great importance in the design of ship channels, harbors, anchorages, etc. Wave amplitude at the shore line is needed to determine the extent of bank protection required. Wave amplitude, being mainly a function of vessel speed, is required to control the velocity of vessels moving past other vessels, barge trains, marinas, and other structures. Since these waves decay as they propagate out from the vessel sailing line, a balance must be maintained bet-

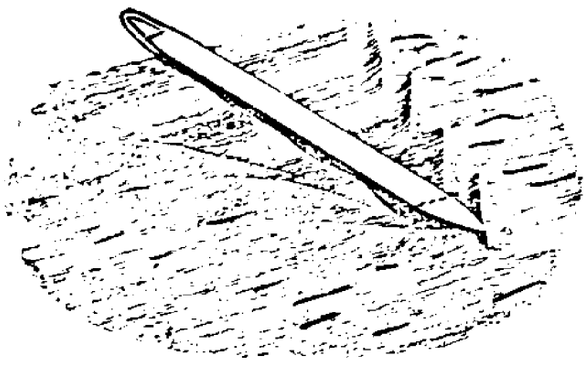

FIG. 40-FROUDE'S SKETCH OF THE CHARACTERISTICS OF SHIP WAVES, TRANS. INST. NAVAL ARCH., 1877 (42)

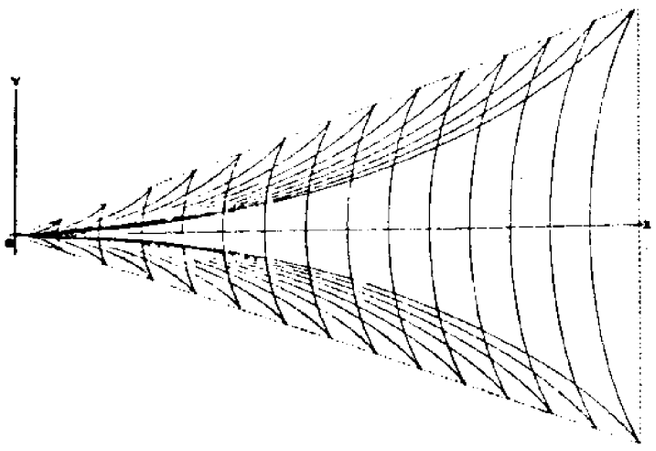

FIG. 41-CREST OF A KELVIN WAVE GROUP IN DEEP WATER CAUSED BY A TRAVELLING DISTURBANCE AT O (TAYLOR, 1943) (47)

ween the distance from the sailing line of the vessel and allowable vessel velocity.

Basic Theory

A vessel moving through the water will create a pressure disturbance. The pressure will be greater than average near the bow and stern and less than average in the mid-length region. Due to separation and eddy effects in a real fluid the pressure increase near the stern is usually substantially less than that at the bow (46,47). These pressure disturbances will in turn create systems of transverse and diverging waves at both the bow and the stern. These wave systems are maximum at the point of pressure disturbance and decrease as they propagate out from the sailing line of the vessel. This decay of the wave has been determined to be caused more by the distribution of energy along the crest of the wave than due to bottom friction which is generally considered to be negligible except in very shallow water (46).

As the diverging and transverse waves propagate away from the sailing line of the vessel, a line of wave cusps is formed at their intersection. It has been theoretically shown by Kelvin and verified by others that this line or locus of cusps forms an angle, α , with the sailing line of the vessel of 19° 28' under deep water conditions (Fig. 42).

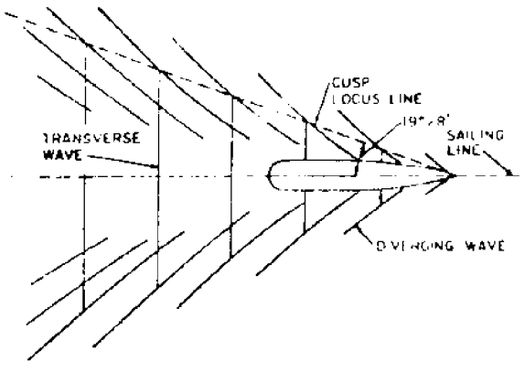

FIG. 42-DEEP WATER WAVE CREST PATTERN GENERATED BY SHIP'S BOW (46)

The maximum wave amplitude always occurs at these cusps. It was also noticed that the diverging wave always played a dominant role in producing these maximum waves. Many researchers have determined that the elevation of the diverging wave was inversely proportional to the cube root of the distance from the sailing line and that the elevations along the transverse wave were inversely proportional to the square root of the distance from the sailing line (13, 46, 47, 52). This shows that the farther away from the sailing line the wave propagates the more dominant the role of the diverging wave becomes.

Ship-generated wave heights seem to be clearly a function of vessel speed and the distance from the sailing line of the vessel. Although ship speed plays a dominant role in wave

generation, ship geometry and bow form are also of great importance (8, 28, 47). Conventional parameters of hull geometry such as block coefficients and speed/length ratios seem to be of little value in grouping ship-generated wave data (8). Brebner, Helwig and Carruthers developed and used two parameters of bow shape which seem to contain most of the dominant characteristics (8). One is a fineness ratio and the other a wave-making breadth.

A fineness ratio is defined as:

$$K_f = \frac{L^*}{(A)^{\frac{1}{2}}} \quad \ldots\ldots\ldots\ldots\ldots\ldots\ldots\ldots \quad (24)$$

Where K_f = fineness ratio

L^* = length of curved part of bow measured horizontally at the waterline

A = cross-sectional area of ship parallel middle body below the waterline

The wave-making breadth is defined as:

$$b = \frac{A}{L^*} \quad \ldots\ldots\ldots\ldots\ldots\ldots\ldots\ldots \quad (25)$$

Where b = wave-making breadth

These parameters seem to group the ship-generated wave data quite well (Fig. 43). Wave-making ability seems to be inversely proportional to the fineness ratio. This is what one would intuitively believe; i.e., the more slender and tapered the bow, the smaller the ship-generated wave for a given speed.

Ship-generated waves are predominantly controlled by gravity and inertial forces (48). It is not surprising then that Froude numbers play an important role in describing the associated phenomena. Deep water conditions will prevail until a Froude number of approximately 0.7 has been reached (Appendix V). Up until this point the α angle between the vessel sailing line and the diverging locus of cusps will remain 19° 28'. When shallow water conditions start, the angle will increase with an increase in vessel speed (assuming constant depth) until the α is 90 degrees at a Froude number of 1.0. At this point, planing of the vessel apparently begins to occur (46). Beyond this point the α angle decreases, although at a lesser rate with an increase in Froude number (Fig. 44). The length term, d, in these Froude numbers is the water depth.

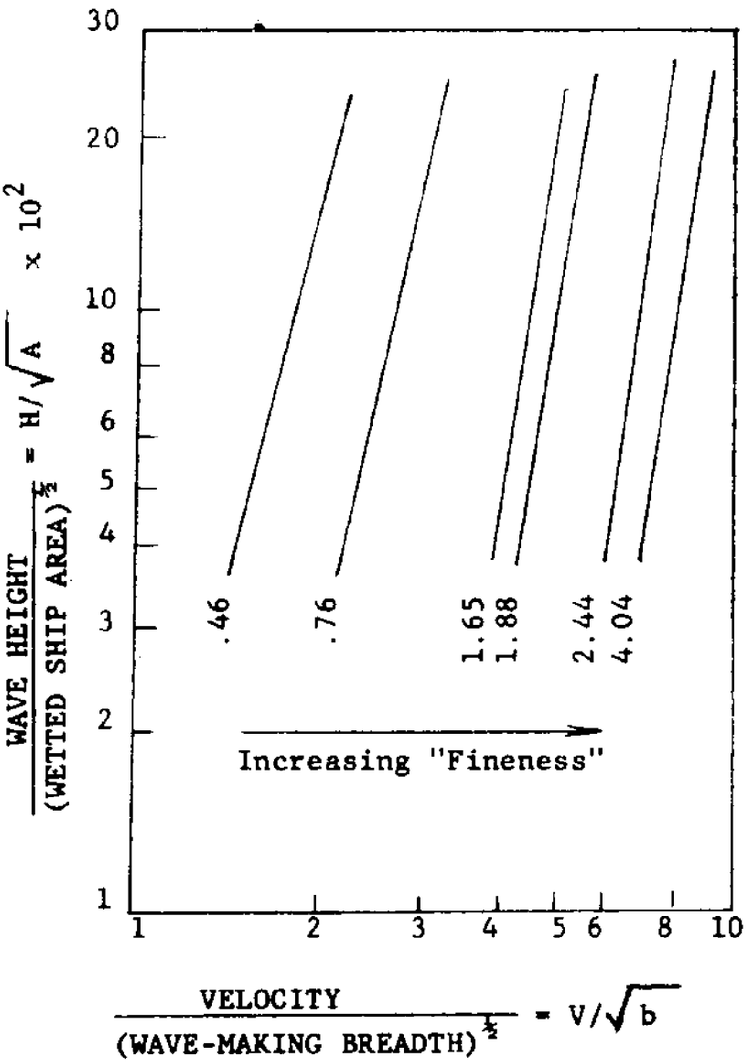

Water depth of 48 feet. H values measured 288 feet from sailing line.

FIG. 43-VARIATION OF WAVE HEIGHT/AREA WITH VELOCITY/WAVE-MAKING BREADTH FOR DIFFERENT VESSELS (8)

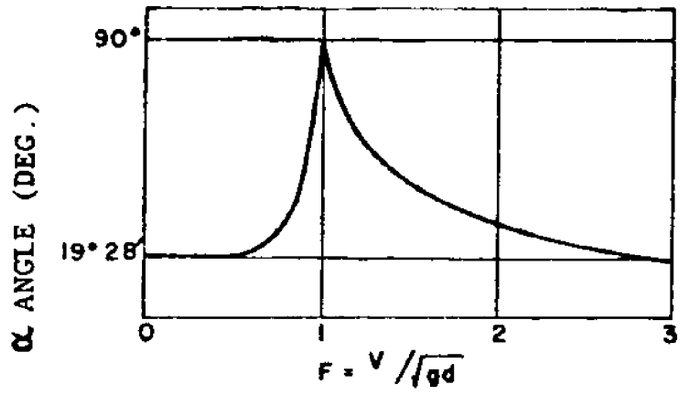

FIG. 44-CUSP LOCUS ANGLE VERSUS FROUDE NUMBER (31)

Model testing at the University of California shows good correlation between the α angle and the Froude number as shown in Fig. 44 (31) and Fig. 45 (26).

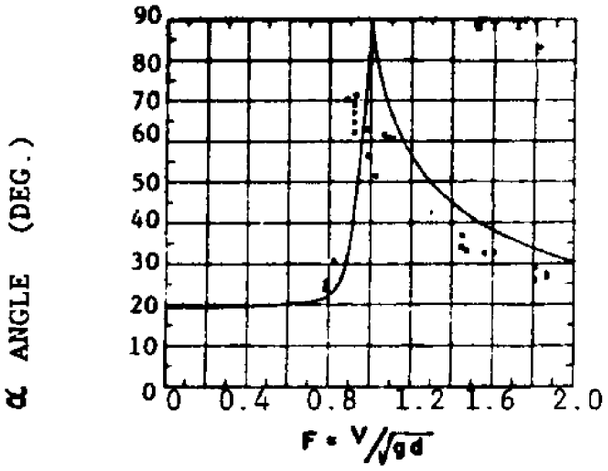

FIG. 45 -EXPERIMENTAL DETERMINATION OF CUSP LOCUS AND OUTER WAVE ANGLES (26)

University of California model tests also showed the relationship between maximum wave height and Froude number (Fig. 46)(47).

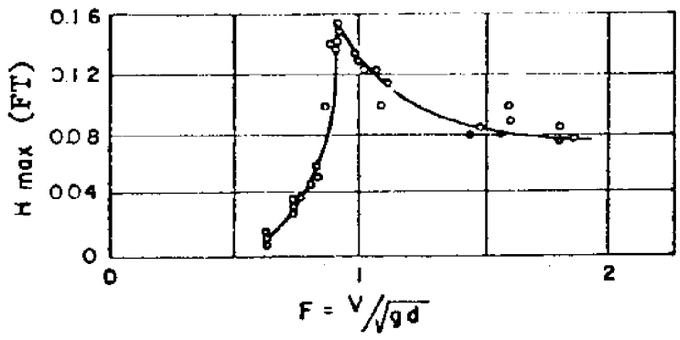

FIG. 46-MAXIMUM WAVE HEIGHT AS FUNCTION OF FROUDE NUMBER FOR TYPICAL SHIP MODEL (26)

The wave shape is wholly dependent on the vessel speed. This is to be expected as the wave periods and velocity should only be dependent on the disturbance velocity and the angle that the waves form with respect to the sailing line (48). The troughs are flattened and are not as deep as the crests are high. The maximum wave height for this type of wave is considered to be from the peak of the highest wave to the base of the preceding trough. Also, the half-period is used as a measure rather than the period. This measure is from the deepest part of the trough to the peak of the wave (Fig. 47 (25).

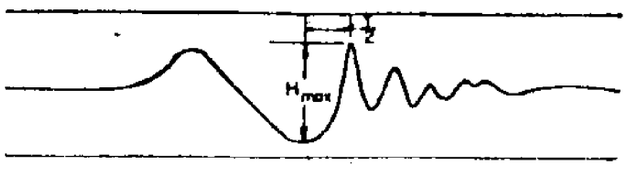

FIG. 47-TYPICAL WATER SURFACE TIME HISTORY OF SHIP WAVES SHOWING MAXIMUM WAVE HEIGHT AND HALF-PERIOD (25)

It is also known that the wave length of the diverging wave actually gets longer with distance from the sailing line of the vessel. In the University of California studies a plot of the half-period and the Froude number was also made. This appears in Fig. 48.

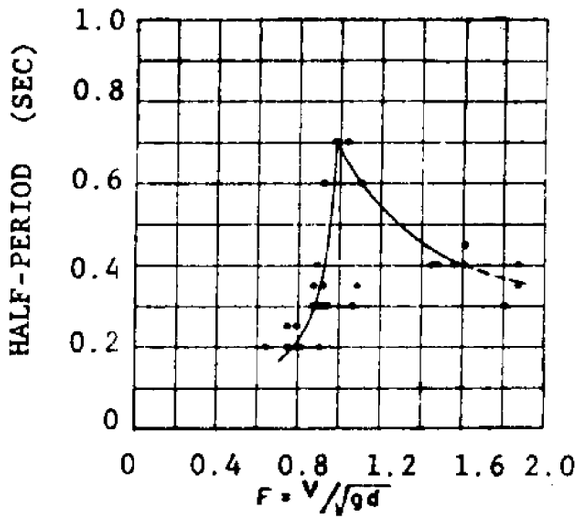

FIG. 48-HALF-PERIOD AS FUNCTION OF FROUDE NUMBER FOR TYPICAL SHIP MODEL (26)

Ships may also generate unseen waves on the interface between two layers of water of different density. Near the mouths of large rivers, a layer of fresh water often rests on the heavier salt water with little or no mixing. These sub-surface waves may be higher and move slower than the visible surface waves generated at the same time (Fig. 49) (5).

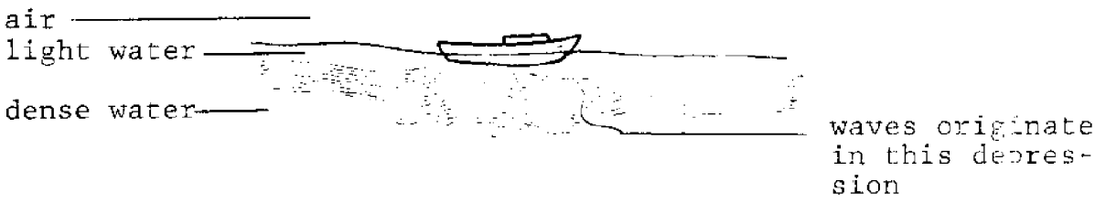

FIG. 49-VESSEL-GENERATED WAVES ON THE INTERFACE BETWEEN FRESH AND SALT WATER (5)

Determination of Wave Heights

Although much theoretical and practical work has been done in the area of wave-making resistance of ships, very little work has been done in obtaining quantitative information on the characteristics of ship waves at a given distance from the sailing line in open and restricted navigation channels (14). A few empirical equations have been developed over the years to determine the amplitude of ship-generated waves in the vicinity of the ship. One of these equations of some interest was presented by Balanin and Bykov (2, 3). They used a modified blockage factor as the prime dimensionless coefficient. This expression for determining the wave height in the vicinity of the ship is as follows:

$$H_s = 2.5\frac{V^2}{2g}\left\{1 - \left(1 - \frac{1}{\left[4.2 + \frac{A}{a}\right]^{\frac{1}{2}}}\right)\left(\frac{\frac{A}{a} - 1}{\frac{A}{a}}\right)^2\right\} \quad . \quad . \quad . \quad (26)$$

Where: H_s = wave height in vicinity of ship (ft)
V = ship speed (ft/sec)
g = acceleration of gravity (ft/sec^2)
A = cross-sectional area of canal
a = cross-sectional area of ship

Using an approach suggested by Sorensen (47), the Froude number at the boundary between shallow and deep water theory was established in Appendix V of this paper. In Appendix VI the author determined the relationship between the vessel speed and water depth at this boundary Froude number (F=0.7). The results of these calculations are presented in Fig. 50. Fig. 50 shows that under normal deep-draft channel operating conditions ship-generated waves would be computed by deep-water theory. For this reason and the fact that deep-water theory is more clearly defined the following paragraphs will stress this theory.

Another method of estimating the height of the ship-generated bow wave is presented in Saunders (42).

$$h = K_w \left(\frac{B}{L_E} \right) \frac{V^2}{2g} \quad \ldots\ldots\ldots\ldots (27)$$

Where:
- h = height of water surface at bow (Ft.)
- K_w = coefficient
- B = ship beam (Ft.)
- L_E = entrance length (Ft.)
- V = ship velocity (Ft/sec)
- g = acceleration of gravity (Ft./sec^2)

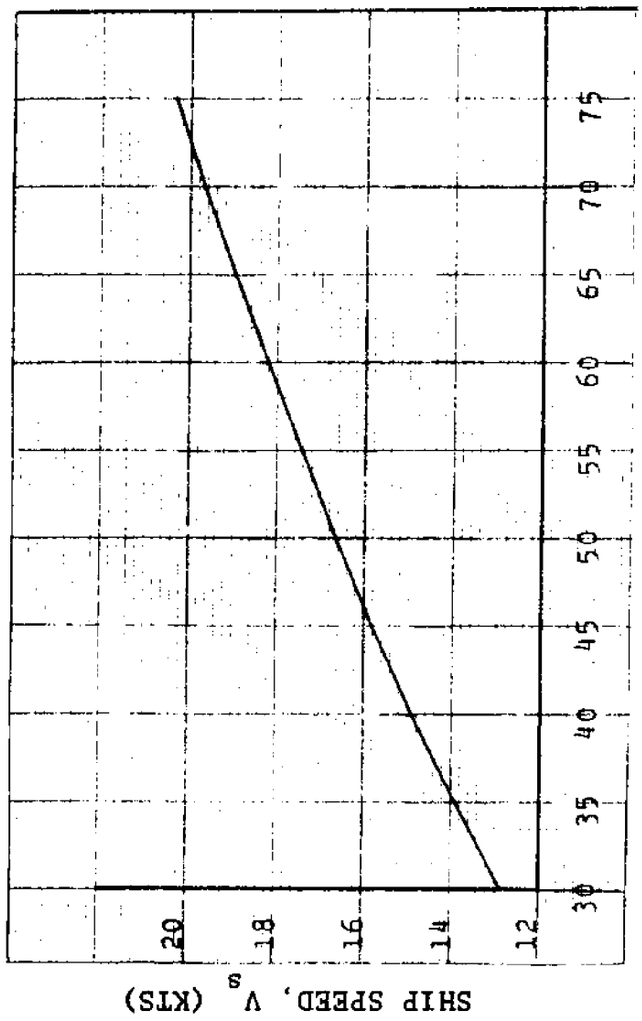

FIG. 50-LIMITS OF DEEP-WATER THEORY

The coefficient K_w is normally determined from the graph shown in Fig. 51.

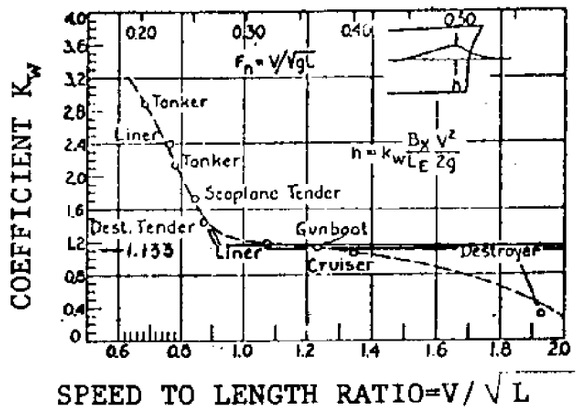

FIG. 51-GRAPH FOR DETERMINING VALUES OF K_w (42)

Equations for these curves were derived and used in the model to determine bow wave heights. However, when an attempt was made to correlate computed values for long parallel middle body cargo vessels with test data, it was found that these values were not in reasonable agreement at high speed to length ratios ($V/\sqrt{L}$), i.e. above approximately 1.5. This is undoubtedly because that portion of the curve in Fig. 51 was determined on the basis of a high performance naval vessel. A determination was made to use a constant value of K_w equal to 1.133 when the speed to length ratio exceeds .9191. This change is shown by the double line in Fig. 51. After this change was made correlation with test data was good. The relatively constant value of K_w in the higher speed to length ratio range would

also explain why Brebner, Helwig and Carruthers (8) found the speed to length parameter of little value in grouping their data.

The entrance length, L_E, is the distance from the stem of the vessel to the point where the parallel middle body begins or in other words the curved portion of the bow. This is a measure of the fineness of the bow. Values of L_E are not normally available to the navigation channel designer so data from 16 tanker bulk cargo ships was used to determine these values (21)(Fig. 52). Should the designer know the value of L_E it may be entered into the model as data. If L_E is not known, a value will be computed based on the following equation (Fig. 52):

$$L_E/L = 0.416 - 0.000235L \quad \ldots\ldots\ldots\ldots\ldots\ldots (28)$$

Where: L_E = entrance length
L = ship length

The original theory for waves generated by a pressure disturbance in deep water was developed by Kelvin (33). Havelock modified Kelvin's theory slightly to eliminate certain undesirable effects (infinite height) occurring at the origin and cusps (52). Kostyukov (31) agrees with the work done by Havelock. The expression for determining the relative amplitude of ship-generated waves at the cusps in deep water is as follows (52):

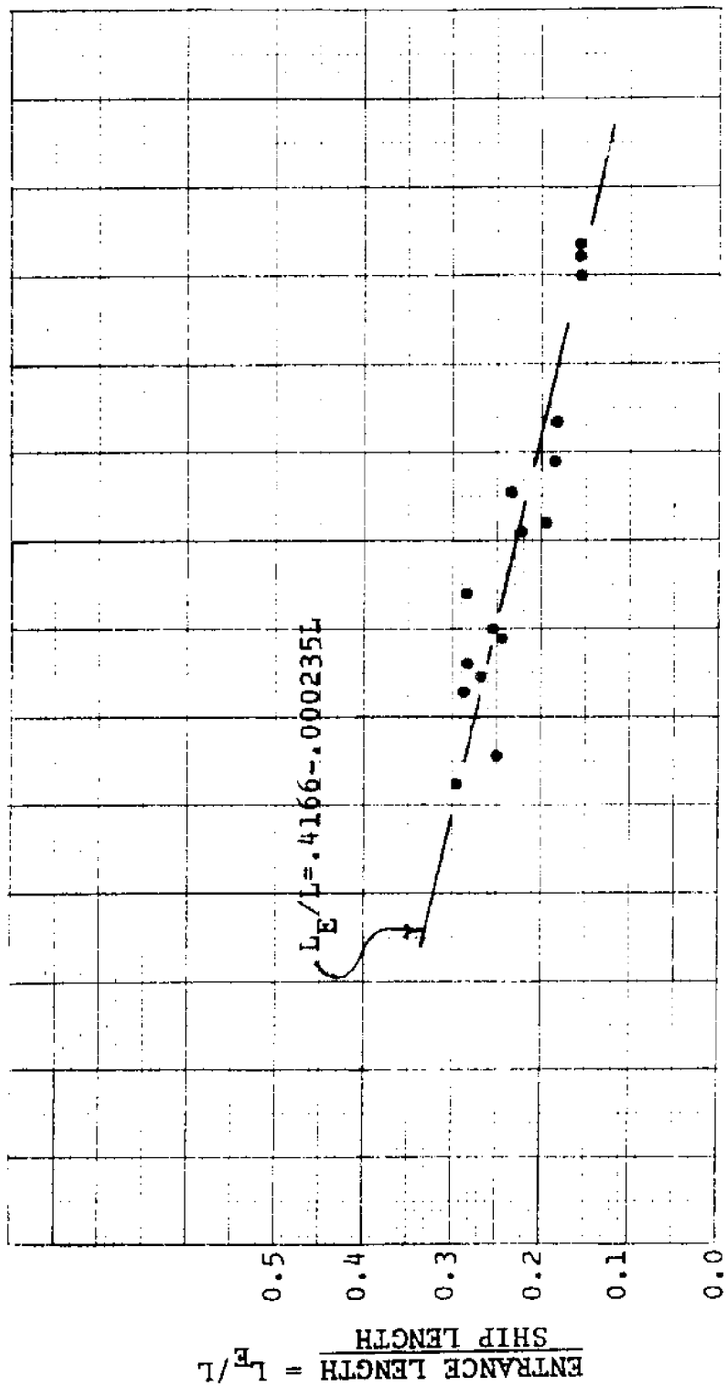

FIG. 52-ENTRANCE LENGTH, L_E AS A PERCENTAGE OF SHIP LENGTH, L_E/L FOR TANKERS AND BULK CARGO VESSELS (21)

$$\zeta_{mc} = \frac{3}{2^{5/6}\Gamma(2/3)(2n+3/2)^{1/3}\ \pi 1/3} \quad \frac{g}{c^4 \rho} \qquad \cdots\cdots (29)$$

Where: ζ_{mc} = height of cusped waves
c = celerity
g = acceleration of gravity
ρ = density
Γ = the gamma-function (See Appendix VII)
n = cusp number

Eq. 29 describes quite well the state of decay of ship-generated waves as they propagate out from the vessel's sailing line. This is quite understandable since the main factors involved are velocity and distance from the sailing line. Although Eq. 28 is for open waters, it serves the purpose of the model well since it is used to estimate the wave heights of the bow-generated cusped waves to the edge of the channel bottom only.

Equation 29 is not suitable in itself to determine wave heights. However, it does describe quite well the decay of the ship-generated wave as it propagates out from the sailing line. A combination of Eq. 27 and Eq. 29 is used to produce the desired values. If a zero value is used in Eq. 29 for n, the value of ζ_{mc} becomes a constant of 69.15 at the point of the pressure disturbance or sailing line of the ship. The value at any distance is equal to:

$$\zeta_{mc} = \frac{153.169}{\rho(2n + 3/2)^{1/3}} \quad \ldots\ldots\ldots\ldots\ldots\ldots\ldots\ldots (30)$$

A good approximation of the wave height at the ship, h_s can be determined from Eq. 27 and of the wave height at any cusp from:

$$h_n = \zeta_{mc} F \quad \ldots\ldots\ldots\ldots\ldots\ldots\ldots\ldots (31)$$

Where: h_n = wave height at cusp n
ζ_{mc} = relative wave height for cusp n from Eq. 29
$F = h/69.15$

The distance from the sailing line to a particular cusp along the cusp line can be found from the following (52):

$$\omega = \frac{2V^2 (2n+3/2)\pi}{g\sqrt{3}} \quad \ldots\ldots\ldots\ldots\ldots\ldots\ldots\ldots (32)$$

Where: ω=distance along cusp line to cusp n
V=vessel speed (ft/sec)

The absolute location of the cusp with regard to the sailing line and the origin is given by the following simple trigonometric relationships (31):

$$Y = \omega \sin\alpha \quad \ldots\ldots\ldots\ldots\ldots\ldots\ldots\ldots (33)$$

$$X = \omega \cos\alpha \quad \ldots\ldots\ldots\ldots\ldots\ldots\ldots\ldots (34)$$

Where: Y = distance out from sailing line
X = distance along sailing line back from bow
α = 19° 28' for deep-water

The computer model was programmed using the method outlined above (Eqs. 27, 30, 31, 32, 33, and 34) with good results (Figs. 53 and 54).

Measured prototype data shown in Figs. 53 and 54 were taken from the work of Brebner, Helwig and Carruthers (8). The two ships measured were the Empress of Canada, EC; length, 650 ft.; beam, 88 ft.; draft, 29 ft. and the Cape Breton Miner, CBM; length, 680 ft.; beam, 75 ft.; draft, 29 ft.. These two vessels represent extreme wave-making capability since the EC is a passenger vessel with a very fine tapered bow while the CBM is an ore carrier with a very blunt bow. One can see from Figs. 53 and 54 that the EC generated wave is much smaller than that of the CBM for the same speed and distance from the sailing line.

The method used by the model gives a general solution. The values computed are well within the accuracy that can be expected with the type of basic input data used. Values of ship-generated wave heights computed by this module will aid the engineer greatly in the design and review of navigation channels.

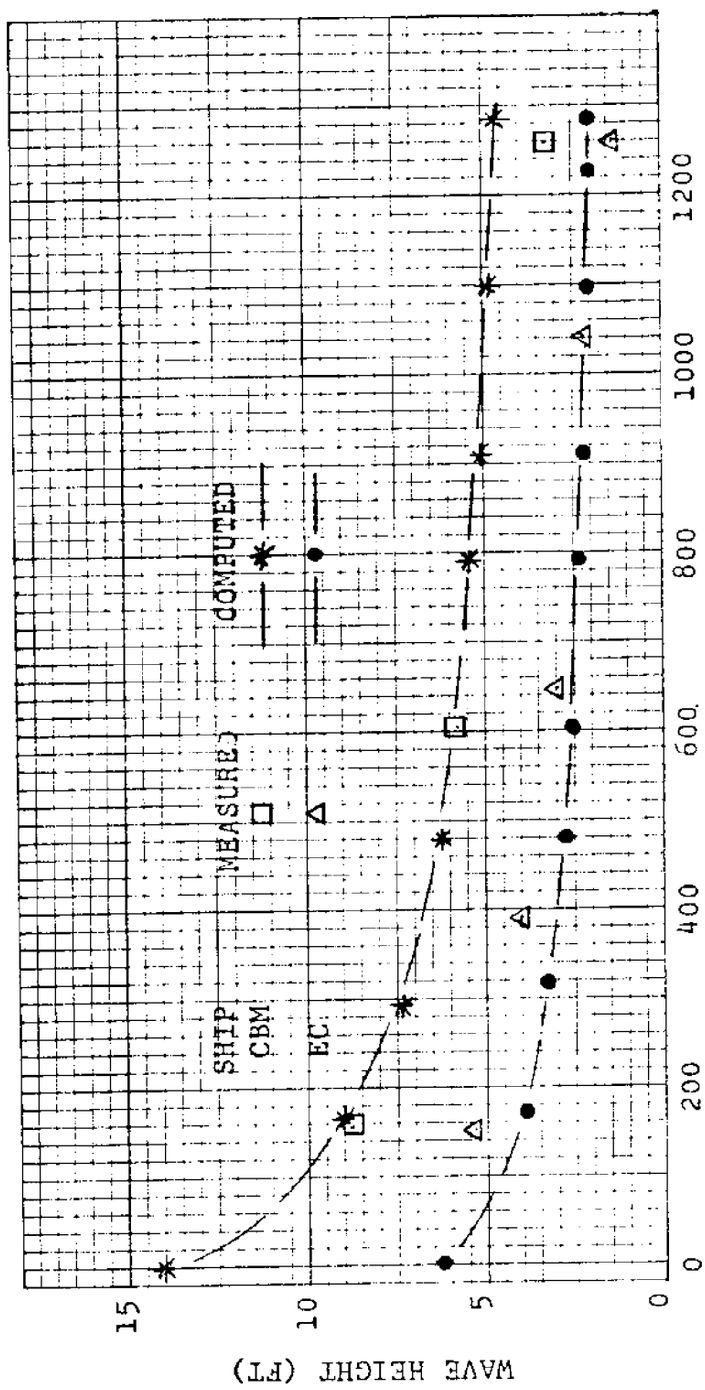

FIG. 53-COMPUTED VS. MEASURED SHIP-GENERATED
WAVE HEIGHTS - WATER DEPTH 48 FEET, SPEED 30 FT/SEC (8)

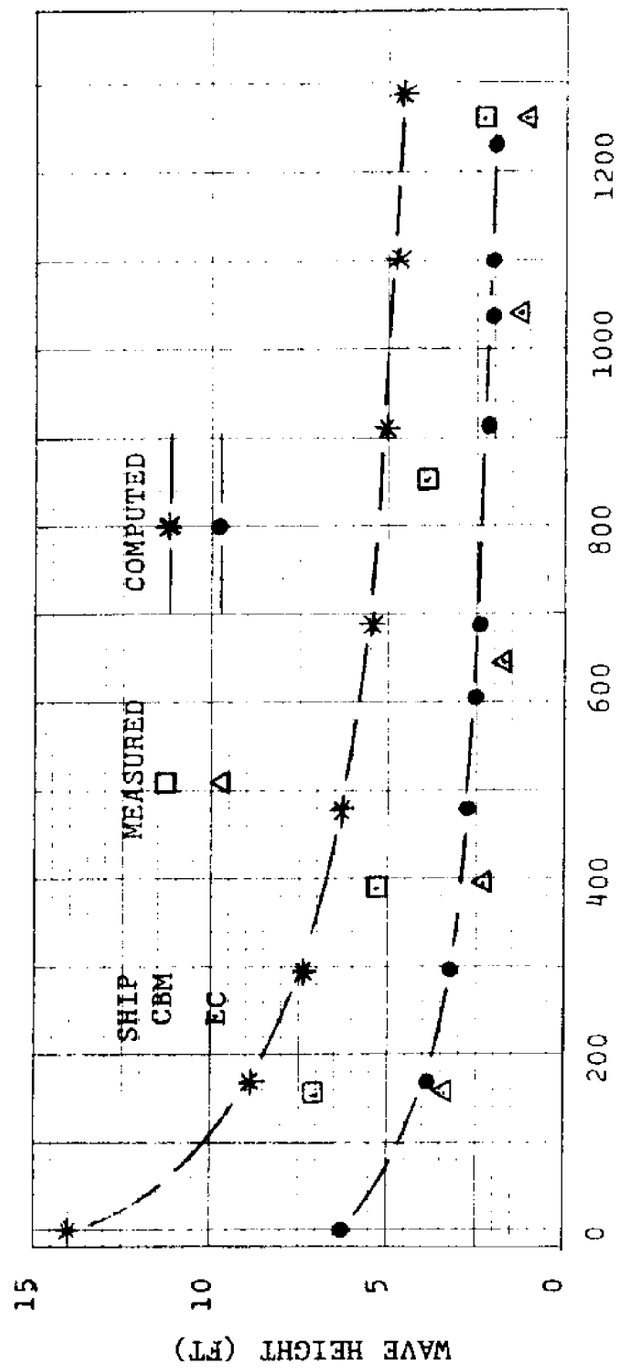

FIG. 54-COMPUTED VS. MEASURED SHIP-GENERATED WAVE HEIGHTS - WATER DEPTH 180 FEET, SPEED 30 FT/SEC (8)

CHAPTER VII

VESSEL STOPPING DISTANCE REQUIREMENTS

Description of Problem

The practitioners of naval architecture and marine engineering have long been interested in the backing power required to stop a vessel in a given distance, the head reach. The purpose of this interest is to insure that the vessel being designed has the proper power plant, propeller size and pitch and various other efficiencies and ratios.

Most texts on naval architecture approach the problem from the same basic energy equation (4, 42):

$$FS=\tfrac{1}{2}MV^2 \quad \ldots\ldots\ldots\ldots\ldots\ldots\ldots\ldots\ldots\ldots \quad (35)$$

Where: F = net stopping force
S = head reach (stopping distance)
M = mass of ship
V = velocity from which ship stops (speed of approach)

The mass term includes an entrained water portion which seems to vary from 8 to 20 percent of the ship's mass. Also, the force term includes the total resistance to the ship moving through the water.

In order to solve the more complex version of this basic equation, a great deal of detailed information must be

known about the vessel such as propeller thrust and torque coefficients, propeller efficiency, dynamic potential terms, moments of inertia of the rotating machinery, propeller speed, various ship resistances and much more. Some of these values can be determined only by model tests (4, 10, 13, 24, 38).

One of the major assumptions of the author during the creation of the channel design model was that the channel design engineer had little or no detailed information about the design vessel. In fact, the design vessel in most cases will not be an existing ship at all, but a composite of existing or expected future vessels. The principal characteristics of these composite design vessels are determined in the Office of the Chief of Engineers (OCE), U. S. Army and are based on the current domestic and world fleets, ships on order and certain economic considerations. Typical design vessel data as received from OCE are contained in Table 6. It then naturally follows that a method was needed to produce stopping distance information that did not require a detailed knowledge of the vessel.

Determination of Stopping Requirements

The head reach (stopping distance) at harbor speeds has been deemed by a majority of operators to be the most

TABLE 6. -PRINCIPAL CHARACTERISTICS OF OCEAN-GOING TANKERS

DWT	Cost per Hour		Length, Overall (feet)	Beam, Overall (feet)	Draft, Overall (feet)
	At Sea	In Port			
20,000	$ 735	$ 615	557	72	31'0"
25,000	780	655	587	84	32'6"
37,000	880	750	660	90	36'0"
50,000	975	825	740	102	39'6"
60,000	1035	875	775	106	40'6"
70,000	1095	925	800	116	42'0"
80,000	1170	980	811	122	43'6"
90,000	1240	1035	820	122	46'0"
120,000	1420	1195	850	138	52'0"
150,000	1585	1350	954	146	55'0"
200,000	1855	1585	1067	155	62'0"
265,000	2210	1905	1107	176	67'0"
325,000	2530	2185	1204	182	73'0"
400,000	2940	2540	1204	228	76'0"
500,000	3545	3105	1314	220	84'0"

essential function of backing power (13). When one restricts stopping distance calculations to harbor speeds one finds that most of the required coefficients reach fairly constant values. By using these constants and assuming 20 seconds of time to establish constant astern thrust, D'Arcangelo produced the following expression (13):

$$S = \frac{80V^2}{\left(\frac{T_1}{\Delta}\right)} + 15V \quad \ldots\ldots\ldots\ldots (36)$$

Where: S = head reach (stopping distance, ft.)
V = velocity from which ship stops (speed of approach, kts.)
T_1 = astern thrust (lbs.)
Δ = ship displacement (long tons)

The coefficient 80 includes 8 percent allowance for entrained water.

Thus, for stopping from harbor speeds, astern thrust per ton of displacement, T_1/Δ, which is a direct measure of rate of deceleration, may be taken as a criterion of stopping ability.

Eq. 36 gives excellent approximations of the head reach for speeds up to 14 knots (Fig. 55).

This increase in mass of 8 percent is for ships operating in open waters, not restricted waterways. Under con-

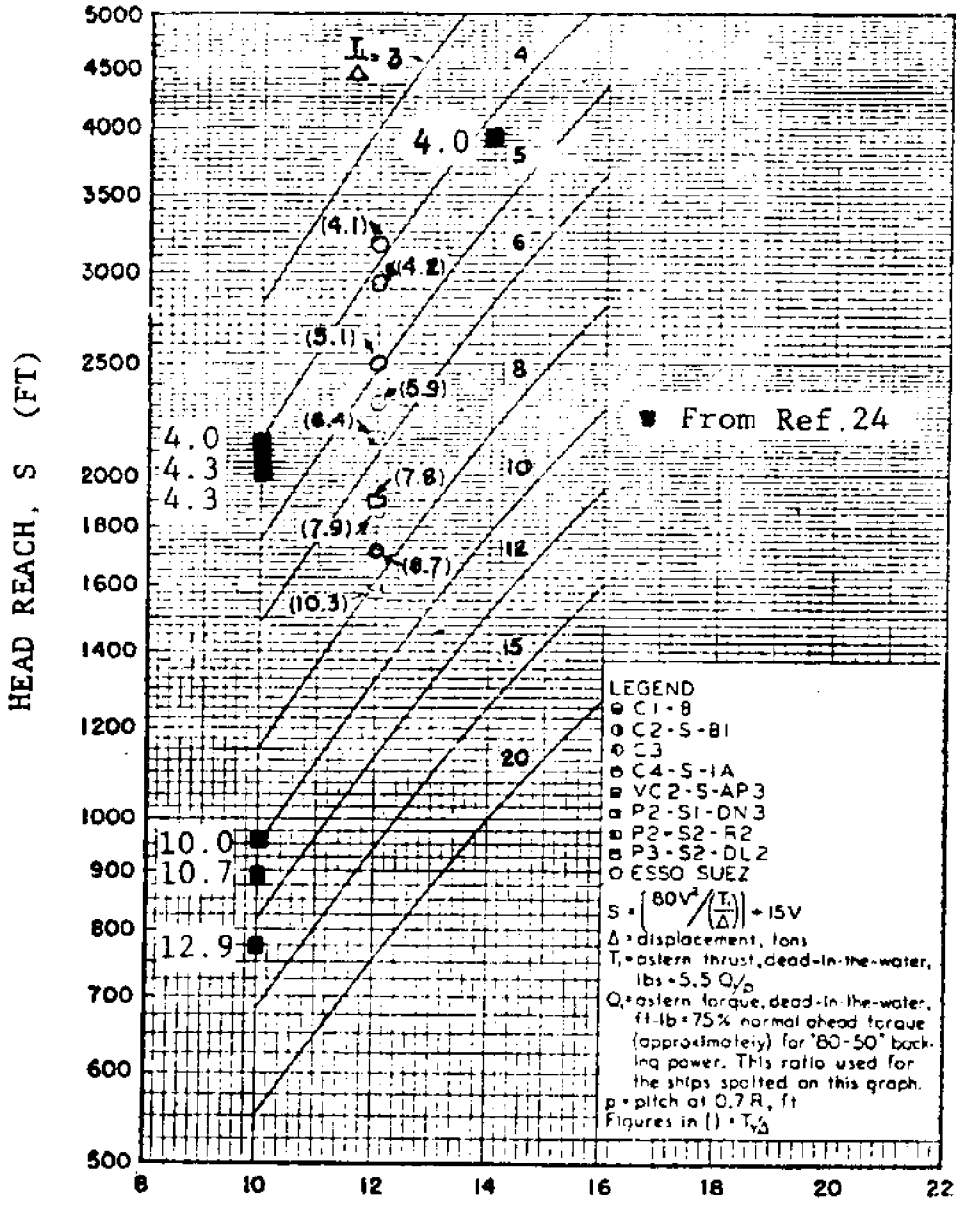

FIG. 55-HEAD REACH AS A FUNCTION OF ASTERN THRUST PER TON OF DISPLACEMENT AND SPEED OF APPROACH (13, 24)

ditions of channel operation, a figure of 20 percent seems to be more appropriate (37, 38). Also, in conversation with ship master (34) and channel pilots (11, 40) the 20 second reverse time was deemed too short. A time of one minute was thought to be much better.

The author, using these increased values of time and mass, derived the following expression:

$$S = \frac{89.3V^2}{\left(\frac{T_1}{\Delta}\right)} + 45.1V \quad \ldots\ldots\ldots\ldots\ldots\ldots (37)$$

Since very little may be known of the design vessel, it was deemed more appropriate to provide stopping distance information in terms of thrust requirements. Eq. 37 was solved for T_1/Δ giving:

$$T_1/\Delta = 89.3V^2/(S-45.1V) \quad \ldots\ldots\ldots\ldots\ldots\ldots (38)$$

Computed values of T_1/Δ can be compared with known values of T_1/Δ for various class vessels. If the known value is greater than the computed value of T_1/Δ, that vessel will be able to stop within the head reach supplied to the model as input and used in the calculation.

CHAPTER VIII

NAVIGATION CHANNEL DESIGN MODEL

Introduction

The statement was made in Chapter I that the navigation channel design engineer should have an in-depth knowledge of both naval architecture and coastal and ocean engineering in order to proficiently complete his tasks. It was also stated that under normal conditions the design engineer does not possess this knowledge and that it is not readily available. In order to provide the engineer with a partial substitute for this in-depth knowledge, a mathematical model of ship behavior in restricted waterways has been programmed for execution on a digital computer. In general, the engineer will describe to the model the channel cross-section to be analyzed, the parameters of the design vessel, and other values of design parameters which have been deemed necessary. The program will then simulate the reactions of the design vessel under these given conditions. The engineer would then analyze the results and make whatever changes are necessary to the channel cross-section to bring the vessel behavior within allowable limits. Successive runs could tell the designer the sensitivity of various changes he might make.

The program was written in the FORTRAN IV language and

it is currently in six overlays on the Honeywell G-225 computer system. The model was written as a series of modules, each module performing a specific analysis. This modularity partitions the design model into distinct parts which may be updated with relative ease as the state-of-the art progresses. Linkage has also been provided to add new modules as basic theory advances or as requirements dictate (Fig. 1, p. 5).

Main Control Module

The main module of the model supplies the control for the entire model. All data cards (Fig. 56, 57) are read by the main module and data transfer to the other modules is made in accordance with control requirements of Card Type No. 1 (Fig. 56).

The main module begins by reading the data cards. The data cards may be in any order as long as each group of data cards is together and the Type 1 card is first. The program will transfer from the data reading phase to the execution phase when it reads the control card for the next execution or when it reads a blank card indicating the end of all data. It is not necessary to repeat all data cards for successive runs. Only the new control card and those cards requiring change need be submitted. For instance, if only one card of the channel section cards is

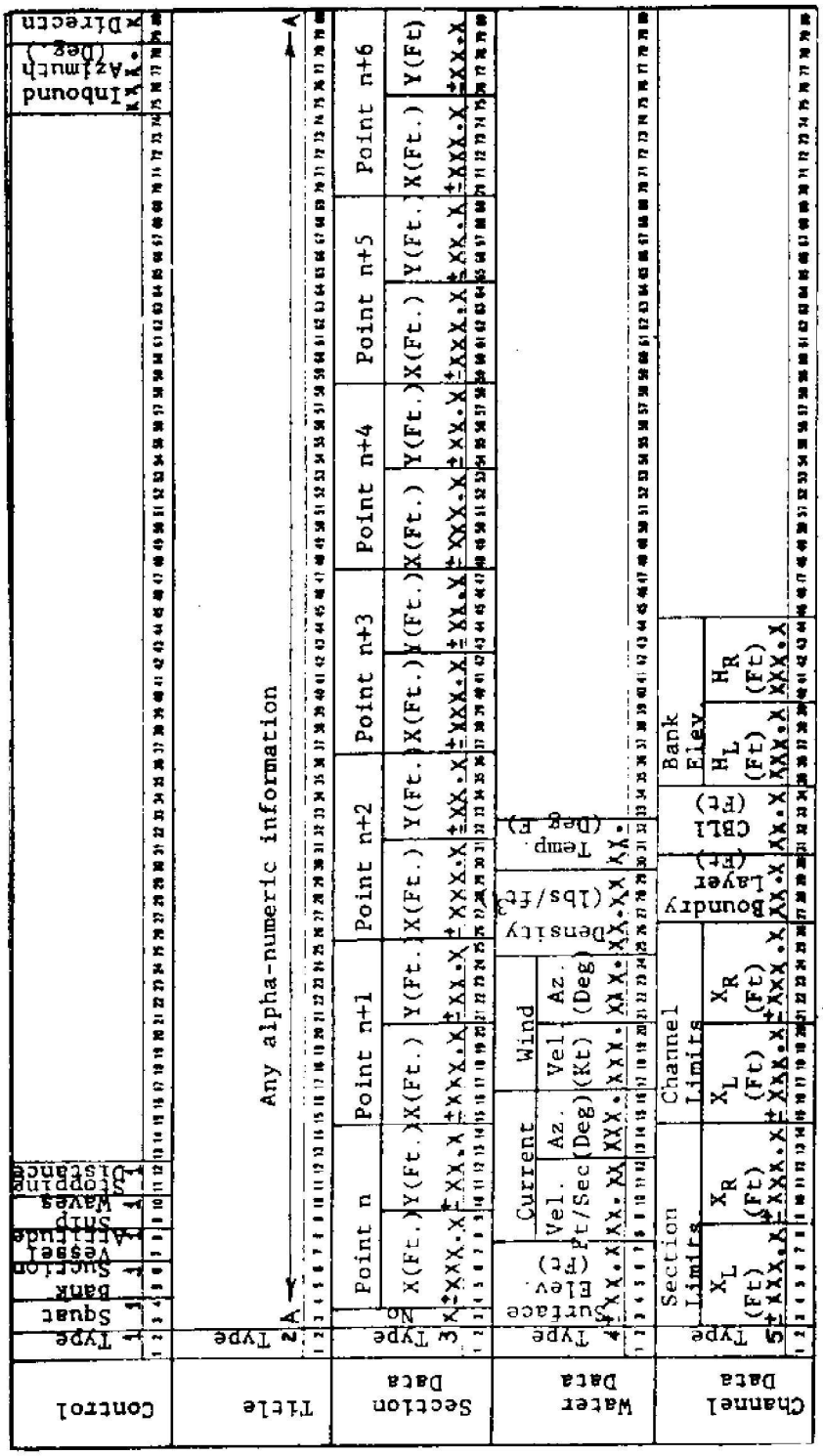

FIG. 56 - INPUT FORMAT-CARD TYPES 1 THRU 5

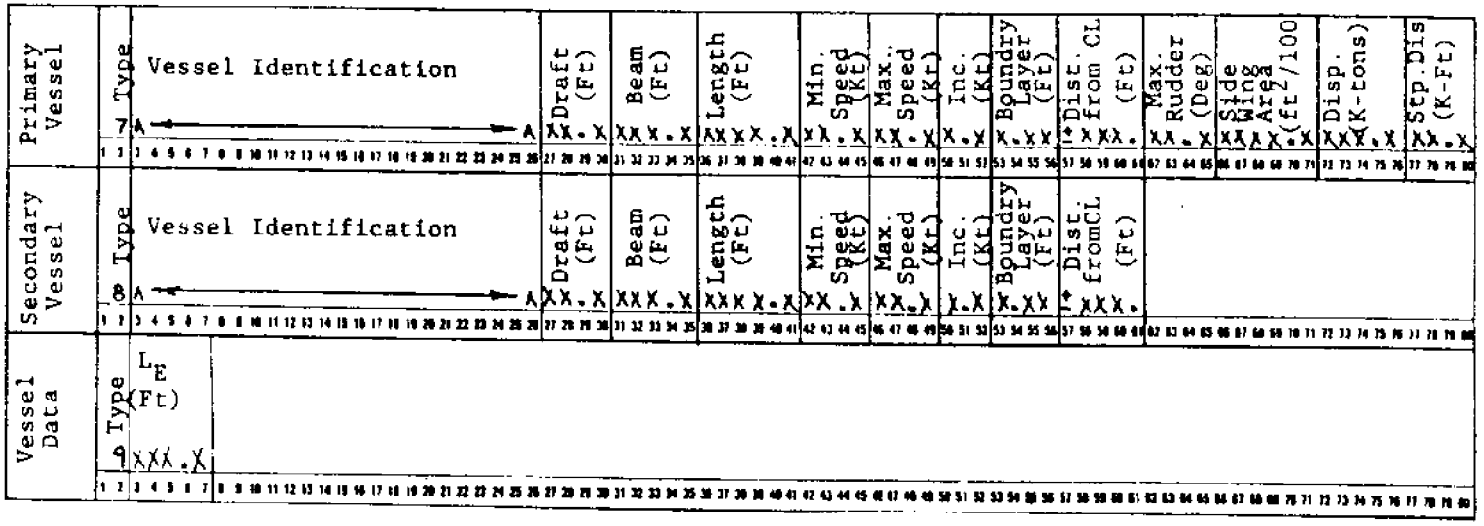

FIG. 59-INPUT FORMAT - CARD TYPES 7 THRU 9

to be changed, only that card preceded by the new control card need be submitted for the next successive run. The new data card will be catalogued into the correct position and execution continued. Once the execution phase has begun, the main control module will call into memory and transfer control to the various modules selected for execution as indicated on the control card. As soon as one module has completed its task, control returns to the main module and the next module is selected. Any number of successive runs may be loaded at one time. Along with its control functions the main module also breaks down wind and current data into component values for use in other modules.

Input Data Cards

Card Type 1, Control, (Fig. 56, p. 109) contains the control information required by the main module to select the type of analysis desired. A "1" punched in any one of the control columns (columns 4-12) will select that particular module for execution. A "0" or blank in these columns will omit that particular analysis from that particular run. The in-bound azimuth (columns 75-78) depicts the azimuth of the vessel in-bound. This is very important as the wind and current data will be broken into components in relation to this azimuth. The direction code in column 80 selects the desired direction(s) of the vessel during the squat analysis. A "1" indicates in-

bound only, a "2" indicates out-bound only, and a "0" in this column indicates that both the in-bound and out-bound analysis is required. The in-bound and out-bound analysis will be identically the same if there is no current. However, if a value of current is indicated, this will either be added to or subtracted from the vessel velocity to give the correct value of squat for those conditions. It should also be kept in mind that if vessel attitude is required, the bank suction module must also be requested as information from one is used in the other. Also, the selection of the bank suction module will automatically pull in the module dealing with the neutral steering line. If the exact location of this line is required as part of an analysis, the bank suction module must be selected.

Card Type 2, Title, (Fig. 56, p. 109) is used for inputting title information. The information in columns 3-80 may be any alphanumeric characters and will be printed as soon as entered into the system. There is no practical limit to the number of title cards that may be used.

Card Type 3, Section Data, (Fig. 56, p. 109) describes the cross-section of the channel itself. This card contains a series of points describing the channel from left to right, in-bound. There are seven points per card and one may use up to seven cards or 49 points. The center-

line of the channel is taken as 0. Points to the left of the centerline will have a negative X value, points to the right of the centerline will have a positive X value. The Y values can be either positive or negative but must increase as the elevation increases. This means that one may input the Y values either as plus and minus values about mean sea level. The user must indicate the correct card number from 1 through 7 in column 3.

Card Type 4, Water Data, (Fig. 56, p. 109) supplies most of the information relative to the channel water conditions. The water surface elevation has the same requirements and restrictions as a Y value on the Card Type No. 3. It may be either positive or negative but must increase as the elevation of the water surface increases. It must have the same base datum as the information given on Card Type 3. The current data is in the form of velocity in feet per second and azimuth in degrees. The wind data is supplied in knots and its directional azimuth in degrees. The water density is given in pounds per cubic foot because this is the form most readily available to the designer. If this field is left blank, the model assumes 64 lbs./cu.ft. The water temperature is in degrees Fahrenheit.

Card Type 5, Channel Data, (Fig. 56, p. 109) describes

the various limits of the channel cross-section and channel bottom. The section limits of Card 5 describe the extreme left and extreme right X values of the channel cross-section. These particular values are of little importance if the channel is of the restricted type, however, if it is of the open type, these values become very important in defining the amount of water taken into consideration for the various analyses performed by the model. The channel limits are normally taken as the prism lines of the channel bottom. These values are used to terminate ship-generated wave calculations. The data entry labeled "Boundary Layer" is the boundary layer on the channel next to the mid-body of the vessel. If a "0" or positive value is entered, the model will use this exact value in all of its computations. However, if a negative value is entered, the model will calculate the value of the displacement thickness at that location considering the speed of the vessel, the current, the temperature of the water, etc. The next data entry labeled CBL1 is the channel boundary layer value in front of the vessel. The next entries labeled "Bank Elevations" are the elevations of the near banks on left and right sides of open channels, in feet, using the same datum as the information given in Card Type 3. This information is used in reducing bank suction values in open channels.

Card Type 7, Primary Vessel, (Fig. 57, p. 110) describes the various parameters associated with the design vessel itself. The vessel identification may contain any alphanumeric data desired. The draft and beam field entries are self-explanatory. For more accurate results, the length between perpendiculars should be entered in the length field. The minimum speed is the lower parameter for speed iteration. This is usually the speed required by the design vessel for steerage. The maximum speed is that speed selected by the designer above which the model will not iterate. The increment is that speed selected by the designer to be added for each iteration. The boundary layer value is the thickness of the boundary layer at the middle-body of the design vessel. As before, if the value is "0" or positive, that value will be used in the various computations, if the value is negative the displacement thickness will be computed by the model for each speed. The next data item, distance from centerline, is the distance that the design vessel is away from the centerline of the channel. The model assumes that the centerline of the channel has an X-coordinate of "0". This particular distance is used in the bank suction computations. The designer need not concern himself with the shift in the neutral steering line due to an asymmetric channel. This shift in the neutral steering line will be computed

by the model and the distance will be adjusted using this distance from centerline. The side wind area is the designer's estimate of the total area exposed to lateral wind forces in hundreds of square feet. This value will change considerably between types of ships and also with the loading condition of a particular ship. Maximum rudder is the maximum rudder deflection possible from centerline to one side. This is normally approximately thirty-five degrees. The designer may subtract from this value whatever amount of rudder swing he wishes to reserve for emergency maneuvering. The displacement data field is for the displacement of the design vessel in thousands of long tons. The stopping distance input field is for the desired stopping distance of the design vessel in thousands of feet.

Card Type 8, Secondary Vessel, (Fig. 57, p. 110) contains the same type of data required for the primary or design vessel required by Card 7. The secondary vessel is used by the model to compute squat values in the passing and overtaking conditions.

Card Type 9, Vessel Data, (Fig. 57, p. 110) contains the entrance length, L_E , of the design vessel. If this value is unknown, this field should be left blank. The model will then compute a value for L_E.

Fig. 58 shows a typical navigation channel cross-section which has been used as a sample problem. Fig. 59 shows the input data cards for this sample problem.

All of the figures illustrating output reports throughout the remainder of this chapter are from this sample problem. It was specifically designed to contain most of the oddities that one might find in a real-life navigation channel design.

Squat Computation

The squat module begins by checking the salinity of the water. If the water is brackish, an adjustment in the draft of the vessel is made. Certain information about the vessels, water surface elevation, current components, etc. is printed at the top of the report including the adjusted draft value (Fig. 60). The program then computes squat values for the primary vessel for both the on-centerline and the while-passing conditions for each speed desired. Values of the displacement thickness for the primary vessel, the secondary vessel, and the channel are also printed. A special code is printed to indicate whether the boundary layer was either turbulent (T) or laminar (L). The kinematic viscosity used by the module in its calculation is also listed for the general information

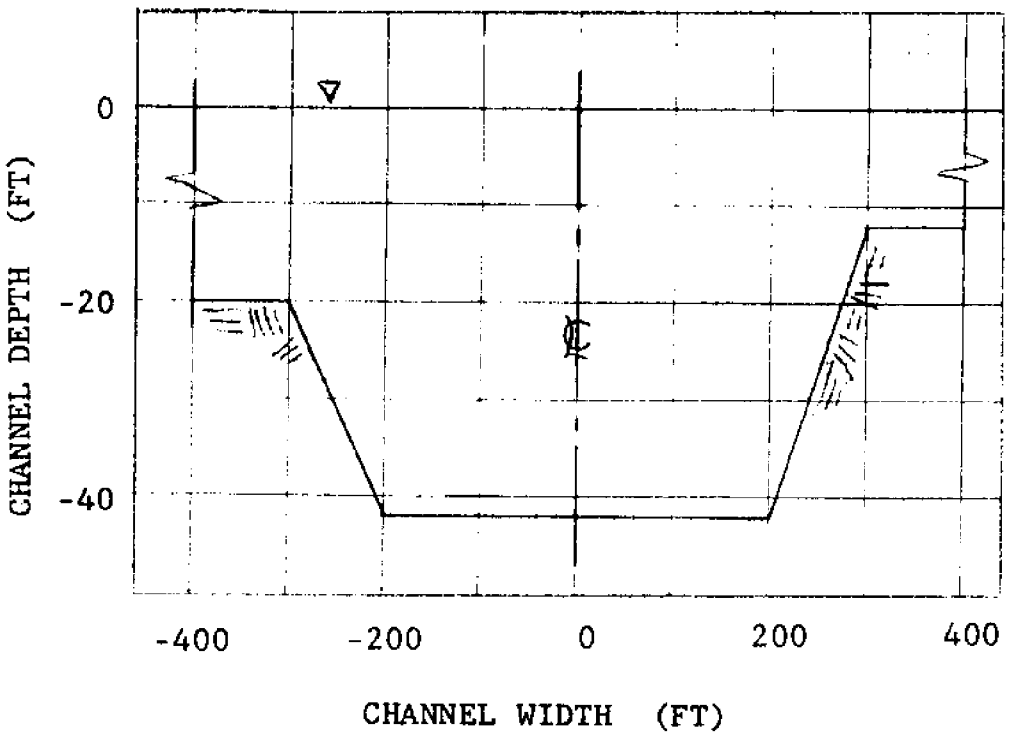

FIG. 58-NAVIGATION CHANNEL CROSS-SECTION

```
$DATA
 1 1 1 1 1 1                                                                  190, 0
 2SAMPLE PROBLEM TEXAS CLIPPER
 31-400,0-20,0-300,0-20,0-200,0-42,0 200,0-42,0 300,0-12,0 400,0-12,0
 4  0,0 2,00 20,  6, 70,63,5070,
 5-300,0 300,0-200,0 200,0 -,1 0,0-20,0-12,0
 7TEXAS CLIPPER           22,0 66,5 450,0 4,012.02.0-,10 100,35.0  110,011,4 2,0
 8MANCHASTER COMMERCE     37,0 62,0 470,0 6,0       0,0
 9
```

FIG. 59-SAMPLE PROBLEM INPUT DATA

SAMPLE PROBLEM TEXAS CLIPPER

SQUAT COMPUTATION
****

WATER SURFACE ELEV, 0.0 FT CURRENT COMPONENT -1.167 KT

PRIMARY VESSEL TEXAS CLIPPER

DRAFT 22.0 FT BEAM 66.5 FT LENGTH 450.0 FT

SECONDARY VESSEL MANCHASTER COMMERCE

DRAFT 37.0 FT BEAM 62.0 FT LENGTH 470.0 FT

SECTION LIMITS LEFT -300.0 FT RIGHT 300.0 FT

DRAFT IN BRACKISH WATER

PRIMARY 22.2 FT SECONDARY 37.3 FT

PRIMARY VESSEL SQUAT

SHIP DIRECTION	VESSEL SPEED (KT)	SQUAT ON CENTERLINE (FT)	SQUAT WHILE PASSING (FT)	BOUNDARY LAYERS (FT) V1	V2	CH	KINEMATIC VISCOSITY
INBOUND							
	4.0	0.2	0.6	0.233 T	0.000	0.376 T	0.1095E-04
	6.0	0.5	1.4	0.218 T	0.000	0.348 T	0.1095E-04
	8.0	0.9	2.9	0.207 T	0.000	0.321 T	0.1095E-04
	10.0	1.6		0.199 T	0.000	0.299 T	0.1095E-04
CRITICAL VELOCITY ON CENTERLINE = 12.6							
OUTBOUND							
	4.0	0.1	0.2	0.262 T	0.000	0.428 T	0.1095E-04
	6.0	0.2	0.5	0.236 T	0.000	0.383 T	0.1095E-04
	8.0	0.4	1.2	0.220 T	0.000	0.351 T	0.1095E-04
	10.0	0.8	2.6	0.209 T	0.000	0.326 T	0.1095E-04
	12.0	1.4		0.201 T	0.000	0.303 T	0.1095E-04

FIG. 60-SAMPLE SQUAT COMPUTATION LISTING

of the designer. The squat computation is terminated when the incremented speed reaches the maximum value, the critical velocity, or the vessel strikes the bottom of the channel. These calculations will be carried out for each speed increment for in-bound or out-bound transits or both as directed by the designer on the control card.

Neutral Steering Line and Bank Suction

When bank suction calculations are requested on the control card, the first program entering main memory is the neutral steering line module. This part of the model computes many values used in the bank suction module but of greatest interest to the designer is the distance from the centerline to the new neutral steering line of the channel. This value along with other items is printed on the bank suction report (Fig. 61). Once the neutral steering line has been determined, the bank suction module is automatically brought into memory. This program computes and lists the lateral force in long tons and the moment in foot-tons due to bank suction effects for each value of vessel speed requested. These values are for a particular distance off the centerline for a symmetric channel, or they could be for on-centerline due to the shift in the neutral steering if an asymmetric channel is described. In themselves these forces are of little value to

BANK SUCTION COMPUTATION
****

VESSEL TEXAS CLIPPER

DRAFT 22.0 FT BRACKISH DRAFT 22.2 FT BEAM 66.5 FT LENGTH 450.0 FT X-OFF 100.0 FT

SECTION DATA

SECT. LIMIT-LEFT -300.0 FT CHANNEL-LEFT -200.0 FT CHANNEL-RIGHT 200.0 FT SECT. LIMIT-RIGHT 300.0 FT

WATER DATA

SURFACE ELEV. 0.00 FT CURRENT COMPONENT -1.167 KT

DEPTH - LEFT OVERBANK 20.00 FT HYDRAULIC DEPTH 37.67 FT DEPTH - RIGHT OVERBANK 12.00 FT

NEUTRAL STEERING LINE

NSL -44.6 FT R-SECTION 37.24 FT R-LEFT 37.34 FT R-RIGHT 37.17 FT

DIMENSIONLESS FACTORS

X-BAR =-0.176 ALPHA = 0.825 CF = 0.0485

BANK SUCTION DATA

VESSEL SPEED (KT)	FORCE (TONS)	MOMENT (FT-TONS)
4.0	1.83	-145.12
6.0	3.92	-279.21
8.0	5.76	-456.78
10.0	8.55	-677.84

FIG. 61-SAMPLE BANK SUCTION COMPUTATION LISTING

the navigation channel design engineer. However, these forces and moments are neutralized by vessel drift angle and rudder action computed in the module on vessel attitude.

Vessel Attitude

The vessel attitude module first computes the values of forces created by cross-currents and winds and adds them to the lateral force computed in the bank suction module. The module then determines the amount of rudder and drift angle required to overcome these computed values of moment and force. The model neutralizes these forces and moments in the same manner that a pilot would on a prototype vessel. Rudder angle in the correct direction is applied to counteract the yawing moment. Drift angle is then added to neutralize the lateral forces. As drift angle is applied, additional yawing moment is generated. Adjustments are then made to the rudder angle to compensate for this additional yawing moment. The listing produced by the vessel attitude module includes the identification of the design vessel, the various wind and current component forces in long tons, and the maximum rudder angle indicated by the design engineer (Fig. 62). This report also lists the total moments in foot-tons, the total force in long tons, and the drift and rudder angles to overcome these

forces and moments for every speed indicated. If the rudder angle exceeds the maximum rudder angle indicated by the designer, a value of 9999.9 will appear in the rudder angle field. The cutoff for this iterative process is similar to that for the squat computations Values of speed above the critical or maximum values will not be used in these computations. The design engineer using the drift angle value can compute the additional width of channel used by the design vessel. He may also verify the safety of vessel operation in regard to allowable rudder angle.

VESSEL ATTITUDE

VESSEL TEXAS CLIPPER

WIND FORCE = 8.5 TONS CURRENT FORCE = 6.9 TONS MAX. RUDDER 35.0 DEG.

SPEED (KTS)	TOTAL MOMENT (TON-FT)	TOTAL FORCE (TONS)	DRIFT ANGLE (DEG)	RUDDER ANGLE (DEG)
4.0	+145.1	9.5	1.9	-28.0
6.0	+279.2	11.0	1.0	-18.0
8.0	+456.8	13.2	0.7	-14.0
10.0	+677.0	16.8	0.5	-11.8

FIG. 62-SAMPLE VESSEL ATTITUDE LISTING

Ship-Generated Waves

The ship-generated wave module will compute the value of the ship wave height at the vessel. It will also compute the value of the wave height at each cusp as the wave propagates out from the sailing line. The report from this module first lists the velocity of the vessel, the Froude number, and the wave height at the vessel. The program will then compute and list the cusp number, the wave height at that cusp, the Y distance from that cusp to the sailing line and finally the distance, R, from that cusp along the cusp line to the bow of the vessel (Fig. 63). These computations are terminated at the extreme far side of the channel. The main purpose of this ship-generated wave data is to determine the effects of ship passage on barge trains

SHIP GENERATED WAVE COMPUTATION

SHIP VELOCITY = 10.0 KNOTS FR = 0.296 WAVE AT SHIP = 4.32 FT

CUSP NO.	WAVE HEIGHT(FT)	Y(FT)	R(FT)
1	3.20	37.	112.
2	2.75	59.	177.
3	2.46	80.	241.
4	2.30	102.	305.
5	2.15	124.	370.
6	2.04	145.	434.
7	1.99	166.	498.
8	1.87	187.	562.
9	1.81	209.	627.

FIG. 63-SAMPLE SHIP-GENERATED WAVE COMPUTATION LISTING

Stopping Power Computation

The stopping distance module computes the thrust required to stop the vessel in the specified distance from each vessel speed. The output is in the form of pounds per ton of mass. This value may be used by the designer as an indication of the reasonableness of this distance requirement (Fig. 64).

STOPPING POWER COMPUTATION
****

VESSEL TEXAS CLIPPER

DISPLACEMENT 11400, TONS (L)

REQD, STOPPING DIST, 2000,

VESSEL SPEED (KTS)	REQD THRUST/MASS (LBS/TON)
4.0	0.8
6.0	1.9
8.0	3.5
10.0	5.8
12.0	8.8

FIG. 64-SAMPLE STOPPING POWER COMPUTATION LISTING

CHAPTER IX

SUMMARY AND CONCLUSIONS

Summary

A gap exists between the knowledge of naval architecture and coastal engineering possessed by the channel design engineer and that required by him to analyze, design and review deep-draft navigation channels. At the present time this knowledge cannot be obtained from either reference material or formal education. To help fill this gap, a computerized mathematical channel design model has been developed.

The channel design model provides the engineer with a powerful tool to determine the behavior of the design vessel in any straight section of the proposed restricted waterway. The model requires as input data only that information that is readily available to the engineer. Detailed information about a specific vessel is not required as the design vessel is normally not an existing vessel at all. The accuracies of the results produced are well within the requirements of a design of this type. Although the channel design model is already a powerful design tool, it is the author's hope that it will serve as a basic framework on

which to build additional capabilities as the state-of-the-art progresses.

Future Research and Study Requirements

During the development of this model the author found certain areas that require further study. Certainly the existing model should be further tested against prototype data. Several areas could be checked without a great deal of expense. An arrangement with the Houston Pilots Association or like organizations could provide data to further verify the neutral steering line, the drift angle, and the rudder angle portions of the model.

It would be desirable to find some ratio of ship dimensions that could be used to determine the vertical side projection area used in the lateral wind force computation. The relationship could be derived by vessel type and class from data supplied by the American Bureau of Shipping.

A method for determining the additional values of squat at the channel prism line should be sought. A starting point is the lateral force due to bank suction effects. This is currently being provided by the bank suction module of the model. It is now required to find the value of the hydraulic gradient between the two sides of the design vessel. An attempt was made by the author to determine this

gradient, however, the value of the difference in the velocity head on either side of the vessel is unknown and is too significant to ignore. It is believed that a method for determining this additional squat could be developed through extensive model testing.

The current design model produces values for lateral forces and yawing moments caused by bank suction effects in relatively well-defined restricted channels only. Limiting values of present equation parameters should be found to determine the bank suction forces and moments for an infinitely wide channel. These values would be of great help in determining the dangers of bank suction forces at channel entrances and during coast-wise transits. Again these values could be determined through model testing.

The question arose during this study as to whether a vessel proceeding with a drift angle on the vessel would produce a larger ship-generated wave because of the greater cross-sectional area taken by a ship in this position. From what has already been discussed about the wave-making parameters of a vessel, one would intuitively believe that higher waves would be generated. The extent of this increase could be found from model testing.

During the course of this study it also became apparent that additional models would eventually be required.

The first of these would be a model to determine vessel behavior in curved sections of a restricted waterway. Some of the modules of the current model could be used in this curved waterway model, however, others would have to be added. Centrifugal force would have to be added to the bank suction forces and the degree of curve would have to be taken into consideration when calculating drift and rudder angles. A considerable amount of information is already in existence and it is believed that a comparable, state-of-the-art model could be produced.

Another model should be developed to determine the values of roll, pitch, and heave caused by open ocean wave action on a vessel approaching the navigation channel entrance. The model would be used by the design engineer to determine the contour that the channel must be dredged to in order to prevent the design vessel from striking the bottom of the channel. It would also be used to determine the economic length of any jetty system protecting the channel entrance. The author at first believed that he could include such a module as part of the present channel design model. However, he found that the present state-of-the-art would not permit this and still keep within the philosophy of the present model. At present, too much specific, detailed information must be known about the vessel to produce any results whatsoever, and so no generalized,

limited solution is currently possible. A tremendous amount of research would go into such a model but its cost is economically justified when one considers the initial costs of dredging and jetty construction along with the repeated cost of maintenance dredging.

In order to complete the total spectrum of analysis, design and review of navigation channels, a channel operation model should be developed. This model should simulate the everyday workings of the harbor channel system itself. It would yield valuable data reflecting the operational and economic efficiency of a channel system and could be used to select the most effective channel design from the many alternates studied. It could also be used in determining cost-benefit ratios. As a review tool this model could be used by regulatory officials in determining the best alternative between expedited maintenance dredging and temporary one-way transit restrictions for a channel where extensive shoaling has occurred. The state of the art of computer simulation and maritime information availability is currently sufficient to build such a model. Its creation and calibration would be costly, however the benefits derived from such a project would more than justify the cost expenditures.

Conclusions

The mathematical model described herein is a new concept in ship channel analysis, design and review. The current criteria-ratio approach to design is inadequate to provide safe, efficient and effective channel systems.

The main assumption of the author which permeates the entire channel design model is that the design engineer has very little detailed information regarding the design vessel. This is evident from the data furnished channel designers by the Office of the Chief of Engineers shown in Table 6 (p. 103). A comprehensive analysis of a navigation channel can be performed using the model with these limited data.

Its relative completeness helps to prevent errors of omission. Its inclusion of local wind and current data tailors the analysis to the specific site location and the overall accuracy of the results is more than adequate.

Successive runs with changed parameters can indicate both the economic and operational sensitivity of these parameters which should lead to a very effective end product. New design considerations can now be effected. For instance, through successive runs of the model the location of the neutral steering lines in transitioning sections of the channel can be found and matched to help achieve greater

steering stability for ships transiting these sections.

The model's shortcomings have already been discussed in the future research and study requirements above. One can assume that many others will surface through usage.

In conclusion, although the navigation channel design model is a very powerful tool at present, it is really only a first step toward safer and more efficient navigable waterways for the nation.

APPENDIX I

REFERENCES

1. Abramowitz, M., and Stegum, I. A., gen. ed., Handbook of Mathematical Functions, National Bureau of Standards, U. S. Department of Commerce, June 1964.

2. Ammar, A. A., Mobarek, I. E., and Hilaly, N., "Design of Navigation Channel Cross-Section and Alignment," Proceedings of the XXIInd International Navigation Congress, PIANC, Paris, 1969

3. Balanin, V. V., and Byvok, L. S., "Selection of Leading Dimensions of Navigation Channel Sections and Modern Methods of Bank Protection," Proceedings of the XXIst International Navigation Congress, PIANC, Stockholm, 1965.

4. Barnaby, K. C., Basic Naval Architecture, Hutchinson Scientific and Technical, London, Sixth Ed., 1969.

5. Bascom, W., Waves and Beaches, Anchor Books, Doubleday and Co., New York, 1964.

6. Bindel, S., Turning Characteristic Coefficients for a Cargo Ship and a Destroyer, Report 1461, David Taylor Model Basin, U. S. Navy, Oct. 1960.

7. Brard, R., "Maneuvering of Ships in Deep Water, in Shallow Water, and in Canals," Paper presented at Society of Naval Architects and Marine Engineers meeting, Washington, D.C., Sept. 1951.

8. Brebner, A., Helwig, P. C., and Carruthers, J., "Waves Produced by Ocean-Going Vessels: A Laboratory and Field Study," Proceedings of the Tenth Coastal Engineering Conference, Tokyo, 1966.

9. Carlstrom, C. G., "Measuring of Squat in Fairways to the Port of Lulea, North Sweden," Proceedings of the Eleventh Conference on Coastal Engineering, London, England, Sept. 1968.

10. Comstock, J. P., Principles of Naval Architecture, SNAME, New York, N. Y., 1967.

11. Coonrod, Jim, Captain, Galveston-Texas City Pilots Assn., Galveston, Texas. Interview, June 1976.

12. Crenshaw, R. S., Naval Shiphandling, U. S. Naval Institute, Annapolis, 1965.

13. Das, M. M., Relative Effect of Waves Generated by Large Ships and Small Boats in Restricted Waterways, Report No. HEL-12-9, University of California, Berkeley, Nov. 1969.

14. D'Arcangelo, A. M., gen. ed., Guide to the Selection of backing Power, Technical and Research Bulletin No. 3-5, Panel M-9, SNAME, 1957.

15. Dickson, A. F., "Navigation of Tankers Through Channels," Sect. II, Subject 2, Proceedings of the XXth International Navigation Congress, PIANC, Baltimore, 1961.

16. Dykhuis, A., North Sea Canal, Delft Hydraulic Laboratory, Translated by the U. S. Army Topographic Command, 1969.

17. Eda, H., Directional Stability and Control of Ships in Restricted Channels, SNAME, New York, 1971.

18. Eda. H., "Dynamic Behavior of Tankers During Two-Way Traffic in Channels," Marine Technology, SNAME, New York, 1973.

19. Eda, H., Ship Controllability in Channels, Davidson Laboratory, Stevens Institute of Technology, Hoboken, 1969.

20. Eden, E. W., "Vessel Controllability in Restricted Waters," Journal of the Waterways, Harbors, and Coastal Engineering Division, ASCE, Vol. 97, No. WW3, Proc. Paper 8310, Aug. 1971, pp. 475-490.

21. Fluor Ocean Services, Inc., "Vessel Design Characteristics," Houston, Tx., Sept. 1970.

22. Garthune, R. S., Rosenberg, B., Cafiero, D., and Olson, C. R., The Performance of Model Ships in Relation to the Design of the Ship Canal, Report 601, David Taylor Model Basin, 1948.

23. Guliev, U. N., On Squat Calculations for Vessels Going in Shallow Water and in Channels, PIANC, 1971.

24. Hewins, E. F., and Ruiz, A. L., Calculation of Stopping Ability of Ships, Technical and Research Bulletin No. 3-4, Panel M-9, SNAME, 1954.

25. Johnson, J. W., "Ship Waves at Recreation Beaches," Shore and Beach, April, 1969.

26. Johnson, J. W., "Ship Waves in Navigation Channels," Proceedings of the Sixth Coastal Engineering Conference, Miami, 1958.

27. Johnson, J. W., "Ship Waves in Shoaling Waters," Proceedings of the Eleventh Coastal Engineering Conference, London, 1968.

28. Johnson, J. W., Das, M. M., "Waves Generated by Large Ships and Large Boats," Proceedings of the Twelfth Coastal Engineering Conference, Washington, 1970.

29. Kline, S. J., Sovran, G., Morkovin, M. V., and Cockrell, D. J., gen. ed., Proceedings Computation of Turbulent Boundary Layers-1968, AFOSR-IFP-Stanford Conference, Vol. 1, Stanford University, California, 1969.

30. Koster, J., Suction Effect of Canal Banks on Ship Behaviour, Publication No. 91, Delft Hydraulics Laboratory, 1971.

31. Kostyukov, A. A., Theory of Ship Waves and Wave Resistance, Effective Communications, Inc., Iowa City, Iowa, 1968.

32. Kray, C. J., "Design of Ship Channels and Maneuvering Areas," Journal of the Waterways, Harbors, and Coastal Engineering Division, ASCE, Vol. 99, No. WW1, Feb. 1973.

33. Lamb, Horace, Hydrodynamics, Dover Publications, New York, 1945.

34. Lane, John, Captain, Texas Maritime Academy, Galveston, Texas. Interviews, 1975-1976.

35. Lloyd's Register of Shipping, Register Book 1965-66, Vol. II, London, July, 1965

36. Moody, C. G., The Handling of Live Super Ships Through Gaillard Cut of the Panama Canal, Report 1277, David Taylor Model Basin, Navy Dept., Oct 1958.

37. Moody, C. G., The Handling of Ships Through a Widened and Asymmetrically Deepened Section of Gaillard Cut in the Panama Canal, Report 1705, David Taylor Model Basin, Dept. of the Navy, Aug. 1964.

38. Moody, C. G., The Stopping of Large Bulk-Cargo Ships in a Canal, Naval Ship Research and Development Center, March 1970.

39. Norrbin, N. H., Bank Effects on a Ship Moving Through A Short Dredged Channel, Swedish State Shipbuilding Experimental Bank, Sweden, 1974.

40. Pearson, James, Captain, Houston Pilots Assn., Houston, Texas. Interview, April 1973.

41. Phillips, Edwin, Chief Naval Architect, Designers and Planners, Inc., Galveston, Texas. Interview, May 1976.

42. Saunders, H. E., Hydrodynamics in Ship Design-Vol. II, Society of Naval Architects and Marine Engineers, New York, 1957.

43 Schlichting, H., Boundary-Layer Theory, Sixth Ed., McGraw-Hill Book Company, New York, N. Y., 1968

44. Schoenherr, K. E., Data for Estimating Bank Suction Effects in Restricted Water and on Merchant Ship Hulls, Report 1461, David Taylor Model Basin, U. S Navy, Oct. 1960.

45. Sorensen, R. M., Investigation of Ship-Generated Waves, HEL-12-1, University of California, Berkeley, April, 1966

46. Sorensen, R M, "Water Waves Produced by Ships," Journal of the Waterways, Harbors, and Coastal Engineering Division, ASCE, Vol 99, No. WW2, May 1973

47. Sorensen, R. M. "Waves Generated by Model Ship Hull," Journal of the Waterways and Harbors Division, ASCE, Vol. 95, No. WW4, November, 1969.

48. Sorensen, R. M., "Waves Generated by Moving Ship," Shore and Beach, April, 1967.

49. Streeter, V. L., Fluid Mechanics, McGraw-Hill Book Co., New York, N. Y., 1971.

50. Tothill, J. T., Ships in Restricted Channels, Report MB-264, National Research Council of Canada, Ottawa, Jan. 1966.

51. Wicker, C. F., ed., Evaluation of Present State of Knowledge of Factors Affecting Tidal Hydraulics and Related Phenomena, Report No. 3, Committee on Tidal Hydraulics, Corps of Engineers, U. S. Army, May 1965.

52. Wigley, C., gen. ed., "The Propagation of Groups of Waves in Dispersive Media, with Application of Waves Produced by a Traveling Disturbance," The Collected Papers of Sir Thomas Havelock on Hydrodynamics, Office of Naval Research, Department of the Navy, 1963.

Supplemental Sources Consulted

Abkowitz, M. A., Stability and Motion Control of Ocean Vehicles, Massachusetts Institute of Technology, 1972.

Bindel, S., Experiments on Ship Maneuverability in Canals as Carried out in the Paris Model Basin, Paris, undated.

Biswas, A. N., and Bhattacharya, S. K., "Evaluation of Harbor Deepening Projects," Journal of the Waterways, Harbors, and Coastal Engineering Division, ASCE, Volume 99, No. WW1, February 1973.

Biswas, A. N., "Selection of Optimum Size of Vessel in Relation to the Voyage Distance," Proceedings of the Institution of Civil Engineers, September 1973.

Blagoveshchenski, S. N., Theory of Ship Motions, Dover Publications, New York, 1962.

Carroll, J. L., and Bronzini, M. S., Planning for Coastal Ports on a Systems Basis: Preliminary Methodological Design, Pennsylvania State University, University Park, Pennsylvania, May 1972.

Constantine, T., "The Behavior of Ships Moving in Restricted Waterways," Proceedings of the Institution of Civil Engineers, London, 1961.

Costa, F. V., and Leipe, J. G., "Influence of the Period of the Waves and of the Velocity of the Ship on the Depth Required in Port Approaches," Proceedings of the XXIst International Navigation Congress, Permanent International Association of Navigation Congresses, Stockholm, 1965.

Def.Quinn, A., Design and Construction of Ports and Marine Structures, McGraw-Hill Book Company, New York, 1972.

Department of the Army, Port Construction and Rehabilitation, TM 5-360, September, 1964.

Department of the Navy, Design Manual-Harbor and Coastal Facilities, DM-26, NAVFAC, July, 1968.

Department of Transportation, U. S. Coast Guard, Load Line Regulations, Subchapter E, February, 1971.

Dickson, A. F., "Underkeel Clearance Required for Tankers in Port Approaches and Seaberth Subject to Wave Action," Proceedings of the XXIst International Navigation Congress, Permanent International Association of Navigation Congresses, Stockholm, 1965.

Dickson, A. F., "What the Engineer Should Know About Ship Handling Problems," Proceedings of the Institution of Civil Engineers, London, November 1971.

Dickson, A. F., Potter, J. H., and Agar, M., "Port Approach Facility for Tankers, Approach Channel Characteristics, and a Floating Off-Shore Tanker Discharge Berth," Proceedings of the XXIInd International Navigation Congress, Permanent International Association of Navigation Congresses, Paris, 1969.

Eda, H., "Steering Characteristics of Ships in Calm Water and Waves," paper presented at annual meeting of the Society of Naval Architects and Marine Engineers, New York, November 1965.

Eda, H., "Study of Ship Maneuvering-Control in Wind," Journal of Ship Research, Society of Naval Architects and Marine Engineers, 1968.

Eda, H., and Savitski, D., Cargo Ships Controllability, Stevens Institute of Technology, December, 1969.

Eda, H., and Savitski, D., Two-Way Traffic and Effectiveness of Tugs, Stevens Institute of Technology, December, 1969.

Eden, E. W., Jr., "Design of Navigation Channels," Paper presented at the 69th Meeting of Committee on Tidal Hydraulics, Charleston, South Carolina, June 1970.

Fujino, M., "Experimental Studies on Ship Maneuverability in Restricted Waters," International Shipbuilding Progress, August, 1968.

Gannett, E., Tanker Performance and Costs, Cornell Maritime Press, Inc., Cambridge, 1969.

Garrelts, E., Grosz, A., Cohler, G., Petersen, H., Wellmann, R., and Wetzel, G., "Measures in Connection with the Sailing of Large Ships in the North Sea," Proceedings of the XXIInd International Navigation Congress, Permanent International Association of Navigation Congresses, Paris, 1969.

Gillmer, T. C., Fundamentals of Construction and Stability of Naval Ships, U. S. Naval Institute, Annapolis, 1959.

Great Britain, National Ports Council, Channel Width Study, London, 1973.

Harlow, E. H., and Small, S. W., "Problems Arising from the Use of Very Large Ships in Connection with Structures for Loading and Discharging Off-Shore," Proceedings of the XXIInd International Navigation Congress, Permanent International Association of Navigation Congresses, Paris, 1969.

Hay, D., "Ship Waves in Navigable Waterways," Proceedings of the Eleventh Coastal Engineering Conference, London, 1968.

Helm, K., Mockel, W., and Woltinger, O., Interaction between Ships and Canals, translated from the German by the Waterways Experiment Station, Corps of Engineers, Vicksburg, 1973.

Henry, C. J., Savitski, D., and Breslin, J. P., Preliminary Study of Ship Maneuverability in a Canal, Stevens Institute of Technology, October, 1968.

Herbich, J. B., Coastal and Deep Ocean Dredging, Gulf Publishing Co., Houston, 1975.

Hooft, J. P., "The Maneuverability of Ships on a Straight Course," International Shipbuilding Progress, February, 1968.

Korvin-Kroukovsky, B. V., Theory of Seakeeping, Society of Naval Architects and Marine Engineers, New York, 1961.

Kray, C. J., "Handling Problems of Very Large Ships in Approach Channels and Maneuvering Areas," Permanent International Association of Navigation Congresses, Quarterly Bulletin No. 5, 1970.

LaDage, J. H., Modern Ships, Cornell Maritime Press, Cambridge, Maryland, 1965.

Lancaster, J. H., The Atlantic Pacific Interoceanic Canal Comments on Vessel Spacing in Convoy, Office of the Chief of Engineers, 1969.

Langeveld, J. M., Mazure, P. C., and Rietveld, C. F. W., "Harbor and Navigation Channel Design," Proceedings of the XXIInd International Navigation Congress, Permanent International Association of Navigation Congresses, Paris, 1969.

Lee, C. A., and Bowers, C. E., "Ship Performance in Restricted Channels," Transactions of the American Society of Civil Engineers, Vol. 114, 1949.

Lott, D. N., Collision Prevention, D. Van Norstrand Company, New York, 1947.

Madciar, J., "Future Tendencies in Sea Transportation and Their Influences on the Setup and Organization of Harbors," Marine Technology and Management, translated from the Polish, 1973.

Makela, G. A., "Design of a Navigation Channel for an Interoceanic Sea-Level Canal," Paper presented at the 69th meeting of the Committee on Tidal Hydraulics, Charleston, 1970.

McCormick, M. E., Ocean Engineering Wave Mechanics, John Wiley and Sons, New York, 1973.

McNown, J. S., Discussion-McNown on Panama Canal, Transactions of the American Society of Civil Engineers, Vol. 114, 1949.

Miller, R. L., "Prediction Curves for Waves Near the Source of an Impulse," Proceedings of the Twelfth Coastal Engineering Conference, Washington, 1970.

Moody, C. G., A Study of the Performance of Large Bulk-Cargo Ships in a Proposed Interoceanic Canal, The Naval Ship Research and Development Center, Washington, D.C., January, 1970.

Moody, C. G., Two Way Traffic for Large Bulk-Cargo Ships in Gaillard Cut of the Panama Canal, Washington, D.C., August, 1970.

Munroe-Smith, R., Notes and Examples in Naval Architecture, Edward Arnold Publishers, Limited, London.

Nagai, S., Oda, K., and Shigedo, M., "Impacts Exerted on the Dolphins of Seaberths by Roll, Sway, and Drift of Supertankers Subject to Waves and Swells," Proceedings of the XXIInd International Navigation Congress, Permanent International Association of Navigation Congresses, Paris, 1969.

Ogilvie, T. F., The Wave Generated by a Fine Ship Bow, University of Michigan, October, 1972.

Plummer, C. J., Ship Handling in Narrow Channels, Cornell Maritime Press, New York, 1945.

Reeves, J. E. and Bourguard, E. H., Design of Channel, Transactions of the American Society of Civil Engineers, Vol. 114, 1949.

Robb, A. M., Theory of Naval Architecture, Charles Griffin and Company, Limited, London, 1952

Saunders, H. E., Hydrodynamics in Ship Design-Vol. I, Society of Naval and Marine Engineers, New York, 1957.

Sorensen, R. M., "Investigation of Ship-Generated Waves, Journal of the Waterways and Harbors Division, ASCE, Volume 93, No. WW1, February 1967.

Taylor, D. W., The Speed and Power of Ships, John Wiley and Sons, New York, 1911.

Tothill, J. T., "Ships in Restricted Channels," Marine Technology, SNAME, Vol. 4, No. 2, April, 1967.

Tryde, P., and Josai, A. V., "Drag on Ships from Transverse Currents in Shallow Water," Proceedings of the XXIInd International Navigation Congress, Permanent International Association of Navigation Congresses, Paris, 1969.

Tsai, C., Study of Total Viscus and Wave Resistance of a Family of Series 60 Models, Iowa University, December, 1972.

Tuck, E. O., "Unstable Squat from Lateral Motion of Ships in Shallow Water," Journal of Ship Research, Society of Naval Architects and Marine Engineers, March, 1974.

Van Houten, L. E., "Ship Motions," Proceedings of the XXIst International Navigation Congress, Permanent International Association of Navigation Congresses, Stockholm, 1965.

Wang, H., and Hwang, L., "Behavior of a Slender Body in Shallow Water Waves," Proceedings of the Twelfth Coastal Engineering Conference, Washington, 1970.

Waugh, R. G., Jr., "Economics of Channel and Maneuvering Areas for Ships," Journal of the Waterways, Harbors, and Coastal Engineering Division, ASCE, Volume 97, No. WW4, November, 1971.

Waugh, R. G., Jr., Problems Inherent in Ship Characteristics as They Affect Harbor Design, (Unpublished).

Waugh, R. G., Jr., "Water Depths Required for Ship Navigation," Journal of the Waterways, Harbors, and Coastal Engineering Division, ASCE, Volume 97, No. WW3, August, 1971.

Wicker, C. F., "Economic Channels and Maneuvering Areas for Ships," Journal of the Waterways, Harbors, and Coastal Engineering Division, ASCE, Volume 97, No. WW3, August, 1971.

APPENDIX II

NOTATION

Many of the symbols used in this paper change in meaning from chapter to chapter in order to match exactly the notation in a referenced paper.

Chapter I

B = beam of design vessel

Chapter II

A = wetted cross-sectional area of channel w/o vessel;
A' = wetted cross-sectional area of channel after squat;
L = length of design vessel;
Q = rate of fluid flow;
V = velocity of design vessel;
d = squat;
W_0 = width of channel before squat;
$\mathfrak{M}$ = midship section area.

Chapter III

R_x = Reynolds number at distance x;
U = free stream velocity;
u = velocity of fluid at distance y;
x = coordinate distance;
y = coordinate distance;
δ = boundary layer thickness;
δ_1 = displacement thickness;
μ = viscosity;
τ = shear stress.

Chapter IV

A = cross-sectional area of channel;
B = beam of vessel;
C_F = dimensionless coefficient;
D = hydraulic depth;
d = draft of vessel;
F = lateral bank suction force;
H = channel depth;

H_1 = depth of water over near bank;
L = length of vessel;
M = yawing moment of vessel;
RF = reduction factor;
V = velocity of vessel;
W = channel width;
$\bar{X}$ = dimensionless coefficient;
Y = distance of vessel from neutral steering line;
α = ratio;
ρ = fluid density.

Chapter V

C_N = yawing moment coefficient;
C_V = velocity coefficient;
C_Y = lateral force coefficient;
F = lateral force due to wind or current;
L = length of vessel;
N = yawing moment;
S = total longitudinal area;
T = draft of vessel;
V = velocity of vessel c.g.;
W = channel width;
Y = lateral force and offset distance;
α = rudder angle;
δ = vessel drift angle;
ρ = fluid density.

Chapter VI

A = cross-sectional area at middle-body;
A = wetted area of canal;
a = wetted area of ship;
b = wave-making breadth;
C = coefficient;
c = celerity;
d = depth of water;
E = width of canal;
F = Froude number;
F_n = height factor;
F_{r_d} = Froude number based on depth;
g = acceleration of gravity;
H = wave height;
H_m = maximum wave height;

H_s = wave height at ship;
h = wave height at bow;
h_n = wave height at cusp n;
K_f = fineness ratio;
K_w = coefficient;
L = length of vessel;
L_E = entrance length;
L^* = length of curved part of bow;
n = cusp number;
T = wave period;
V_p = velocity of point;
V_s = velocity of ship;
X = coordinate distance;
Y = coordinate distance;
α = angle from sailing line;
Γ = Gamma function;
ζ_{mc} = wave height at cusp;
ρ = fluid density;
ω = distance along cusp line.

Chapter VII

F = net stopping force;
L = length of vessel;
M = mass of vessel;
R = resistance;
S = head reach;
T_1 = astern thrust;
V = velocity from which ship stops;
Δ = vessel displacement.

Chapter VIII

X = coordinate distance;
Y = coordinate distance;
R = distance along cusp line from a particular cusp to the bow of the design vessel.

Appendix III

A = wetted cross-sectional area of channel w/o vessel;
A' = wetted cross-sectional area of channel after squat;
A_s = wetted cross-sectional area of ship;

d = depth of water before squat;
d' = depth of water after squat;
g = acceleration of gravity;
Q = rate of flow before squat;
Q' = rate of flow after squat;
V = velocity of fluid on ship;
V' = $V + \Delta V$;
W = width of channel;
Δd = squat;
ΔV = increase in velocity due to bank flow;
θ = side slope of channel.

Appendix IV

A = cross-sectional area of channel w/o vessel;
A' = area of channel minus area of vessel;
C_f = coefficient of skin friction;
C^*_1 = laminar flow constant;
H_{12} = shape factor;
L = shape factor;
m = constant 4;
n = constant 6;
p = pressure;
R_n = Reynolds number;
U = fluid velocity at boundary;
U = free stream velocity;
x = distance from stem;
x_t = distance from stem to beginning of turbulent flow;
Y = beam/2 at entrance station;
Y_N = beam/2 (max.);
Δp = change in pressure;
δ_1 = displacement thickness;
δ_2 = momentum thickness;
l = length of ship;
ζ = intermediate contraction variable;
ρ = density.

Appendix V

c = celerity;
d = depth of water;
F = Froude number;
g = acceleration of gravity;
V_s = velocity of ship;
λ = wave length.

Appendix VI

d = depth of water;
F = Froude number;
g = acceleration of gravity;
V_s = vessel speed.

APPENDIX III

DERIVATION OF BASIC SQUAT EQUATIONS

ASSUMPTIONS (20, 50):

1. Friction losses may be neglected. This allows the use of Bernoulli's equation.
2. All water displaced by the vessel, moves back to fill the void astern of the ship. This allows the use of a continuity equation.
3. The ship is a prism with a cross-sectional area of that at the ship station where squat is to be determined.
4. For the range of speed associated with the squat to be determined, wave and hydrodynamic effects on the vessel may be neglected.
5. Conditions are such in the restricted waterway that transverse variations in water levels may be neglected.

DERIVATION (20, 50) See Fig. III-1 and III-2:

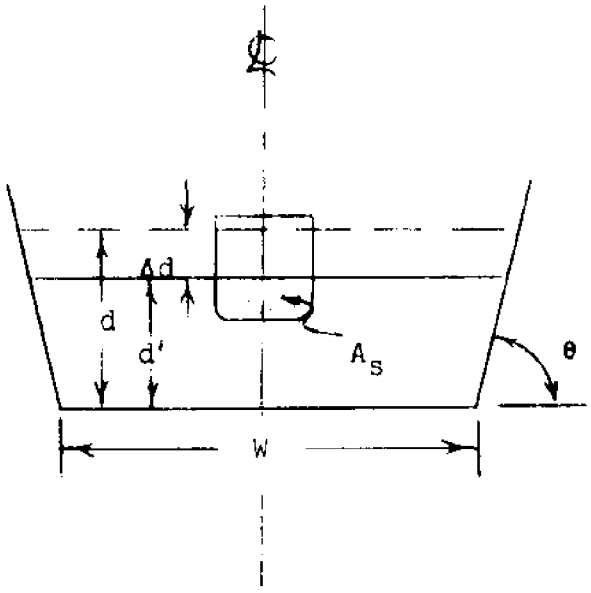

FIG. III-1-CHANNEL TERMS CROSS-SECTION

Area of water w/o ship or motion

$$A=Wd + d\cot\theta d$$

$$=Wd + d^2\cot\theta \quad \ldots\ldots\ldots\ldots\ldots\ldots\ldots \quad (1)$$

Area of water with ship and motion

$$A'=Wd' + d'^2 \cot\theta - As \quad \ldots\ldots\ldots\ldots\ldots \quad (2)$$

When ship moves through channel with velocity V, the water surface will drop by a distance Δd.

Consider the ship stationary with the water flowing past at velocity V. Ahead of the ship the total flow will be:

$$Q=AV$$

Abreast of the ship the flow will be:

$$Q'=A'(V + \Delta V)$$

Continuity dictates that:

$$Q=Q'$$

$$AV=A'(V + \Delta V) \quad \ldots\ldots\ldots\ldots\ldots\ldots\ldots \quad (3)$$

Where ΔV is the change in water velocity as $A \rightarrow A'$. Let:

$$V' = V + \Delta V \quad \ldots\ldots\ldots\ldots\ldots\ldots\ldots \quad (4)$$

Eq. (3) becomes:

$$AV=A'V'$$

Solve for V'

$$V' = \frac{A}{A'} V$$

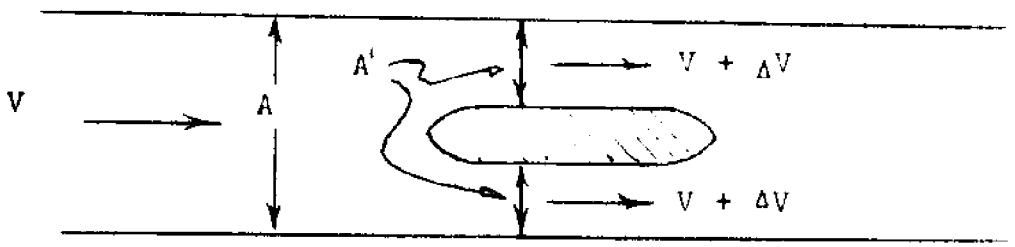

FIG. III-2-CHANNEL TERMS PLAN

The Bernoulli equation:

$$d + \frac{V^2}{2g} = d' + \frac{V'^2}{2g}$$

Solve for d:

$$\Delta d = d - d' = \frac{V'^2}{2g} - \frac{V^2}{2g}$$

Factor the 2g:

$$\Delta d = \frac{1}{2g}\left(V'^2 - V^2\right)$$

From Eq. (4) substitute for V':

$$\Delta d = \frac{1}{2g}\left[\left(\frac{A}{A'}\right)^2 V^2 - V^2\right]$$

Factor the V^2:

$$\Delta d = \frac{V^2}{2g}\left[\left(\frac{A}{A'}\right)^2 - 1\right] \quad \ldots\ldots\ldots\ldots\ldots\ldots (5)$$

Eq. (5) is the basic equation for determining squat. The squat of the vessel and the water surface is Δd.

To make the basic equation more useful, express V in Eq. (5) in knots; enumerate g:

$$\Delta d = \frac{V^2}{22.6}\left[\left(\frac{A}{A'}\right)^2 - 1\right] \quad \ldots\ldots\ldots\ldots (1)$$

Where:

Δd=Squat in feet
V=Velocity of vessel in knots. Current effects must be included.
A=Area of the selected channel w/o ship in square feet.
A'=Area of the selected channel after squat with ship cross-sectional area subtracted in square feet.

It is sometimes necessary to know the vessel velocity for a given squat:

$$V = \left[\frac{22.6\Delta d}{\left(\frac{A}{A'}\right)^2 - 1} \right]^{\frac{1}{2}} \quad \ldots\ldots\ldots\ldots\ldots (2)$$

APPENDIX IV

COMPUTATION OF ENTRANCE EFFECTS ON DISPLACEMENT THICKNESS

A complete derivation of the method of determining values for incompressible turbulent boundary layers with pressure gradients due to Truckenbrodt may be found in Chapter XXII of Schlichting (43).

To determine the displacement thickness, δ_1, in a pressure gradient which occurs along the fore-body of a vessel, one must determine the momentum thickness, δ_2, and working with various shape factors L and H_{12} finally compute δ_1.

The sample case used in the computations consisted of a restricted channel 500 ft. wide and 45 ft. deep. The vessel used was 707.5 ft. in length with a beam of 75 ft. and a draft of 40 ft. The computations used an assumed vessel speed of 10 knots with no current.

Required relative velocities were obtained from Saunders (42). See Fig. IV-1.

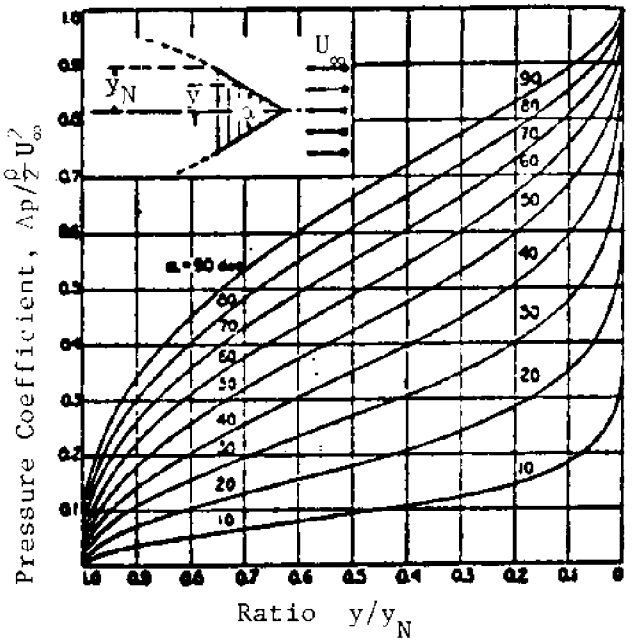

FIG. IV-1-PRESSURE COEFFICIENTS FOR FLOW ALONG A TWO-DIMENSIONAL VEE ENTRANCE (42)

The pressure coefficient, $\Delta p/((\rho/2)U^2_\infty)$, may be used to determine velocity ratios since:

$$\frac{\Delta p}{(\rho/2)U^2_\infty} = 1 - \left(\frac{U}{U_\infty}\right)^2 \quad \ldots\ldots\ldots\ldots\ldots\ldots \quad (1)$$

Where: Δp = change in pressure
ρ = density
U = velocity at the boundary
U_∞ = free stream velocity

Transposing Eq. (1)

$$\frac{U}{U_\infty} = \left(1 - \frac{\Delta p}{(\rho/2)U^2_\infty}\right)^{\frac{1}{2}} \quad \ldots\ldots\ldots\ldots\ldots\ldots \quad (2)$$

A bow angle, α, of 40° was used with a fore-body section of 103 ft. The fore-body was divided into 10 equal

segments of 10.3 ft. each and data read from the graph (Fig. IV-1).

A correction was made to the velocity ratios to account for the restriction of flow due to the vessel body being in the channel using continuity relationships.

$$\frac{U}{U_\infty}\left(\frac{A}{A'}\right) = \frac{U}{U_\infty}\ \text{corrected} \quad \ldots\ldots\ldots\ldots\ldots\ldots \quad (3)$$

Where: A = Cross-sectional area of channel w/o vessel
A' = Cross-sectional area of channel minus the cross-sectional area of vessel at that station

The expression to determine the momentum thickness, δ_2 is (43):

$$\frac{\delta_{2(x)}}{l} = \left(\frac{U}{U_\infty}\right)^{-3}\left\{C^*_1 + \left(\frac{C_f}{2}\right)^{\frac{(n+1)}{n}} \int_{x_t/l}^{x/l} \left(\frac{U}{U_\infty}\right)^{3+2/n} d\left(\frac{x}{l}\right)\right\}^{n/(1+n)} \quad \ldots\ldots \quad (4)$$

Where:
x = distance from stem
x_t = distance from stem to beginning of turbulent flow
l = length of ship
C^*_1 = laminar flow constant (see below)
C_f = coefficient of skin friction
n = 6 for high Reynolds numbers

The laminar flow constant, C^*_l, is formed from the following expression (43):

$$C^*_l = \left[\tfrac{1}{2} C_{f_l} \left(\int_0^{x_t/l} \left(\frac{U}{U_\infty} \right)^5 d\left(\frac{x}{l} \right) \right)^{\frac{1}{2}} \right]^{(n+1)/n} \quad \ldots\ldots\ldots (5)$$

Where: C_f = laminar coefficient of skin friction

The constant C^*_l takes into account the laminar portion of the boundary layer, however, since the transition point, x_t, occurs within 3 inches of the vessel stem, C^*_l is essentially zero.

The integral portion of Eq. (4) was determined using a method of quadrature the main elements of which appear in Table IV-1.

The value of the coefficient of skin friction, C_f, was determined by a method adopted by the International Towing Tank Conference (ITTC), Madrid, 1957 (10).

$$C_f = \frac{0.075}{(\log_{10} R_n - 2)^2} \quad \ldots\ldots\ldots (6)$$

Where: R_n = Reynolds number

For a Reynolds number of 1.0535×10^8, $C_f = 3.195 \times 10^{-3}$.

TABLE IV-1- δ_2 QUADRATURE ELEMENTS

1	2	3	4	5	6	7	8	9	10
Y/YN	X	X/ℓ	$\Delta p/(\rho/2)U^2_\infty$	U/U_∞	A/A'	U/U_∞	$(U/U_\infty)^{10/3}$	Coef	(8x9)
.1	10.3	.015	.595	.636	1.0135	.645	.232	4	.928
.2	20.6	.029	.510	.700	1.0274	.719	.333	2	.666
.3	30.9	.044	.480	.721	1.0417	.751	.385	4	1.540
.4	41.2	.058	.395	.778	1.0563	.822	.520	2	1.040
.5	51.5	.073	.350	.806	1.0714	.864	.614	4	2.456
.6	61.8	.087	.305	.834	1.0870	.906	.720	2	1.440
.7	72.1	.102	.260	.860	1.1029	.949	.840	4	3.360
.8	82.4	.117	.205	.892	1.1194	.998	.993	2	1.986
.9	92.7	.131	.140	.927	1.1364	1.053	1.188	4	4.752
1.0	103.0	.146	.000	1.000	1.1538	1.154	1.611	1	1.611
								Σ	=19.779

The momentum thickness, δ_2, was determined as:

$$\delta_2 = (1.154)^{-3}\left\{\left(\frac{3.195\times10^{-3}}{2}\right)^{7/6}\left(\frac{.0146}{3}\right)(19.779)\right\}^{6/7}(707.5) = .0989 \quad \cdots (7)$$

The next step is to determine Truckenbrodt's shape factor, L. however, to do this a new construction much be introduced (43):

$$\xi = \left[C^*_1 + \left(\frac{C_f}{2}\right)^{(n+1)/n}\int_{x_t/\ell}^{x/\ell}\left(\frac{U}{U_\infty}\right)^{3+2/n} d\left(\frac{x}{\ell}\right)\right]^m \quad \cdots (8)$$

Where: $n = 6$
$m = 4$

Due to the requirement of a later step, ten values of ξ were computed again using quadratures. These values of are shown in Table IV-2.

TABLE IV-2-COMPUTED VALUES OF ξ

Y/YN	ξ
.1	3.00×10^{-21}
.2	2.61×10^{-20}
.3	3.90×10^{-19}
.4	1.23×10^{-18}
.5	7.81×10^{-18}
.6	1.72×10^{-17}
.7	6.90×10^{-17}
.8	1.31×10^{-16}
.9	4.41×10^{-16}
1.0	6.19×10^{-16}

The value of Truckenbrodt's shape factor can be determined from (47):

$$L = \frac{\xi_1}{\xi}\left\{L_1 + 0.23+0.0076\ \frac{n}{n+1}\right.$$
$$-0.030+\ \ln\left(\frac{U_\infty\ \ell}{\nu}\right)\ \ln\left(\frac{U_1}{U_\infty}\right)$$
$$\left.-0.0076\ \frac{n}{n+1}\ \ln\xi_1\right\}-0.23-0.0076\ \frac{n}{n+1}$$
$$+0.0304\ln\left(\frac{U\ \ell}{\nu}\right)+\ln\frac{U(\xi)}{U_\infty}\ +.0076\ \frac{n}{n+1}\ \ln\xi$$
$$-1.0608\ \frac{1}{\xi}\int_{\xi_1}^{\xi}\ln\left(\frac{U(\xi)}{U_\infty}\right)d\xi \qquad \ldots\ldots\ldots\ (9)$$

The subscript 1 in Eq. (9) indicates the value of that variable at the transition point, x_t. Since the flow becomes turbulent so close to the stem of the vessel, $x_t \approx 0.0$, $\xi_1 \approx 0.0$ and the entire first term of Eq. (9) goes to zero.

In order to evaluate the integral in the last term of Eq. (9) by quadrature methods, values of U/U_∞ at equal intervals of t are required. Values of ξ from Table IV-2 were plotted against values of U/U_∞ from Table IV-1 in Fig. IV-2. The range of ξ was divided into ten equal segments and related values of U/U_∞ obtained from Fig. IV-2. These values and related quadrature elements are shown in Table IV-3.

The value of L from Eq. (8) is:

$$L = -.23 - .0076\left(\frac{6}{7}\right) + .0304 \ln\left[\frac{(1.68889)(707.5)}{1.1342X10^{-5}}\right] + \ln(1.154) + .0076\left(\frac{6}{7}\right)\ln(6.19X10^{-16}) - \frac{1.0608}{6.19X10^{-16}}(1.46558X10^{-17}) = .215 \quad \ldots\ldots\ldots (10)$$

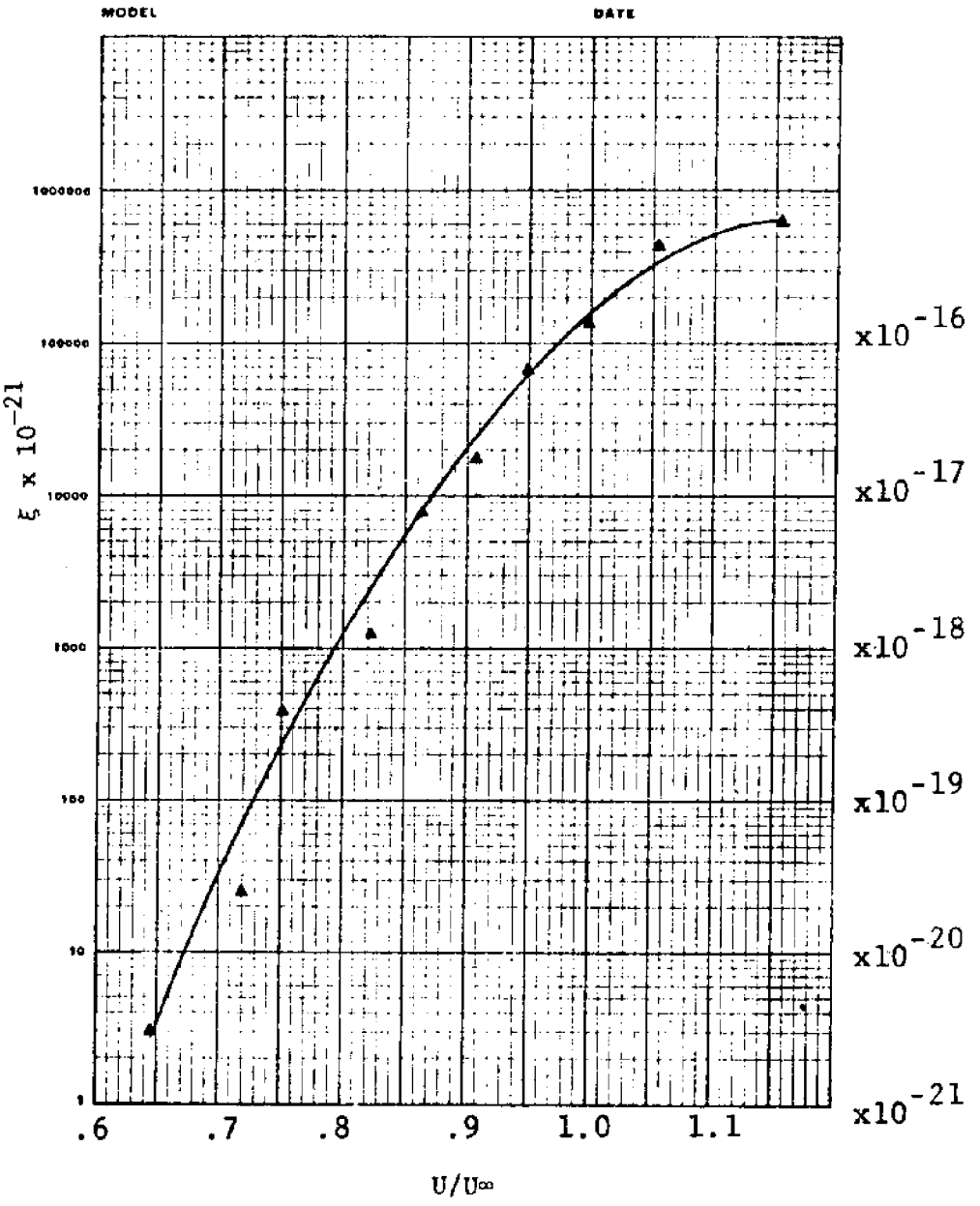

FIG. IV-2-PLOT OF ξ VERSUS U/U_∞

TABLE IV-3- ξ QUADRATURE ELEMENTS

1	2	3	4	5
ξ	$U(\xi)/U_\infty$	$\ln(U(\xi)/U_\infty)$	Coef	(3x4)
3.00×10^{-21}	.645	-.438505	1	-.4385
6.19×10^{-17}	.946	-.055512	4	-.2220
1.24×10^{-16}	.983	-.017146	2	-.0343
1.86×10^{-16}	1.005	.004987	4	.0199
2.48×10^{-16}	1.031	.03052	2	.0610
3.10×10^{-16}	1.045	.044016	4	.1761
3.71×10^{-16}	1.061	.059211	2	.1184
4.33×10^{-16}	1.077	.074179	4	.2967
4.95×10^{-16}	1.090	.086178	2	.1724
5.57×10^{-16}	1.110	.104360	4	.4174
6.19×10^{-16}	1.154	.143234	1	.1432
				Σ = .7103

Truckenbrodt's slope factor, L, must be converted to shape factor, H_{12} through use of Fig. IV-3(35). The value of H_{12} extrapolated from Fig. IV-3 is 1.25.

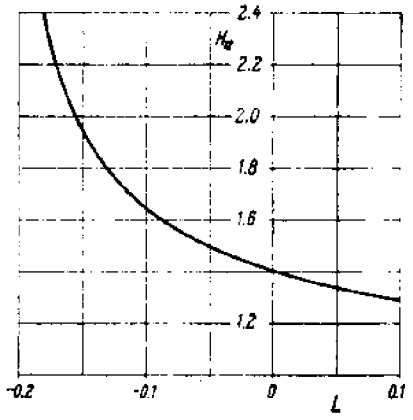

FIG. IV-3-SHAPE FACTOR RELATIONSHIP (43)

The shape factor H_{12} is defined as (43):

$$H_{12} = \frac{\delta_1}{\delta_2} \quad \ldots\ldots\ldots\ldots\ldots\ldots (11)$$

Solving for δ_1:

$$\delta_1 = H_{12}\,\delta_2 \quad \ldots\ldots\ldots\ldots\ldots\ldots (12)$$

Substituting into Eq. 12 and solving for δ_1:

$$\delta_1 = 1.25(.0989) = \underline{.124 \text{ ft.}} \quad \ldots\ldots\ldots (13)$$

Solving for δ_1 using the flat plate turbulent equation (Eq. 6) from Chapter III:

$$\delta_1 = \frac{.04625(103)}{\left[\frac{(1.1538)(1.6889)(103)}{1.1342X10^{-5}}\right]^{1/5}} = .169 \text{ ft.}$$

The difference between the values of the displacement thickness, δ_1, determined by the flat plate equation and the Truckenbrodt method is:

$$.169-.124=.045 \text{ ft.} \quad \ldots\ldots\ldots\ldots (14)$$

APPENDIX V

FROUDE NUMBER FOR DEEP-WATER CONDITIONS

I. Wave velocity for deep-water conditions:

$$C = \left[\frac{g\lambda}{2\pi}\right]^{\frac{1}{2}} \quad \ldots\ldots\ldots\ldots\ldots\ldots \quad (1)$$

Where: C=wave velocity (ft/sec)
λ=wave length (ft)
g=acceleration of gravity (32.2 ft/sec^2)
π=Pi (3.14159)

II. Froude number:

$$F = \frac{V_s}{\left[gd\right]^{\frac{1}{2}}} \quad \ldots\ldots\ldots\ldots \quad (2)$$

Where: F=Froude number
V_s=velocity of ship (ft/sec)
d=depth of water (ft)

III. Wave velocity is equal to ship speed:

$$V_s = C = \left[\frac{32.2\lambda}{2(3.14159)}\right]^{\frac{1}{2}} = \left[5.125\lambda\right]^{\frac{1}{2}} \quad \ldots \quad (3)$$

IV. Substitute (3) into (2):

$$F = \left[\frac{5.125\lambda}{32.2d}\right] \quad \ldots\ldots\ldots\ldots\ldots\ldots \quad (4)$$

V. Waves begin to "feel" bottom when the water depth, d, equals one half the wave length, λ or:

$$\frac{d}{\lambda} = \frac{1}{2} = .5 \quad \ldots\ldots\ldots\ldots\ldots\ldots \quad (5)$$

VI. Substitute (5) into (4) and solve for F:

$$F = \left[\frac{5.125}{32.2(.5)}\right]^{\frac{1}{2}} = \left[.3183\right]^{\frac{1}{2}} = .57 \quad \ldots \quad (6)$$

VII. The diverging wave system plays the dominant role in producing the maximum wave height, Hmax. Since the transverse waves are longer than the diverging waves, they will feel bottom at lower velocities. It is also known that the length of diverging waves increases with distance from the vessel sailing line. For these reasons the diverging wave system will not be significantly affected by the bottom until the Froude number is greater than the .57 derived above. The author believes .7 to be satisfactory.

APPENDIX VI

MAXIMUM VESSEL SPEED FOR DEEP-WATER CONDITIONS

I. In Appendix V it was determined that .7 was an appropriate Froude number to define the boundary between deep and shallow water for ship-generated waves.

II. Solve for vessel speed and substitute .7 for F:

$$V_s = F\left[gd\right]^{\frac{1}{2}} = .7\left[32.2d\right]^{\frac{1}{2}} \quad \text{(1)}$$

Where V_s=vessel speed (ft/sec)
F=Froude number
g=acceleration of gravity (32.2 ft/sec^2)
d=water depth (ft)

III. Convert V_s from (1) to knots:

$$V_s = .41447\left[32.2d\right]^{\frac{1}{2}} \quad \text{(2)}$$

IV. Determine limiting deep-water speeds for a range of water depths (Table VI-1):

TABLE VI-1-DEEP-WATER WAVE LIMITS

Water Depth (Feet)	Vessel Speed (Knots)
30	12.882
35	13.914
40	14.875
45	15.777
50	16.630
55	17.442
60	18.218
65	18.962
70	19.678
75	20.368

APPENDIX VII

COMPUTATION OF $\Gamma\left(\frac{2}{3}\right)$

$$\Gamma(x) = \int_0^\infty e^{-t}\, t^{x-1}\, dt \quad \ldots\ldots\ldots\ldots\ldots\ldots\ldots\ldots\ldots\ldots \quad (1)$$

$$\Gamma(x) = \Gamma(x+1)/x \quad \ldots\ldots\ldots\ldots\ldots\ldots\ldots\ldots\ldots\ldots \quad (2)$$

$$\Gamma\left(\frac{2}{3}\right) = \Gamma\left(\frac{2}{3}+1\right)\Big/\frac{2}{3}$$

$$= \frac{3}{2}\Gamma\left(\frac{5}{3}\right) \quad \ldots\ldots\ldots\ldots\ldots\ldots\ldots\ldots\ldots\ldots\ldots\ldots \quad (3)$$

From Gamma table (Fig. VI-1):

$$\Gamma\left(\frac{5}{3}\right) = .9024728748$$

$$\Gamma\left(\frac{2}{3}\right) = \frac{3}{2}(.9024728748)$$

$$= 1.3537093122 \quad \ldots\ldots\ldots\ldots\ldots\ldots\ldots\ldots \quad (4)$$

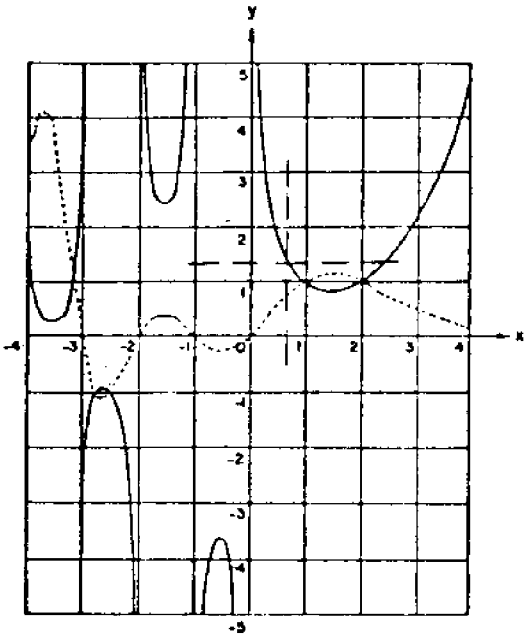

FIG. VII-1 GAMMA FUNCTION (1)